STUDIES ON THE INTERACTION OF COPPER (I) AND MERCURY (II) HALIDES IN SOLID STATE

THESIS SUBMITTED FOR THE DEGREE OF

Doctor of Philosophy

IN

Chemistry

BY

AFAQ AHMAD

M. Sc., M. Phil.

DEPARTMENT OF CHEMISTRY
ALIGARH MUSLIM UNIVERSITY
ALIGARH

1979

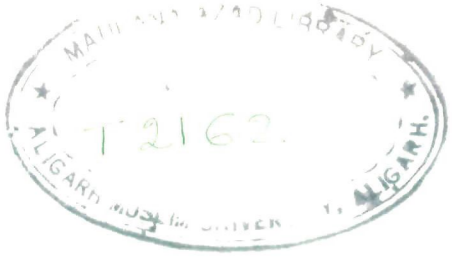

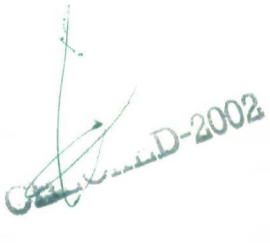

ALIGARH MUSLIM UNIVERSITY
ALIGARH, U.P., INDIA

Phone : Office : 3345

Department of Chemistry

Date

This is to certify that the thesis "Studies on the Interaction of Cu(I) and Hg(II) halides in solid state" is the original work of Mr. Afaq Ahmad, carried out under my supervision and is suitable for submission for Ph.D. Degree.

(Dr.) Mirza Aijas Beg
Supervisor

C O N T E N T S

ACKNOWLEDGMENTS

It is a pleasure to express my thanks to Dr. Mirza Aijaz Beg for his advice and direction in the course of this work. His interest in every stage of this research has always been a source of inspiration.

I am also grateful to Dr. B. Rama Rao, Regional Research Laboratory, Hyderabad for providing facilities for X-ray measurements; to Miss Safia Mehdi and Mir Raza Hussain of the same lab. for helpful discussion in the analysis of X-ray diffraction patterns. Thanks are also due to Prof. A. Rahman, Head of the Chemistry Department for providing research facilities.

The comments and suggestions of the members of the laboratory colleagues, particularly, Dr. S.M. Ansari, Mr. R.P. Singh and Mr. M.A. Iraqi are highly appreciated.

Financial assistance by the Council of Scientific and Industrial Research and University Grants Commission, New Delhi is gratefully acknowledged.

Afaq Ahmad

Afaq Ahmad

C H A P T E R - I

I N T R O C U C T I O N

The last quarter-century has been marked by the rapid growth of the solid state sciences. This has exerted an increasingly larger and broader impact on newer areas of science and technology. Their growing applications in metallurgy, ceramic technology, electrochemistry, lasers, semiconductors, polymers and propellants have added new dimensions to their importance. And it is only the application of solids that has stimulated a growing interest[1,2] in solid state reactions.

Due to their practical and theoretical importance numerous investigations of reactions involving solids have been carried out. In the early period, dating from 1912 to about 1930, a variety of solid state reaction systems were studied[3,4]. The pioneering work in the area has been carried out by J.A. Hedvall. Formation of solid solutions have been reported for systems exhibiting complete miscibility such as CoO-ZnO, CoO-MgO, NiO-MnO etc. as well as for such systems of partial solubility as Al_2O_3 - Cr_2O_3, CdO-MnO, MgO-MnO.

Many reactions of actual compound formation involving acidic oxides and basic oxides to form the corresponding salts, or specific reactions to give spinels have been reported.

Similar reactions occur between oxides and salts decomposing into a solid and a gas. Such reactions are of practical importance. Another class of reactions which has been thoroughly investigated in the early period is represented by base exchange of the type $MeO + MeXO_4 \rightleftharpoons MeXO_4 + MeO$, and this type of reactions may also lead to the formation of spinels.

In solid-solid reactions, the reactants have only restricted access to each other as compared to reactions in gases or liquids where intimate contact between reactant molecules is a natural consequence of kinetic nature of reactants. In order to understand solid state reactions which means an understanding of the atomistic reaction mechanism, it is first of all necessary to explain the transport of matter in the reaction product. Since this transport in solids is due primarily to the mobility of point defects, it is therefore necessary to understand the behaviour of point defects in binary and higher order metallic systems and in ternary and higher order ionic systems. The emphasis should be on the dependence of point defect concentrations on the activities of the components since these activities change locally in the reaction product during a solid state reaction.

In the middle of 1920, Hedvall observed the first evidence that reactions may be carried out by the motion of

lattice ions. This was concluded from the fact that reaction commenced to take place at about the same temperature at which ionic conductivity becomes noticeable. Among the important developments of this period was the well-known interpretation by Wagner[5], of the formal rate expressions in terms of the gradient of chemical potential, mobility of ionic particles in solids, and of the lattice disorder models as postulated by Frenkel and by Schottky. This earlier work provides the foundation of the present knowledge.

The general problem of the solid state reaction is two fold. Firstly, the experimental determination of reaction rate and morphology as a function of all independent variables. Secondly, the calculation of the reaction rates and a prediction of the morphology under a given set of independent variables in terms of known thermodynamic and transport properties of the system under consideration. And these require the knowledge of the atomistic mechanism of the fundamental steps such as nucleation, phase boundary reaction, sintering and diffusion. Such studies will doubtless provide valuable aid in furthering the practical utilisation of reactions in solid state. However, as Stringer et al.[6] have pointed, theoretical models are in general not adequate for interpretation of real cases and to account for the kinetic analysis, more data and observations are needed. Real systems

are usually in a state of considerable imperfections. Indeed, enhanced and desirable activity and lattice reactivity are often obtained by producing a solid in the form of imperfect crystal. Effect of normal structure have been found in many processes, the rate of which is controlled by bulk or surface reaction or by sorption phenomena. Their appearance is also obvious in cases where topotactic relationships are important. Lattice imperfections influence all types of elementary steps in a solid state reactions. They often constitute preferred sites for reaction and nucleation, either in bulk of the solid or at the surface. In addition, lattice imperfection makes solid state diffusion possible and enable the reactants to reach each other.

Obviously, for a quantitative treatment of the reaction kinetics, one has to make several assumptions. Among them, the most important are the assumption of local thermodynamic equilibrium in the solid phases taking part in the reaction and a thermodynamically well-defined system in which the proper number of independent thermodynamic variables are predetermined. This is why the solid-solid reactions in binary or quasibinary systems have been quantitatively studied. In principle, knowledge of point defect thermodynamics, thermodynamic properties of the systems, and that of Fick's law are sufficient to treat the kinetic problems quantitatively.

This treatment can be satisfactorily applied to precipitation and decomposition reactions in solids, taking into account the elastic part of the chemical potential[7,8]. Similarly, the relevant problem associated with solid state electrical battery working with solid electrolytes can be solved by taking into the consideration the diffusion theory in ionic crystal together with point defect thermodynamics[9].

This highlights the broad field falling systematically under solid state chemistry topic. The gradient of chemical potential is the local driving force for the fluxes of the components. There are other solid state reactions in heterogeneous systems which proceed under the action of other kinds of driving forces such as relative temperature gradients or phase boundary free energies. The kind of reaction under the action of a temperature gradient has been analysed recently in detail[10], and the solid state reactions driven by phase boundary free energies are the so called Ostwald ripening process[11,12].

The reaction between heterogeneous solid phases, where phase boundary controls the overall rate, are very important and have been studied in a number of solid gas reactions where a linear rate law indicates that diffusion control does not play the predominant role[13]. Although it has been found in a number of solid state reactions in ionic systems that the

linear rate law is the initial rate determining step, the atomistic reaction mechanisms are not yet understood. This is due to the fact that in contrast to gas solid reactions, it is extremely difficult to study the linear reaction rate as a function of the component activities at solid-solid interfaces. But a knowledge of the reaction rate as a function of the independent variables is a pre-requisite for a correct analysis of the atomistic reaction steps of a phase boundary reaction.

It is now obvious that these factors influence the reaction kinetics in solid phase in practical applications to such systems as refractories, ceramics, cement, glass, semi-conductor, catalyst, etc. The reactivity of the raw mixes of the constituents, the effect of the various types of the diffusing species in the course of solid-solid reactions influence the quality of the final product.

From the industrial point of view, reactions in solid state have a universal importance. New technologies based on nuclear energy, space exploration and solid state electronic devices have stressed the need for high temperature solid state materials and for a systematic understanding of their chemical behaviour.

Ferrites of the general composition $MeOFe_2O_3$, constitutes an important class of compound having high electrical resistance with magnetic permeabilities comparable with those of metallic systems. Even before the introduction of ferrites to solid state devices, the formation of ferrites and of other spinels by reaction in the solid state had been studied extensively[14] to elucidate phenomenologically the various stages of interaction between two solids leading finally to the formation of a new crystalline material. Since ferrites have become practical materials for commerce, many more studies are being carried out.

Since the end of the last century, it has been known that there exist solid electrolytes, that is, solid compounds with practically pure ionic conductivity. This was first established by transference measurements[15]. Galvanic cells with solid electrolytes have been built. The solid electrolytes have attained a faster growth during the last decade, and a number of review articles[15], are available dealing generally the electrical conductivity behaviour of solid electrolyte.

Catalytic processing is becoming increasingly important. The majority of industrial catalytic processes are heterogeneous and employ solid catalysts. All factors affecting the reactivity of solids are important for the preparation of highly active catalysts. The thermal decomposition reaction is commonly

used to prepare active catalysts. An example of catalysts comprising ionic solids are zeolite-containing catalysts, which in recent years have been introduced to such important industrial processes as cracking isomerisation and polymerisation, and many others.

These technological applications underline the profound importance of the kinetics of the reactions involving solid phases not only in the understanding of the fundamental principles involved in many aspects of the industrial development. These relationships, which are certainly complex, cover a very broad area from the initial interaction through all stages of reaction to nucleation and growth of each individual phases. The varied academic values and applied implications demand much more attention than this branch has received so far.

Despite their importance and usefulness in every field of life, reactions in solid state, in particular, and many facets of solid state chemistry, in general, had remained unrecognized for a long time. However, some fifty years ago, a remarkable revival took place and new vistas has been added both experimentally and theoretically to reveal the secrets of the atomic structures and their reactivity. Although the first reaction of this kind seemed to have been reported as early as in 1820 by Faraday[16], the systimatisation of solid state reactions can be regarded to be started from 1920 onwards by

Hedvall[17-19], and Tammann[20], and was further developed to a satisfactory interpretation by Wagner[21-23] and Jander[24-26].

The processes associated with the solid state reactions are fundamentally more complicated than those involved in gas phase or liquid phase processes. In the latter, mixing occurs at molecular level so the kinetics of the reactions in a liquid or a gas phase can be expressed as a function of concentrations of reactants. In contrast, this is usually of little significance in kinetic studies when solids are involved. Since here the reacting species are very much restricted in their motion so their availability for reaction can not be described by simple statistical laws. In solid state reactions, at least one reactant diffuses into the others in order that the reaction may be initiated and propagated. Or, in other words, solid state reactions are diffusion initiated. Thus, the main point on which chemical reactions with solids distinguish themselves from those occurring in liquid or gaseous phase is the effect of lattice structure[27,28], and diffusion mechanism. Whether it is transformation of crystal structure or formation of a chemically different solid, they involve the rupture of old bonds and the formation of new ones to form the new product[29,30]. Furthermore, as the solid state processes involve movement of the interphase boundary, the mathematical formulation of the rate processes must be expressed in terms of space and time co-ordinates.

Very few efforts have been made to describe the classification of solid state reactions. The first attempt to classify the solid-solid reactions in a systematic way was due to Jander[31] which was based on simply the nature of the chemical reaction only. It has got no theoretical basis and hence it is ignored today. Muller[32] introduced a number of simplified ideas for chemical processes and reduced the former's classification to seven. Later Jost[33], giving priority to the formation of solid solutions and ignoring the solid state reactions forming new products, classified into three categories. Therefore, his classification is good only for the system of the metallurgical interest. Roginskii[34], studying the topochemical reactions, proposed the classification on the basis of the state of the product formed.

In reactions involving solids, five reaction types have been distinguished, namely: solid state decomposition, dimerisation, etc., reaction between a solid and a gas, another solid or a liquid, and reactions at the surface of a solid which does not enter into the overall reaction equation. Mechanismwise, solid state reactions are roughly classified as under.

1. diffusion controlled reactions in which atomic motions are largely uncorrelated.

2. diffusionless phase transformations which involve co-operative motion of atoms; and

3. reactions that involve extended defects and that combine features of the first two classes. Christian[35] has given a detail discussion of the classification of reactions and transformations of metallurgical interest.

There are, however, alternative schemes for classifying solid state reactions in which the product structure has a definite relationship to that of the reactants. The reference has been made to the phenomenon of topotaxy[36] and to such processes as topotactic reactions[37,38]. In the terminology of Bernal and Mackay[39], the term reconstructive transformation is used when a major rearrangement of bonds precludes any correlation between the orientation of the reactant and product. The detailed atomic mechanism by which these orientation relation come about is a topotactic mechanism, hence topotaxy thus describes the mechanism of reactions which involve structural relations between reactant and product. Likewise, epitaxy is a two dimensional correlation between the reactant and product, but having no correlation in the third dimension. Ubbelohde[40] distinguished between discontinuous and continuous phase transformations according to classical thermodynamics. Phases related structurally are usually not independent in thermodynamic sense and their interconversions are usually continuous transformations. The structural relationship is given much importance for solid state reactions.

The properties of solids may be divided into two groups. (i) Structure insensitive, and (ii) structure sensitive properties. Structure insensitive properties are well-defined under given external conditions and are independent of the history of the specimen and of its dimensions like chemical formula, lattice dimension, density, etc. Structure sensitive properties, on the otherhand, are directly affected by factors like the mode of preparation of the specimen, the particle size and shape, for instance, the mechanical strength and the actual value of cohesion, electric conductivity and absorption spectra of real crystals. The chemical reactivity is usually structure-sensitive as is evidenced by the fact that the catalytic activity of solids and the ability to luminence fluoresce may vary with the mode of preparation or treatment.

Solid state reaction is the reaction between two solids to form one or more product phases. During the course of this heterogeneous solid-solid reaction, the product thus formed separates out. Therefore, the progress of the reaction has to be attributed to a transport of the reactants across phase boundaries and through the reaction product. In order to understand solid-solid reactions, it is required to explain the transport of matter in the reaction product under the action of chemical or electrochemical potential gradients. Since this transport in solids is essentially due to the

movement of point defects, the understanding of the behaviour of point defects is important. And the importance should be given to the dependence of defect concentrations on the activities of the components. Since these activities vary locally in the reaction product during a solid state reaction.

In a solid-solid reaction, different steps such as nucleation, transfer of matter across phase boundaries and diffusion in reaction product occur. Therefore, besides defect thermodynamics, the diffusion theory is the basis for the explanation of solid-solid reactions.

In general, solid-solid reactions are exothermic. This follows from the fact that the overall driving force for the reaction is the difference between the Gibbs energy of the crystalline reactants and the reaction products and that the reaction entropies are in general quite small. However, unless solid state reactions are not conducted as reactions between very fine powders with a corresponding high surface area, in most cases, one may easily impose isothermal conditions, due to the low reaction rates in the solid state.

The problem of determining the mechanism of a solid state reaction is easily understood provided that the macroscopically measured reaction rate is interpreted in terms of the change in the Gibbs energy and the respective fundamental

transport co-efficients. This can be achieved if the number of possible variables are minimized and rigorously defined. This is possible at best if the reactants are single crystals and if, in addition to pressure and temperature, the appropriate number of chemical potentials of components is predetermined according to the phase rule. Only in the case of binary or quasi-binary systems, a cross section of the phase diagram can be obtained[41]. If phases with extended homogeneity ranges are present and the above parameters are known, then one can calculate the composition versus distance curves in the related system[42]. A number of reviews and books[4,43-55] are now available which have contributed significantly towards the understanding of some of the fundamental aspects of solid state reactions such as nucleation, transfer of matter beyond phase boundaries and above all the role of imperfections. Extensive treatments are available in the literature[56-58].

DIFFUSION

In view of the role of diffusion phenomenon in controlling solid state reaction rates, the study of diffusion in solid bodies is very significant, both theoretically and experimentally. Diffusion of gases and liquids is a relatively simple process and has been explained quite satisfactorily. In contrast, diffusion in solids is quite complex. A number of reviews[29,59-61]

have appeared during the last few decades that explain the diffusion mechanism in solids. Also, recently accounts of self-diffusion are available for metals[62], halides[63], oxides and other compounds.[64,65]

Depending on the mode of migration of the atoms, ions, etc. we have bulk diffusion, surface diffusion and diffusion along crystal faces, the former of which has been a subject of thorough study.

Elucidation of the diffusion mechanisms is very often difficult and is quite complex. As a matter of fact, it was not clear in the early stages whether solid state reactions actually go through diffusion in solid state or via vapour phase[66-68]. The first idea of the diffusion mechanism appeared to be given by Havesy[69]. In 1923, Joffe[70] suggested other ideas on the mechanism of mass transfer in crystalline lattice, which was the basis of the quantitative treatment of the diffusion theories of Frenkel[71] and latter Wagner and Schottky[75].

According to the work of Frenkel, and of many others, the diffusion mechanism can be classified, depending on the type of elementary jump as follows[72,73]:

1. Rotation mechanism[74] such as exchange mechanism, ring mechanism. This happens in a purely perfect crystal.

2. Defect mechanism[75-77] such as interstitial mechanism, interstitially mechanism, crowdion mechanism, vacancy mechanism, etc.

3. Grain boundary and dislocation mechanism[78-80] and

4. Vapour phase diffusion.

The more extensive and detailed studies in diffusion have been made on metals and on ionic crystals, and the current understanding of diffusion phenomena is largely due to these studies.

Self-diffusion in most pure metals is characterized by the obedience of the Arrehenius equation, $I = A\exp(-\frac{E}{KT})$ with an activation energy, E, given by the relation, $E = 34\ T_F$ where T_F is the melting point. It has been pointed out that self-diffusion in metals is by vacancy mechanism. A recent application to Silver[81] provided strong evidence for a vacancy mechanism for T below 750°C. Experiments on iron[82] also suggest vacancy diffusion in both the body centred cubic (b.c.c.) and face centred cubic (f.c.c.) phases. However, extremely careful measurements over wide ranges of temperatures have indicated that there may be a very slight curvature in the Arrehenius plots of log D vs 1/T. This provides strong evidence for the simultaneous operation of more than one mechanism[83,84]. And this is more pronounced in Sodium[85] and is thought to be due to divacancy migration contributing to the total diffusion.

Deviations from normal self-diffusion are found in certain other metals[86] as well like β-zirconium, β-Hafnium, γ-Uranium, β-Prutonium, etc. There has been no satisfactory explanation for this anamolous behaviour. It seems that owing to difficulty in getting these metals pure, the diffusion is enhanced due to an excess intrinsic vacancy concentration associated with an impurity such as oxygen. Or it may be due to a different mechanism in operation either alone or together with a vacancy mechanism. Dislocation diffusion may be another possibility, because there will be an unusually high dislocation content on account of the phase change, necessary in all case to reach the diffusion temperature, and which may be retained during the diffusion because of the high impurity content. Another important factor is the diffusion of very dilute solutes, or impurities in metals[86,87]. The first systematic study on a wide range of solutes in the noble metals revealed a pattern of behaviour with which all later measurements are compared. The main features of this impurity diffusion are the total obedience to the Arrehenius equation with values of activation energy, E, and frequency factor, A, that do not differ appreciably from the values for solvent self-diffusion. This close similarities between solute and solvent diffusion rates justify the assumption of a vacancy mechanism for both. But recent measurements on impurity diffusion in Aluminium show

some deviation from normal behaviour, but this does not warrant to propose another mechanism[88]. Nevertheless deviations have been noteably more profound from normal behaviour for the diffusion of the noble metals and some other transition metals like Cd, Co, etc. in solvents as alkali metals[88,87]. Such behaviour suggest to invoke another mechanism and currently it is believed that this fast impurity diffusivity is due to the solute being dissolved interstitially and its diffusion is by interstitial or interstitially mechanism[89,90].

The effect of the activity of one of the components on self-diffusion has been studied in several binary compounds especially oxides[91]. For example, the observation of a cation diffusion co-efficient proportional to δ in an oxide $M_{1-\delta}O$ provides some evidence of a cation vacancy mechanism. The knowledge of defect present can contribute to the understanding of diffusion as much as the identification of the defect, for example, Schottky or Frenkel type can be attributed in the prediction of diffusion mechanism in ionic crystals. Recent work has utilised this fact and evidence for interstitial Uranium diffusion in UO_2[92], cation vacancy diffusion in MnO[93] and NiO[94] and anion interstitial diffusion in CaF_2 and BaF_2[95] and in UO_2[96] have been explained on the basis of defect theory. Comprehensive evidence of mechanism has not been found for

diffusion of both species in a binary compound. Even in important oxides with the rock-salt structure, the diffusion mechanism of oxygen is not clearly known. It has been suggested that interstitial diffusion of the anion occurs in these materials[97], but studies on pure and doped CoO provide good support for anion-vacancy diffusion[98]. It is quite possible that diffusion mechanisms change with temperature and defect concentrations.

Fundamental studies of more concentrated solution have mostly been associated with the phenomena of chemical diffusion- Kirkendal Effects, Darken equations, vacancy wind effects, etc. - the general treatment is given here for brevity. However, a comprehensive treatment is available elsewhere[99].

We consider here reactions in which the composition of a solid phase is changing with time because of the interdiffusion of two components A and B. The inter-diffusion coefficient may best be defined in terms of the difference of velocity Δv of the two components or equivalently in terms of the difference in flux of A and B, thus[100],

$$\tilde{D} = V\,(C_B J_A - C_A J_B)/\,\Delta C_B \qquad (1)$$

Here C_A and C_B are mole fractions and J_A and J_B, the fluxes of A and B while V is the molar volume. The flux is related to the velocity by $\nu C = JV$ and will depend on the

co-ordinate system, so that one may define diffusion co-efficient, D_A and D_B as

$$D_A = V.J_A / \Delta C_A, \text{ etc.} \quad (2)$$

So that $\tilde{D} = C_B D_A + C_A D_B$ (3)

If chemical and tracer diffusion occur by the same mechanism, it may be shown that[101]

$$I_A = D_A^* (\delta \ln a / \delta \ln c) \quad (4)$$

Where D_A^* is the tracer diffusion co-efficient and a the thermodynamic activity.

The activity in these equations refer to the activity in the crystal undergoing diffusion and may include the effects of stress and electrostatic potential[101].

The general problem of interdiffusion in multicomponent systems is much more complicated. One can sometimes usefully define an effective binary diffusion co-efficient relating the flux of a species to its concentration gradient[102]. A good general discussion of this problem has been given by Kirkaldy[103].

Role of Defects

In the majority of solid state reactions, the movement of atoms over many lattice distances and the choice of certain sites for nucleation of a new phase is required to be explained. It basically requires to understand the nature and the role played by imperfections in crystalline solids. Indeed, ideally ordered crystalline solids do not occur in nature, and even crystal growth itself depends on the presence of structural defects, at least one dislocation with a screw component. However, even a single crystal with a very small number of dislocations has lattice defect on atomic scale which increase with the rise in the temperature. Therefore, to each temperature, there corresponds a precise concentration of defects. Apart from the properties of crystals, therefore, the temperature alone determines the concentration of such lattice defects. There are all known as point-defects. Lattice defects play an important role in solid state reaction because diffusion processes in solids are controlled by the concentration and mobility of such defects. The simple lattice defects, vacancies and interstitial atoms, take part in a variety of processes leading to phase changes, precipitation, order-disorder transformation and chemical reactions in solids.

Frenkel[104] in 1926 and Schottky[105] in 1935 developed theories regarding the presence of interstitial and vacancy defects in crystals. The idea of the dislocation was developed by Taylor[106] and Orowan[107]. Impurities are also considered as defect because their presence cause disturbance in the periodicity of lattice. In addition to these imperfections, there are other species like electrons, holes etc. However, very few attempts have been made to correlate such effects to specific problems of phase transition and chemical reactions in solid state[108].

It is now clear that the reactivity of solids is due to their defect structure and it is the point defects which play a crucial role in solid state reactions. If local thermodynamic equilibrium is established, the local concentration of these defects in the reaction product can be calculated provided that all the independent thermodynamic variables are correctly predetermined. As long as the concentration of point defects are small, the ideally dilute solutions theory can be adopted to calculate the dependence of concentration of point defects on the component activities. This has been done comprehensively in the past, on the basis of the Wagner-Schottky treatment for binary metallic and ionic compounds[5,109]. For non-metals, the Kroger-Vink approach based on the proposals by Brouwer[110] using the chemical potential of structure elements and neglecting minor defects, blancing equations have been

accepted quite generally. Therefore, the majority defects which constitute a disorder type[105] govern the activity dependence of defect concentrations. This means that point defect equilibria are established in the reaction product. If reaction between point-defects in order to maintain the internal equilibria are homogeneous, it can be shown that their relaxation times are small compared with the time of the solid state reaction[111].

In all other cases, the relaxation of internal equilibria depend on the density of the sources and sinks of point defects. The relaxation time then may be calculated with the help of appropriate models[112,113], or measured independently[111,114].

The direct interchange of atoms without the intervention of a lattice defect is energetically very unfavourable, particularly in case of close packed structures. Diffusion is therefore occuring through lattice defect. Diffusion may occur by the successive interchange of lattice atoms with an interstitial atom, but the energy of formation of an interstitial is so high that it can not be produced in a significant quantity by thermal means. The energies of formation and migration of a lattice vacancy are, however, of the right order of the magnitude for the vacancy to be responsible for self-

and inter-diffusion. This vacancy mechanism of diffusion are for more prevalent than others. Experimental evidence for vacancy diffusion is provided by the Kirkendal effect. If, therefore, diffusion occurs by the vacancy mechanism, then the diffusion co-efficient is proportional to the concentration of vacancy present. An excess concentration of vacancy in a metal can be produced by various ways, such as quenching, plastic deformation and irradiation[115]. At a temperature where vacancies are mobile, the excess vacancies must tend to anneal out of sample. During their migration the excess vacancies cause atomic interchange and therefore may influence many diffusion controlled solid state processes; for instance, the acceleration of the ordering of Cu_3Au alloys by rapid quenching from high temperature has been observed[116,117]. Excess vacancies introduced by quenching increase greatly the pre-precipitation clustering in precipitating alloys[118].

Defects in a solid are able to alter its composition and a phase with homogeneity range can be defined in the broadest sense as a solid solution where one or more kinds of atom are gained or lost[119]. The extent to which a binary compound can exist as a unique phase can be measured by a variety of physical and chemical techniques and many classes of inorganic compounds are reported to have wide composition limits reflecting high concentration of random defects. The concept of non-stoichiometric

compound is important, for it can retain, simple formulae for inorganic compounds, and extracting or adding atoms from or to a rigid three-dimensional infinite lattice framework. For example, the high temperature form of Nb_2O_5 has a complex X-ray powder diagram, and preparations in the region $NbO_{2.5}$-NbO_2[120] could, therefore, be described sometimes ago as a non-stoichiometric compound with a wide homogeneity range. This could have been caused either by the presence of additional niobium atoms interstitially, which could increase the density or by vacancies, following the removal of oxygen atoms, which would decrease it. However, this picture seems over-simplified. Instead, a number of discrete phases are often present within the composition region of non-stoichiometric compound.[121] The formulae of the newly recognised compounds are no longer simple, but their structures are closely related to each other.

They all contain an ordered and recurring abnormality, which may be a vacancy in case such as Cr - S[122], Pr - O[123] systems. Also, the fault may be interstitial as for the alkali metals in the cubic tungsten bronzes[124] and oxygen or fluorine in the fluorite structures[125]. The replacement of non-metal by metal is known for certain metallic selenides and tellurides with structures derived from the common NiAs type[126]. While these examples define in principle the physical

nature of the three well-established classes of defects, it is only at temperatures sufficiently high for them to be disordered[127], that a truly non-stoichiometric compound containing them can be said to exist. Studies on such systems support the presence of these types of defect in dilute as well as in the more concentrated systems. However, there are well-documented families of closely packed phases amongst the higher oxides of Tungsten, Molybdenum, etc. where there is no direct evidence of these classical defects. An ordered fault can be recognised instead, known as crystallographic Shear[121]. In this, one part of the parent structure is displaced or sheared relative to the next, forcing its collapse along certain parallel planes, and bringing the metal-oxygen octahedra at these ends into closer union. The sharing of octahedral edges rather than corners, or faces rather than edges, may increase the stability of structures, and reflect a chemical bonding system more covalent than ionic[127].

In general, the fault planes reflect a dynamic state existing within a crystal at high temperature, which is almost retained even if cooling is applied. The fault may be attributed to one of two causes. In the first place, it may be virtually impossible to find a flawless crystal of any one of these phases because of the experimental difficulty of assuming an exact stoichiometry. Secondly a real equilibrium state may not

have reached, either because the materials had been given insufficient time to react, or because the phase had begun to disproportionate during cooling. Both arguments support the idea that the planar faults are an integral part of the physical processes by which the compound is formed or decomposed.

In high temperature chemical processes, part played by point imperfections tend to predominate over that played by line imperfections; and, therefore, the mechanism of diffusion is in favour of migration via point-defect. This is the basis of Wagner's theory[128] of high temperature oxidation, which proved very successful and, has since been applied to describe the high temperature oxidation of a number of metals[129]. The growth of an edge dislocation by the addition of an atom at the dislocation line generates a vacancy or removes an interstitial atoms. Dislocation arising out in this way act as a source for point defects and there is found an intimate relation between the two types of imperfections. Many of these have been discussed by Frank[130] and others[131,132]. Also, because of the differing energies of formation of anion and cation vacancies, dislocation in ionic crystal are surrounded by an excess of vacancies of one sign. High diffusion coefficients for alkali halides can be explained in this way[133]. This brief discussion underlines that the reactivity of solids is a

structure-sensitive property, that is, due to the existence, the nature and number of defects they contain.

SINTERING

Sintering is one of the most important phenomena which occur when a metal or ceramic powder is transformed into a dense, solid product or the phenomena by which useful solid products are formed from metallic or non-metallic inorganic powders, at temperature between half and three-half of the absolute melting point. It can affect both the rate of the reaction between solid substances and also the properties of the final product/s. Hence, the role played by sintering has far reaching influence in the study of the solid state reactions.

Several stages are involved in the sintering process. First, the surface roughness is destroyed, that is, surface becomes smooth. This is followed by the welding of the particles at the contact site and finally there is the socalled densification phenomenon; where much of the void volume which resulted from the initial misfit of the powder particles is eliminated. There is naturally a change in the area of entire surface of the particles and the surface of the contact between them. The former decreases while the latter increases. During sintering, there is also an increase in the numbers of non-

equilibrium grains, a decrease in the lattice defects and removal of existing stresses in the contact area of material. It is thought earlier that a liquid phase has to be present, but now it is recognised that particles that are solids at all times can be joined by sintering.

The phenomenon of sintering has interested scientists and technologists for many years and a great number of papers and reviews have been written describing the various aspects of sintering process[134-139]. The aim has been to establish the driving force of the mechanisms of matter transport, and the kinetics of the processes that lead to particle joining and porosity elimination; describing the mathematical formulation of the kinetics of the shrinkages as a function of important variables such as diffusion co-efficients, particle sizes, etc. Also, factors influencing processing times and temperatures, the structures and properties of the final product has been established.

The sintering process has been divided into three stages. The first stage, initial stage, describes the growth of necks between particles. The separate particles of the compact maintain their identity during this stage and relatively little shrinkage occurs.

Kuczynki[134,135] treated the kinetics of the growth of a neck between a sphere and a plane, and a cylinder and a plane. He considered four mechanisms of neck growth, namely, viscous flow, surface diffusion, evaporation-condensation, and volume diffusion. In dealing with the diffusion mechanism, he referred to the flow of vacancies instead of flow of atoms. The driving force for this flow was taken to be the difference between the vacancy concentration in the region just under the strongly curved neck surface and that in the rest of the system. The neck growth process is visualized as occurring because vacancies have the neck surface for interior so that they may achieve their equilibrium concentration. In doing so, they increase the neck radius, thereby decreasing stress and finally the magnitude of the equilibrium concentration. Some of the vacancies may be freed to diffuse to grain boundaries and cause shrinkage. Kingery and Berg[137] also came to similar conclusions. Johnson and Cutler[140] contended that grain boundary diffusion is a significant contributor to the initial neck growth, which was omitted by Kuczynki, Kingery etc. in their earlier treatments. Johnson and Cutler analyzed the initial shrinkage of Al_2O_3 and concluded that it is controlled by grain boundary diffusion.

The second stage is called the <u>intermediate stage</u>. In this stage, the contact grew so that the initial powder

particles lose their identity and a considerable amount of grain growth occurs. Most of the densification occurs during this stage. This stage is of most importance from the point of view of kinetics and mechanism, according to Tammann[141].

The initial development of a theory of intermediate stage sintering has been due to the work of Colbe and his co-workers[139,142]. Using a greatly simplified model to describe the vacancy flow by volume diffusion from a single pore to the boundaries of the adjacent grains, he obtained the densification equation as

$$P = P_o - (KD\gamma_s V / G^3 KT)(t-to)$$

where P is the porosity, t is the time, D is the diffusion co-efficient of the sintering rate limiting species, G is the grain size, K is a geometric factor, and subscript zero indicates the initial value. Colbe use his equation to obtain values for the diffusion of Cu in Cu and Al in Al_2O_3, and found values equal to that obtained by tracer method.

Values of diffusion co-efficient D, obtained by Colbe's equation are generally larger than those obtained with tracer. This is because he did not make allowance for grain growth. Change in grain sizes during this stage causes reductions of the number of pores. Johnson[143] has, however, proposed a technique where grain growth may be taken into account.

Nevertheless, his method does not yield an explicit relation between porosity and time and so it has never been applied.

Roscolowski and Greskovich[144] have analysed the intermediate stage sintering assuming the pores cylindrical and located on grain edges, with distribution of radii to occur. They did not place any restriction on sizes and shapes of the grains, and grain growth according to any time dependence was allowed to occur. They also assumed the pore shrinkage took place by volume diffusion. The equation thus obtained was

$$\ln (1-P) = \frac{K D \gamma_{sv} \Omega}{KT} \left[\int_{to}^{t} \frac{dt}{G_{av}^3} \right] + \ln (1-P_o)$$

The values of diffusion co-efficient obtained by this equation were found in several cases, in good agreement of the values obtained by other methods.

In the final stage of sintering the pores occur as isolated species located either on the grain corners, or totally enclosed within grains as a result of moving grain boundaries having swept by them. This stage of sintering has been studied very little. This is because the porosity is only a few percent and changes slowly. Hence the shrinkage in the last stages could only be studied by examining change in the number of pores and their size distribution with time. Since large grain growth in the final stage causes a large fraction of the

pores to end up inside the grains, the shrinkage rate is greatly reduced. Rosolowski and Greskovich[145] have examined the flow of vacancies by volume diffusion from pores in the final stage.

The experimental studies aimed at distinguishing between these stages of sintering in individual cases were performed by Kuczynki. He observed that the rate laws expected from the mechanism detailed above are as follows:

For viscous or plastic flow $\frac{x^2}{\gamma 2} = K_2 t$; for evaporation condensation $\frac{x^3}{\gamma 2} = K_2 t$, and for diffusion $\frac{x^5}{\gamma 2} = K_3 t$.

Where x is the radius of contact, and γ is the radius of sphere or cylinder undergoing sintering.

Surface area of the solid bodies in the sintering and also the thermodynamic potential of the system which is then the driving force for the sintering are decreased. A reduction in the total grain surface in a sintering process reduces the surface energy and hence complete energy of the system. It follows, therefore, that the greater is the surface energy, the greater its thermodynamic potential. This implies that the fine grain powders sinter more rapidly than the coarser one.

The sintering process is greatly influenced by the variation in the grain size composition, pores of different

sizes and shapes, and difference in the viscous flow of the crystalline and liquid bodies. Among the many aspects which are essential for sintering, the following appear to be of major significance[146].

(a) Establishment of the chemical bonds between adjoining particles.

(b) Modifications of these infinite bonds to normal lattice bonds in the contact area.

(c) Surface diffusion of atoms or ions into the vicinity of the contact area.

(d) Transfer of material into or through the contact area by surface or volume diffusion.

(e) Recrystallization, nucleation and crystal growths.

Nucleation

When we assume that in the solid state reaction, initially surface diffusion rapidly coats the surface of the reacting particles with a continuous product layer, the rate of reaction is taken to be the rate of diffusional growth of the product. However, this is not always the case, especially in phase transformations and decomposition reactions or new crystalline phase formation from a super saturated solutions. Phase transformation often appear to take place more rapidly than is expected from the reaction rate theory[147].

Although several explanations have been advanced[149], none is generally accepted[150]. Nevertheless, this abnormal behaviour i.e. abnormal rates of transformations are governed by diffusion and nucleation processes.

Nucleation is the initial process in overall steps of solid state reactions - more commonly occurring in phase transformation and decomposition reactions. The surface of solids is supposed to contain a specific number of potential nucleus-forming sites which on receipt of a critical quantity of energy become germ nuclei, which are latter transformed to active growth nuclei. Reaction is confined to the reaction-product interface with a gradual increase in size of the nuclei. Thus, the kinetics can be described in terms of a rate of nucleus formation, or of nucleation, and a rate of growth of these nuclei. The activation energy associated with this latter process is normally less than that of nucleation. This leads to the viewpoint that the nearness of product and reactant molecule enhances the decomposition, which has been actually found for few systems[151]. The surface area of the interface between the nuclei and the reactant matrix and therefore the reaction rate is thus controlled by the laws governing the formation and growth of the nuclei.

Since nucleus growth is essentially a three-dimensional phenomenon, it may be isotropic or anistropic. If the length to which a nucleus grows in a particular direction in time Δt is Δl_j, then,

$$\lim_{\Delta t \to 0} \left(\Delta l_j / \Delta t \right) = G_j \qquad (1)$$

is the rate of the nucleus growth in jth direction. Growing nuclei are characterised generally by three different growth functions G_1, G_2 and G_3 corresponding to growth along three principal crystallographic directions. For large nuclei, G_1, G_2 and G_3 are constant, in other words, they are independent of the size of the nuclei.

Nucleation may be either a single step or multi-step process. In the former case, it is assumed that a single molecular decomposition produces a stable nucleus that immediately proceeds to grow. The concept of germ nucleous i.e. one that go back to its initial stage is not possible, since the negative free energy change of the chemical transformation of reactant to product is comparatively large. In other words nucleus formation is irreversible. On the other hand, in phase transformation, which is in effect same as the solid decomposition accompanied by nucleus formation and growth[152], small nuclei will be unstable[153] and may either

reform the reactant phase or form stable growths nuclei.

If there are n_0 potential nucleus forming sites and the number of these formed in time t is n_1. If each of n_0 sites has the same a priori probability of being converted into a nucleus, then,

$$\frac{dn_1}{dt} = K_0 [n_0 - n_1]$$

$$\text{or} \quad n_1 = n_0 (1-e^{-Kot}) \qquad (2)$$

which is the law of random nucleation at a finite number of sites.

In the analysis of the single step nucleation, it is essential that the rate of growth must exceed that of nucleus formation, otherwise nucleation is not distinguished from growth. But in multi-step nucleation process such a distinction is by no means evident. This process was put forward for decomposition in which the number of nuclei present at time t was found to obey a power law, first applied by Bagdassarian[154] to the problem of photographic sensitivity.

In this model an active growth nucleus is considered to be formed by p successive molecular decompositions at a single site. The rate of change of population of nuclei is given by a set of coupled differential equation

$$\frac{dn_j}{dt} = K_{j-1} n_{j-1} - K_j n \qquad (3)$$

where n_j is the number of nuclei comprising j germ nuclei and K_j represents the rate constant for the addition of a germ nucleus to a nucleus comprising j of such nuclei.

For the limiting case $K_j t \ll 1$ for all j, a condition often in practice, the simplified form for an active growth nucleus comprising a cluster of two germ nuclei is obtained by limited expansion of the exponential terms to give

$$n_2 = K_o K_1 N_o t^2/2!$$

To generalize, Bagdassarian used the term K_g which is the rate constant of growths for the addition of a germ nucleation to the active growth nucleus containing p germ nuclei, and $K_g = K_o = K_1 - - - = K_{p-1} = K_p = K_{p+1} = \cdots$

With this approximation, the generalized form becomes

$$n_p = \left[N_o (Kot)^p / p! \right] e^{-Kot} \qquad (4)$$

when $Kot \ll 1$

then $$n_p = No\ (Kot)^p / p! \qquad (5)$$

However, the assumption that all K are equal until a growth nucleus is formed is not justified. Such a nucleus is formed at the selective site by successive addition of adjacent germ nuclei.

Allnatt and Jacobs[155] derived general solutions for two cases (i) all K_j different and (ii) K_j different upto $j = p-1$ and all equal to K_g for $j \geqslant p$.

The solutions are in general, in the limit of small value of t,

$$n_p = K_p t^p \qquad (6)$$

As soon as the active growth nuclei containing p germ nuclei are formed no further assumption about K_j are required, since K_j is then determined by the characteristics of the growth process.

Since nucleation is the initial process in all solid state reactions the energy parameters associated with the initial act of nucleation are those relevant to the overall chemical reaction modified by the crystal environments. In other words in a gas reaction, we may confine to the energy changes resulting from bringing the reactants sufficiently close together to favour the formation of an activated complex. In solid reaction, there is,in addition, a strong interaction between the reactants, the product lattices and at the interface between the old and new structures. Hence, it is necessary to know the morphology of crystal in order to understand the main factors contributing to the act of nucleation.

Solid state transformations are usually nucleated preferentially at such sites as external or internal impurities or point defect clusters[156]. Nucleation over such preferred sites is called heterogeneous nucleation. Nucleation that takes place uniformally throughout the parent phase is called homogeneous nucleation.

The basis for a molecular kinetic treatment was given by Kossel and Stranski[157], who considered the deposition of single molecules in the formation of a new crystal and by Volmer[158] who derived the equation for the rate of growth of the nucleus. Basing his postulates on Gibb's concept[159], he assumed that nucleation was also necessary for the addition of each new lattice plane. The formation of these two-dimensional nuclei determines the rate of growth. The introduction of separation[160] led to a link between thermodynamic and statistical methods of treatment. Volmer-Stranski Becker-Doring has proposed the theory of homogeneous nucleation to the problem of nucleation of a new crystalline phase, II, in the interior of an unstable crystalline phase, I. Successive clustering of kinetic units occur to form embyros. There is a critical size of cluster, the critical nucleus, which is in metastable equilibrium with the unstable phase. After creating the instability, the size distribution of embyros may become steady, and then there will be stable flow through the critical size. This is called the

rate of nucleation, J_o per unit volume, and is given by

$$J_o = n_1 g_K \exp\ (-\ \Delta G_K/KT) \qquad (7)$$

Where n_1 is the number of kinetic units for unit volume of phase, I, g_K is the rate of kinetic units transformation onto to the ctirical nucleus of size K and ΔG_K is the free energy of formation of a critical nucleus.

It is assumed in general that when a nucleus of critical size has been produced, it will grow.

There are two main concepts about the mechanism of progression of the reactant/product interface through solid. In the interfacial mechanism, reaction proceeds by successive decomposition of reactant molecules and does not involve the mobility of any species in the reactant matrix. In the diffusion controlled mechanism the species that finally form the product are assumed to be mobile and diffuse to and react with reactant/product interface.

The theory of nucleation at dislocation site has been given by Cahn[161] and calculations of rate of heterogeneous nucleation, when there is a distribution of catalysing sites have been performed successfully for various types of transformations[162,163]. From the above theory, it has been postulated that the diffused product in the dislocation net work will create adjacent nuclei, i.e. increase the rate of nucleation[164].

As a result the boundary between the reactant and product becomes a rather diffuse zone, having reaction almost complete on the product side and just starting on the reactant side. The rate of advance of this zone depends on the rate of nucleation. It is therefore obvious that nucleation and growths are complimentary and take place almost simultaneously. At high temperature, growths is rapid, which automatically lowers the nucleation rate, whereas at low temperature, the nucleation rate is comparatively fast which is the cause of the yields of fine grains at low temperature[165].

Kinetic equations of Nucleation Formation and Growth - Avarami and Erofeev equations

The extent of decomposition or phase transformation as a function of time can be calculated by combination of the rate of nucleus formation and that of growth. We define the fractional decomposition as $\alpha' = V(t)/V_f$

Where V(t) is the total volume of product i.e. of all growth nuclei present at time t. The rate constants for linear growth for the three crystallographic directions are devoted by $G_1(x)$, $G_2(y)$ and $G_3(z)$ and may vary with extent of decomposition or transformation. Consequently, the extended fractional decomposition is given by

$$\alpha' = \left(\frac{\sigma}{V_f}\right) \int_0^t \int_\tau^t G_1(x)dx \int_\tau^t G_2(y)dy \int_\tau^t G_3(z)dz \left[\frac{dn}{dt}\right]_{t-\tau} d\tau \quad ..$$

Where $\frac{dn}{dt}$ is the rate of nucleus formation at $t = \tau$, and σ is a shape factor (e.g. $\frac{4\pi}{3}$ for spherical nucleus). For constant growths rates, this reduce to

$$\alpha' = \left(\frac{\sigma}{V_f}\right) \int_0^t G_1 G_2 G_3 \, (t-\tau)^3 \left[\frac{dn}{dt}\right]_{t-\tau} d\tau \qquad (7)$$

for $Kot \ll 1$ for a single-step nucleation, from equation (2)

$$n = K_o n_o t$$

where Ko is the rate constant for the nucleation function, then eqn.(7) becomes

$$\alpha' = \left(\frac{\sigma}{V_f}\right) G_1 G_2 G_3 \, K_o n_o t^4$$

or for isotropic growth $G_1 = G_2 = G_3 = G$

$$\therefore \alpha' = \left(\frac{\sigma}{V_f}\right) G^3 K_o n_o t^4 \qquad (8)$$

For multi-step nucleation with $K_p t \ll 1$, eqn (5) holds, Therefore, $n_p = K_p N_o t^p$ where $K_p = \frac{K_o^p}{p!}$ and therefore eqn.(7) becomes

$$\alpha' = \left(\frac{\sigma}{V_f}\right) \int_o^t G_1 G_2 G_3 \, (t-\tau)^3 K_o n_o \, e^{-K_1 \tau} \, d\tau$$

$$= \frac{6\sigma G_1 G_2 G_3 n_o}{(V_f) \quad K_o^3} \left[e^{-K_o t} - 1 + K_o t - \frac{(K_o t)^2}{2!} + \frac{(K_o t)^3}{3!} \right] \qquad (9)$$

However, with increasing extent of decomposition

Some of the n_o potential sites are destroyed by incorporation in the growth of other nuclei in near-neighbour range[166]. Similarly, growth of nearby nuclei results in their impingement on each other and the formation of a smaller number of combined nuclei which then form the subsequent growth unit. The fractional decomposition or transformation, α', that would have occurred in absence of destruction of potential nucleation sites and formation of combined nuclei is therefore greater than the measured fractional decomposition, α, that has actually occurred. It is assumed that both nucleation and growths are random i.e. all topochemically equivalent segments of reactant have the same probability of decomposition in given time increment dt,

$$d\alpha = d\alpha'(1-\alpha) \qquad (10)$$

which satisfies the following conditions:

$d\alpha'/dt = d\alpha/dt$ at $\alpha = 0$, $d\alpha/dt = 0$

$d\alpha'/dt$ is finite and nonzero at $\alpha = 0$

Equation (10) on integration yields

$$-\ln(1-\alpha) = \alpha' \qquad (11)$$

Since $\alpha = \alpha' = 0$ at $t = 0$, hence by equation (9), the following equation is obtained:

$$-\ln(1-\alpha) = (6\sigma/V_f)(G^3/K_o^3)\left[e^{-K_o t} - 1 + K_o t - \frac{(K_o t)^3}{2!} + \frac{(K_o t)^3}{3!}\right] \qquad (12)$$

This is the Avrami equation[166] for isotropic nucleation.

For $K_o t \gg 1$

$$- \ln (1-\alpha) = (Gt)^n \times \text{const.} \qquad (13)$$

with K, the rate constant, given by

$$K^n = 6 \sigma G_1 G_2 G_3 K_p N_o / (p+1)(p+2)(p+3) V_f$$

For $K_o t \ll 1$

$$-\ln (1-\alpha) = \text{const.} \times G^3 K_o t^4 \approx \alpha \quad \text{for} \quad \alpha \ll 1 \qquad (14)$$

Corresponding to three dimensional growth of a constant number n_o of nuclei. Both these limiting cases given by (13) and (14) give the general Erofeev equation[167]

$$-\ln (1-\alpha) = (Kt)^n \qquad (15)$$

Evidently the Erofeev equations are the limiting cases of the Avrami equation.

Reaction Mechanism:

To gain an insight in the solid state reactions, Huttig[165] investigated reactions with mixtures of metals with the rise in temperature. He concluded and generalized the following sequence of changes.

(i) Coating of the surface

(ii) Activation and formation of surface molecular films.

(iii) Deactivation of the surface molecular films.

(iv) Activation occurs followed by volume diffusion

(v) Formation of a crystalline reaction product, and

(vi) Defect correction in the lattice of the product formed.

However, the studies carried on latter, revealed that in a mixture of solid the physiochemical changes taking place both under gradual heating like Huttig's researches and at constant high temperature, are not much different. It is generally agreed that it may proceed in the following various stages.

(a) The development of defects and breaking of the crystal lattice.

(b) Reconstruction of the lattices due to polymerphic process.

(c) Formation and decomposition of solid solutions.

(d) Diffusion phenomenon takes place.

(e) Sintering and recrystallization may occur.

(f) Fusion solution of the system component in the melt.

(g) Liquid phase crystallization.

(h) Sublimation.

(i) Dissociation and

(j) The chemical reaction proper.

The processes outlined as (e) and (j) are essential steps in every reaction of solid, while others may or may not take place at all.

Systematic studies of the reactions in solid mixtures started as far as 50 years back by Hedvall[169] and Tammann[170]. They arrived at a series of fundamental conclusion on the mechanism of reactions in crystalline mixtures on the basis of their studies. Wagner, Huttig[168], Jander, and many other researchers supplemented and developed the Tammann-Hedvall theory.

In 1930, Wagner and Schottky[171] proposed a thermodynamic theory of solids which takes into account imperfection and impurities. They suggested that there are two fundamental processes involved in a solid state reaction.

(1) Phase boundary processes such as chemical reaction itself, formation of nuclei and growths of the reaction product.

(2) Transport of matter to the reaction zone, i.e., diffusion through the layer of the reaction products. They developed the well known parabolic rate law assuming a unidirectional diffusion accross the product layer, which is given as,

$$\frac{dy}{dt} = D \frac{k}{y}$$

Where y is the thickness of product layer, t is the reaction time, D is the diffusion co-efficient of the migrating species and K is the proportionality constant. Assuming

diffusion co-efficient to be independent of time and area of contact as constant, we get;

$$Y^2 = 2K\,Dt + C$$

or when $t = 0$, $Y = 0$

$$Y^2 = 2KDt = K_p t \qquad (1)$$

Where K_p is the parabolic rate constant. It has been assumed and showed latter that initial stage of the solid state reaction in a number of reactions follows the parabolic rate law.

Using oversimplying assumptions, Jander[172] arrived at an expression for the reaction rate of powders, which has been widely used, although its physical basis is unreal. Jander's model is based on the following assumptions:

1. The reaction under consideration can be classified as an additive reaction.
2. Nucleation, followed by surface diffusion, occurs at a temperature below that needed for bulk diffusion, so that a coherent product layer is present when bulk diffusion does occur.
3. The chemical reaction at the phase boundary is considerably faster than the transport process and thus the solid state reaction is bulk-diffusion controlled.

4. Bulk diffusion is unidirectional.
5. The product is not miscible with any of the reactants.
6. The reacting particles are all spheres of uniform radii.
7. The ratio of the volume of the product layer to the volume of the material reacted is unity.
8. The increase in the thickness of the product layer follows the parabolic rate law.
9. The diffusion co-efficient of the species being transported is not a function of time.
10. The activity of the reactants remains constant on both sides of the reaction interface.

Let V denote the volume of material still unreacted at time t; then

$$V = \frac{4\pi}{3} (r - y)^3 \qquad (2)$$

Where r is the initial radius of the reacting particles. Letting x be the fraction reaction completed at time t, the volume of the material unreacted is also given by

$$V = \frac{4\pi}{3} r^3(1-x) \qquad (3)$$

Equation (2) and (3) can be equated to yield,

$$y = r\left[1-(1-x)^{1/3}\right] \qquad (4)$$

Combining equation (4) with equation (1) and rearranging yields

$$K_J t = \frac{2KDt}{r^2} \left[1-(1-x)^{1/3}\right]^2 \qquad (5)$$

Equation (5) is the well-known Jander equation relating the fraction of reaction completed to time, where K_J is the rate constant.

If the Jander model applies to the system being studied, the rate constant should not drift as the reaction proceeds. If the rate constant does drift, another model must be sought. The Jander equation has been applied to many systems, but practical evidence does not satisfy it well. This is because of the fact that Jander's assumptions that spherical symmetry of the diffusion does not conform to a parabolic rate of growth of the reaction layer thickness, and the molar volumes of reactant and reaction product are the same.

Kroger and Ziegler[173,174] indicated that Jander's assumption of a constant diffusion co-efficient was not applicable to all solid systems, particularly during the early stage of a reaction. They used Jander's geometry i.e. Jander's assumption 1-7, except that of the diffusion co-efficient, and assumed that the diffusion co-efficient of the transported species was inversely proportional to time. This is equivalent to assuming that rate of change of product thickness is inversely proportional to time, which is the basis of Tammann theory. The Kroger-Ziegler equation is

$$K_{kx} \ln t = (2K/r^2) \ln t = \left[1-(1-x)^{1/3}\right]^2 \qquad (6)$$

Zhurarlev, Lesokhin, Tempelman[175] modified the Jander relation by assuming the activity of the reacting substance proportional to the formation of unreacted material (1-x). Their relationship between fraction of reaction completed and time is

$$K_{Z-T}t = \left[\left(\frac{1}{1-x}\right)^{1/3} - 1\right]^2 \qquad (7)$$

Ginstling and Brounshtein[176] arrived at a model using Jander's assumptions with the exception of the parabolic rate law. They indicated that the parabolic rate law asserted that the reaction surface area remained constant; however, when they considered spherical particles this surface actually decreased in area as the reaction proceeded. They discarded the parabolic rate law in favour of an equation relating the growth of the product layer to Barrer's[177] growth of the product layer equation for steady state heat transfer through a spherical shell. They arrived at the final form,

$$K_{G-B}t = \frac{2KDt}{r^2} = 1 - \frac{2}{3}x - (1-x)^{2/3} \qquad (8)$$

Carter[178,179] further improved the Ginstling-Brounshtein model by accounting for the difference in the volume of the product layer with respect to that of volume of the reactants. He also introduced a new term, Z, to account for the change

in volume, where Z represents the volume of the reaction product formed per unit volume of the reactant consumed. Carter's equation as obtained is,

$$K_{C-V}t = \frac{Z-(Z-1)(1-x)^{2/3}-\left[1+(Z-1)x\right]^{2/3}}{(Z-1)} \qquad (9)$$

Valensi[180] developed the same solid state reaction model mathematically from a different starting point. Hence, this equation is referred to as Carter-Valensi equation.

Dunwald and Wagner[181] derived an equation for solid state reaction analysis using a solution to Fick's second law of diffusion into or out of a sphere. Serin and Ellickson[182] expressed the Dunwald and Wagner equation in terms of the fractional completion of the process;

$$K_{DW}t = \frac{\pi^2 Dt}{r^2} = \ln\left[\frac{6}{\pi^2(1-x)}\right] \qquad (10)$$

All the models discussed here have drawback that they are based on the reaction of spherical particles of uniform radius. They described many solid state reactions in a satisfactory way[183]. There have been attempts to introduce particle size gradation into a workable model. These have been resulted in models which involve complicated mathematics and contain parameters that are difficult to measure. Such

models have been advanced by Miyagi[184], Sasaki[185] and Gallagher[186].

When the reaction starts only at rhe contact zones between particles and the reaction proceeds by diffusion through the contact zones, Jander's assumption that the surface of one component is obviously not valid. To account for the effect of the number of contact points, Komatsu[187] introduced into the Jander's equation, the mixing ratio of the two components, the ratio of the radius of the two compcnents, and a parameter which describe the packing state of the powders.

The models of the solid state reactions thus far discussed have been based on the assumption that initially surface diffusion coats rapidly the surface of the reacting particles with a continuous product layer, the subsequent rate of diffusion is taken to be the rate of diffusional growths of the product layer. However, when diffusion through the product layer is so fast that the reactants can not combine as rapidly at the reaction interface as to establish equilibrium the solid state reaction is phase-boundary controlled, and the product layer is discontinuous when the molar volume of the product phase is considerably different from that of the reactant upon which it is growing. According to Laidler[188], in such cases the rate determining step may be the chemical

process occurring at the phase boundary.

Equations relating x and t have been derived for simple geometrical system with the following assumptions:

(i) the reaction rate is phase boundary controlled,

(ii) the reaction rate is proportional to the surface area of the fraction of unreacted material, and

(iii) the nucleation step occurs virtually instantaneously so that the surface of each particle is covered with a layer of product.

The models developed on the basis of above boundary conditions are called as phase boundary kinetic models. For a sphere reacting from the surface inward[188] the relation between x and t is

$$K_{PB}t = 1-(1-x)^{1/3} \qquad (11)$$

and for a circular disk reacting from the edge inward or for a cylinder[189]

$$K_{PB}t = 1-(1-x)^{1/2} \qquad (12)$$

Equation similar to classical rate equations have often been applied to solid state reactions. The integrated form of the general kinetic equation based on the concept of an order of reaction is

$$Kt = \frac{1}{n-1}\left[\frac{1}{(1-x)^{n-1}} - 1\right] \qquad (13)$$

Where n is the customary order of the reaction.

When $n = \frac{2}{3}$, equation (13) is identical with equation (11), and when $n = 1/2$, it is identical with that of equation (12).

REFERENCES

1. Hedvall, J.A.: J. Chem. Educ. 30, 638 (1953).

2. Hedvall, J.A.: Reactions fahigkeit, fester Stoffe (Edwards Brothers Inc, Michigan), 67 (1963).

3. Hedvall, J.A.: Einführung in die Festkörperchemie, Branuschweig, (1943).

4. Cohn, G.: Chem. Rev. 42, 527 (1948).

5. Wagner, C. and Schottky, W.: Z. Physik Chem. B11, 163(1930).

6. Stringer, R.K., Warble, C.E. and Williams, L.S.: Material Science Research, Vol. 4 (Plenum Press, New York) Chapt. 4, Eds. Gray, T.J. and Frechette, V.D. (1969).

7. Blakely, J.M. and Che-Yu Li: Acta Met. 14, 279 (1966).

8. Oriani, R.A.: Acta Met. 14, 84 (1966).

9. Schmalzried, H.: Festkörperreaktionen (Verlag-Chemie, Weinheim), (1971).

10. Wagner, C.: Progress in Solid State Chemistry, eds. Reiss, H. and McCaldin, J.O. Vol. 7, pp. 1 (Pergamon, Oxford), 1972.

11. Wagner, C.: Ber. Bunsenges.: Physik. Chem. 65, 581 (1961).

12. Lifshilz, I.M. and Slezov, V.V.: Soviet Phys. - JETP, 35, 331 (1959).

13. Hüttig, G.: Z. angew. Chem. 49, 882 (1936).

14. Warburg, E.: Wiedemann. Ann. Physik. 21, 622 (1884); Tubandt, C. and Lorenz, P.: Z. Physik. Chem. 87, 543 (1914); Tubandt, C. and Reinhold, H.: Z. Elektrochem. 29, 313 (1923).

15. Steele, B.C.H.: in Progress in Solid State Chemistry, ed. Reiss, H. (Pergamon Press, Oxford), 1972; Rapp, R.A. and Shores, D.A.: Physicochemical Measurements in Metal Research, ed. Rapp, R.A. pp. 123-192 (Wiley, New York, London), 1970; Foley, R.T.: J. Electrochem. Soc. 116, 13c (1969).

16. Faraday, M. and Stodart, J.: Quart. J. Sci, 9, 319 (1820).

17. Hedvall, J.A.: Z. anorg. Chem. 93, 313 (1915).

18. Hedvall, J.A. and Henberger, J.: Z. anorg. allg. Chem. 122, 181 (1922); 135, 49 (1924).

19. Hedvall, J.A.: ibid, 128, 1 (1923).

20. Tammann, G.: ibid, 149, 21 (1925).

21. Wagner, C.: Z. Physik. Chem. 34, 309 (1936).

22. Wagner, C.: Z. anorg. allg. Chem. 236, 320 (1938).

23. Wagner, C.: Trans. Farad. Soc. 34, 851 (1938).

24. Jander, W.: Z. anorg. allg. Chem. 168, 113 (1927).

25. Jander, W.: ibid, 190, 654 397 (1930); 191, 171 (1930); 192, 286 (1930).

26. Jander, W.: ibid, 231, 345 (1937).

27. Bernal, J.D.: Trans. Farad. Soc. 34, 834 (1938).

28. DeBoer, J.H.: Discuss. Farad. Soc. 23, 171 (1957).

29. Hulbert, S.F.: J. Brit. Ceram. Soc. 6, 11 (1969).

30. Tompkins, F.C.: Pure and Applied Chem. 9, 387 (1964).

31. Jander, W.: Z. anorg. Chem. 41, 73 (1928).

32. Muller, M.: Chem. Fabrik, 32, 333 (1933).

33. Jost, W.: Diffusion und Chem. Reaction infesten Stoffen (Dresden), 47 & 60 (1937).

34. Reginskii, S.Z.: Zhur. Fiz. Khim. 12, 427 (1938).

35. Christian, J.W.: The Theory of Transformations in Metals and Alloys (Pergamon Press, Oxford), 1965.

36. Lotgering, F.K.: J. Inorg. Nucl. Chem. 9, 113 (1959).

37. Bernal, J.D.: Dasgupta, D.R. and Mackay, A.L.: Clay Minerals Bulletin, 4, 15 (1959).

38. Mackay, A.L.: Min. Mag. 32, 545 (1960).

39. Bernal, J.D. and Mackay, A.L.: Tschermakds Mineral. Petrog. 10, 331 (1965).

40. Ubbelhode, A.R.: Quart. Rev. Chem. Soc. 11, 246 (1957).

41. Brindley, G.W. and Hyani, R.: Phil. Mag. 12, 505 (1965).

42. Shmalzried, H.: in Progress in Solid State Chemistry, II, (Pergamon Press, Oxford), 1965.

43. Moore, W.J.: A. Rev. Phys. Chem. 10, 409 (1959).

44. Rastogi, R.P.: J. Sci. Indust. Res. 29(4), 177 (1970).

45. Hedvall, J.A.: Solid State Chemistry - Whence, where and Whither (Elsevier Publishers, Inc. London), 1967.

46. Garner, W.E.: Chemistry of the Solid State (Butterworths Scientific Publication, London), 1955.

47. Morawetz, H.: Physics and Chemistry of the Organic Solid State, Vol. I, edited by D. Fox, M.M. Labes and A. Weissenberger (Interscience Publishers Inc., London), 1963.

48. Bowden, F.P. and Yoffe, A.D.: Fast Reactions in Solids (Academic Press, Inc.), 1958, New York, London.

49. Childs, P.E. and Wagner, J.B.: Heterogeneous Kinetics at Elevated Temperatures (Plenum Press, New York), 1970.

50. Kuczynki, G.C., et al. eds.: Sintering and Related Phenomena (Gordon and Breach, New York), 1969.

51. Gray, T.J. and Frechette, V.D. eds.: Kinetics of Reaction in Ionic System (Plenum Press, New York) Mat. Sci. Res. Vol. IV, 1969.

52. Roberts, L.E.J., editor: Solid State Chemistry: Inorganic Chemistry Series, Vol. 10, MTP (Butterworths, London), 1972.

53. DeBoer, J.H. et al. editors: Reactivity of Solids(4th Symposium)(Elsevier, Amsterdam), 1967.

54. Schwab, G.M. editor: Reactivity of solids (5th Symposium, Elsevier, Amsterdam), 1965.

55. Mitchell, J.W. et al. editors: Reactivity of solids (6th Symposium, Wiley & Sons, New York), 1969.

56. Jost, W.: Diffusion in solids, liquid and gases (Academic Press, Inc., New York), 1952.

57. Kroger, F.A.: The Chemistry of Imperfect crystals (North-Holland, Amsterdam), 1964.

58. Schmalzried, H.: Festkorperreaktionen (Verlag. Chemie, Weinheim), 1971.

59. Barrer, R.M.: Diffusion in and through solids (University Press, Cambridge), 1941.

60. Moore, W.J.: J. Chem. Educ. 38, 232 (1961).

61. Wever, H.: Naturwissenschoften, 50, 55 (1962).

62. Peterson, N.L.: Solid state phys. 22, 409 (1968).

63. Süptitz, P. and Teltow, J.: Phys. Status Solidi 23, 9 (1967).

64. Drago, A.L.: J. Res. Nat. Bur. Stand., A, 72, 157 (1968).

65. Harrop, P.J.: J. Mater. Sci. 3, 206 (1968).

66. Balarew, D. and Tammann, G.: Z. anorg. allg. Chem. 160, 92 (1927).

67. Ginstling, A.M.: Zhur. Prikl. Khim. Leningr. 24, 567 (1951).

68. Ginstling, A.M. and Fradkina, T.R.: J. Appl. Chem. USSR, 25, 1199; 1325 (1952).

69. Groh, J. and Hevesy, G.: Ann. d. Phys. 63, 85(1920); 65, 216 (1921).

70. Joffe, A.F.: Ann. d. Phys. 72, 261 (1923).

71. Frenkel, Y.I.: Ztschr. Phys. 35, 652 (1926).

72. Shewmon, P.G.: Diffusion in Solids (McGraw Hill Book Co., New York), 1963.

73. Manning, J.R.: Diffusion Kinetics in Crystals (Van Nostrand, Holland), 1968.

74. Zenner, C.: Acta Crystallogr. 3, 346 (1950).

75. Koch, E. and Wagner, C.: Z. Phys. Chem. B38, 295 (1937).

76. Frank, F.C.: Phil. Mag. 42, 573 (1953).

77. Manning, J.R.: Can. J. Phys. 46, 2633 (1968).

78. Leclaire, A.L.: Brit. J. Appl. Phys. 14, 351 (1963).

79. Balluffi, R.W.: Phys. Stat. Sol. 42, 11 (1970).

80. Gleiter, H. and Chalmers, B.: Progress in Material Sci., Vol. 16 (Pergamon Press, London), Chapter IV (1972).

81. Rothman, S.J. et al.: Phys. Status. Solidi 39, 635 (1970).

82. Graham, L.: J. appl. Phys. 42, 2386 (1969).

83. Nowick, A.S. and Dienes, G.J.: Phys. Stat. Solid. 24, 461 (1967).

84. Bakker, H.: ibid, 28, 569 (1968).

85. Mundy, J.N.: Phys. Rev. 133, 2431 (1971).

86. Peterson, N.: Solid Stat. Phys. 22, 409 (1968).

87. Aaronson, H.I. editor: Diffusion American Society of Metals Ohio (1974).

88. Barr, L.W. et al.: Phil. Mag. 14, 299 (1966); Mundy, J.N. and Smith, F.A.: Phil. Mag. 20, 389 (1969).

89. Barr, L.W. and Smith, F.A.: ibid. 20, 293 (1969).

90. Anthony, T.R.: Acta Met. 18, 877 (1970).

91. Drago, A.L.: J. Res. Nat. Bur. Stand, A.: 72, 157 (1958).

92. Matske, H.: J. Nat. Sci. 5, 831 (1969).

93. Volpe, M.L. and Reddy, J.: J. Chem. Phys. 53, 1117 (1970).

94. Price, J.B. and Wagner, J.B.: J. Electrochem. Soc. 117, 242 (1970).

95. Matzke, H.: J. Mat. Sci., 5, 831 (1970).

96. Belle, J.: J. Nucl. Mater. 30, 3 (1969).

97. O'Keeffe, M.: Sintering and Related Phenomena, eds. Kuczynki, G.C. et al.(Gorden Breach, New York), pp. 57 (1959).

98. Chen, W.K. and Jackson, R.A.: J. Phys. Chem. Solid, 30, 1309 (19 69).

99. LeClaire, A.D.: Diffusion in Treatise on Solid State Chemistry, Vol. 4, ed. N.B. Hannay (Plenum Press, New York) Chapter one (1976).

100. Wagner, C.: Acta Met. 17, 99 (1969).

101. O'Keeffe, M.: The Chemistry of Extended Defects in Non-metallic Solids (North-Holand, Amsterdam), eds. Eyring, L. and O'Keeffe, M.), pp. 609, (1970).

102. Cooper, A.R.: In Mass Transport in Oxides, NBS Special Publications (Washington, D.C., U.S. Govt. Printing Press)m pp. 79, (1968).

103. Kirkaldy, J.S.: Adv. Mat. Res. 4, 55 (1970).

104. Frenkel, Y.I.: Ztscher. Phys. 35, 652 (1926).

105. Schottky, W.: Z. Physik Chemie, B29, 335 (1935).

106. Taylor, G.I.: Proc. Roy Soc. London, 145, 362 (1934).

107. Orwan, E.: Z. Physik. 89, 634 (1934).

108. Harustra, T.: J. Phys. Chem. Solids, 15, 311 (1960).

109. Kroger, F.A., Stieltjes, F. and Vink, H.J.: Philips Res. Repts. 14, 557 (1959).

110. Brouwer, G.: ibid, 9, 366 (1954).

111. Rogalla, H. and Schmalzried, H.: Ber. Bunsenges. Phys. Chem. 72, 12 (1968).

112. Peuming, P.: Philips Res. Repts. 14, 337 (1959).

113. Schols, A.: Z. Physik, 161, 267 (1961).

114. Stasiw, O. and Teltow, J.: Abh. Dtsch. Akad. Wiss., Kl. Math. Phys. Techn. 7, 295 (1960).

115. Damask, A.C. and Dienes, G.J.: Point Defects in Metals (Gordon and Breach, New York), 1963.

116. Dugdale, R.A.: Phil. Mag. 1, 537 (1956).

117. Benci, S.; Gasparrini G. and Germagnoli, E.: Nuovo Cemento, 31, 1165 (1964).

118. Panseri, C. and Federigh, T.: Acta Met. 8, 217 (1960).

119. Hagg, G.: Zeit. Krist. 91, 114 (1935).

120. Braner, G.: Z. anorg. allg. Chem. 248, 1 (1964).

121. Wadsley, A.D.: Non-Stoichiometric compounds, Mandelcoru, L. (Academic Press), pp. 98-209 (1964).

122. Jellinek, F.: Acta Cryst. 10, 620 (1957).

123. Hyde, B.G.; Bevan, D.J.M. and Eyring, L.: Phil. Trans. Roy. Soc. A259, 583 (1966).

124. Hägg, G.: Z. Phys. Chem. (Leipzig), B29, 192 (1935).

125. Bevan, D.J.M., Cameron, R.S. and others: Inorg. Nucl. Chem. Lett. 4, 241 (1968).

126. Grønvold, F.; Kjekshus, A. and Raaum, R.: Acta Cryst. 14, 930 (1961).

127. Wadsley, A.D.: Helv. Chim. Acta. Fasc. extraord. Alfred Werner, p. 207 (1967).

128. Wagner, C. and Grunwald, K.: Z. Phys. Chem. B40, 455 (1938).

129. Hauffe, K.: Reaktionen in und, an fester Stoffen (Springer-Verlag, Berlin), Chapter 10, (1955).

130. Frank, F.C.: Discuss. Farad. Soc. 23, 122 (1957).

131. Dekeyser, W.: Proc. Fourth International Reactivity of Solids Eds. DeBoer, J.D. (Elsevier, Amsterdam), pp. 390 (1960).

132. Mitchell, J.W.: Repts. Prog. in Phys. 20, 433 (1957).

133. Barr, L.W. and others: Trans. Farad. Soc. 56, 697 (1960).

134. Kuczynki, G.C.: Trans. Ann. Inst. Min. Met. Eng. 185, 169 (1949).

135. Kuczynki, G.C.: J. Appl. Phys. 21, 632 (1950).

136. Kuczynki, G.C. et al. (editors), Sintering and Related Phenomena (Gordon and Breach, New York), 1967.

137. Kingery, W.D. and Berg. M.: J. Appl. Phys. 26, 1205 (1955).

138. Thummler, F. and Thomma, W.: Metals and Materials, Volume One, pp. 69-108 (1967).

139. Colbe, R.L.: J. Appl. Phys. 32, 787 (1961).

140. Johnson, L.L. and Cutler, I.B.: J. Am. Ceram. Soc. 46, 541 (1963).

141. Tammann, G.: Z. anorg. Chem. 157, 321 (1926).

142. Colbe, R.L. and Gupta, T.K.: See ref. 136, pp. 423-444.

143. Johnson, D.L.: J. Am. Ceram. Soc. 53, 574 (1970).

144. Rosolowksi, J.H. and Greskovich, C.: J. Am. Ceram. Soc. 58, 177 (1975).

145. Rosolowksi, J.H. and Greskovich, C.: J. Appl. Phys. 44, 1441 (1973).

146. Gray, T.J.: The Defect Solid State (Interscience, New York) pp. 93 (1957).

147. Bradley, R.S.: J. Phys. Chem. 60, 1347 (1956).

148. Mott, N.F.: Proc. Phys. Soc. London, 60, 391 (1948).

149. Garner, W.A.: Diss. Farad. Soc. 5, 194 (1949).

150. Burke, D.C. and Turnbull, J.H.: "Progress in Metal Physics", Chap. 7, Volume, 3 (1952).

151. Reginskii, S. and Schultz, F.: Z. Phys. Chem. A138, 21 (1928).

152. Burger, W.G. and Green, L.J.: Diss. Farad. Soc. 23, 183 (1957).

153. Hollomon, J.H. and Turnbull, D.: "Progress in Metal Physics", pp. 333, Volume 4 (1953).

154. Ch. Bagdassarian: Acta Physicochim URSS, 20, 441 (1945).

155. Allnatt, A.R. and Jacobs, P.W.M.: Can. J. Chem. 46, 111 (1968).

156. See ref. No. 155.

157. Stranski, I.N. et al.: Z. Physik. Chem. 136, 259 (1928).

158. Volmer, M. and Weber, A.: Z. Physik Chem. 119, 227 (1926).

159. Gibbs, J.W.: Trans. Connecticut Acad. 3, (1875-1878).

160. Volmer, M.: Kinetik der Phasenbildung, Steikopf, Dresden and Leipzig (1939); Becker, R. and Döring, W.: Ann. Physik, 24, 719 (1935).

161. Cahn, W.: Acta Met. 5, 169 (1957).

162. Turnbull, D. and Fischer, J.C.: J. Chem. Phys. 17, 7 (1949).

163. Cohen, M.: Trans. AIME, 212, 171 (1958).

164. Cech, R.E. and Turnbull, D.: Trans. AIME, 206, 124 (1956).

165. Hill, R.A.W.: Trans. Farad. Soc. 53, 1136 (1957); 54, 685 (1958).

166. Avrami, M.: J. Chem. Phys. 7, 1103 (1939); 8, 212 (1940); 9, 177 (1941).

167. Erofeev, B.V.: Compt. rend. Acad. Sci., URSS, 52, 5111 (1946).

168. Hüttig, G.: Z. angew. Chem. 49, 882 (1936).

169. Hedvall, J.A.: Z. anorg. Chem. 162, 110 (1927).

170. Tammann, G.: ibid, 135, 77 (1924).

171. Schottky, W.: Z. Electrochem. Angew Chem. 45, 33 (1939).

172. Jander, W.: Z. anorg. allg. Chem. 163, 1-30 (1927).

173. Kroger, C. and Ziegler, G.: Glastech. Ber. 26, 346-53(1953).

174. Kroger, C. and Ziegler, G.: Glastech. Ber. 27, 199-212(1954).

175. Zhuravlev, V.F. Lesokhin, I.G. and Tempel'man, R.G.: J. Appl. Chem. USSR, 21, 887 (1948).

176. Ginstling, A.M. and Brounshtein, B.I.: J. Appl. Chem. USSR, 23, 1327 (1950).

177. Barrer, R.M.: Phil. Mag. 35, 802 (1944).

178. Carter, R.E.: J. Chem. Physics, 34, 2010 (1961).

179. Carter, R.E.: ibid, 35, 1137 (1961).

180. Valensi, G.: Compt. rend. 202, 309 (1936).

181. Dunwald, H. and Wagner, C.: Z. Physik. Chem. (Leipzig), B24, 53 (1934).

182. Serin, B. and Ellickson, R.T.: J. Chem. Phys. 9, 742 (1941).

183. Giess, E.A.: J. Am. Ceram. Soc. 46, 374 (1963).

184. Miyagi, S.: J. Japan. Ceram. Soc. 59, 132 (1951).

185. Sasaki, H.: J. Am. Ceram. Soc. 47, 512 (1964).

186. Gallagher, K.J.: Proceed of Reactivity of Solids, ed. Schwab, G.M. (Elsevier, New York), 1965, pp. 192.

187. Komatsu, W.: ibid, pp. 182-191.

188. Laidler, K.J.: Chemical Kinetics, McGraw Hill, New York, 1965, pp. 316.

189. Sharp, J.H., Brindley, G.W. and Narahavi Achar, B.N.: J. Am. Ceram. Soc. 49, 379 (1966).

C H A P T E R - II

CHEMISTRY OF COPPER (I) AND MERCURY (II) HALIDES

Among the first row transition elements, only copper in its first valence state shows the typical class behaviour, characterised by the halide affinity sequence $F^- \ll Cl^- < Br^- < I^-$ in aqueous solution.[1] The complex formation of an acceptor in such a unique position is of special interest. Their complex formation has indeed been studied since the beginning of the century[2]. With the possible exception of copper (I) fluoride, all the monohalides of copper are known.

It has been shown that copper (I) fluoride is thermodynamically unstable[3], and Wartenberg[4] has suggested that CuF_2 dissociates at higher temperatures into copper (I) fluoride and fluorine gas. Therefore, it might be possible to prepare copper (I) fluoride as a metastable entities at low temperatures in the absence of catalysts such as moisture or hydrogen fluoride. CuF is white, having rutile crystal structure[5]. Cuprous chloride is white and crystals cubic. Wyckoff and Posnjak[6] found that X-radiograms correspond with the double centred cubic lattice of zinc blende. Similar structures have been reported for cuprous bromide and cuprous iodide crystals. However, the cuprous iodide crystal does not retain its zinc blende structure above 300°C but has a disordered distribution of Cu^+ ions. Above 400°C, cuprous iodide belongs to hexagonal system[7]. The vapour density at 1700°C indicates

that cuprous halides consist almost entirely as dimer[8], the adsorption data supports this conclusion. Even at high temperatures, substantial amounts[10] of cyclic Cu_3X_3 are present[11]. Nevertheless, the structures of cuprous halides, but for cuprous fluoride, is cubic in polymerized form. Some of the physical properties of cuprous halides are given in Table I.

TABLE - I

Physical properties of Cuprous halides

Properties	CuCl	CuBr	CuI	Ref.
Melting point	430°C	483°C	588°C	12
Boiling point	1359°C	1345°C	1293°C	13
Colour	White	White	White	12
Solubilities in water in mg/l at 25°C	110	29	0.42	12
Cu-X in A°				
- $\triangle H_{298}$ in Cal/mole	32.2	24.9	16.2	12
- $\triangle S_{298}$ "	20.8	23.0	23.1	12
- $\triangle G_{300}$ "	28.0	24.2	19.0	12
CuCl radius in Cu_3Cl_3	1.17A°	-	-	14
				13

The addition of halide ions greatly increases the solubilities of the cuprous halides due to the formation of halocuprate (I) anions[15,16,17] of the type CuX_2^- and CuX_3^{--}.

Complexes of copper (I) halides are formed by all the halogens except fluorine and contain 2,3 or 4 atoms. Remy and Laves[18] found that of the complex chlorides known, the number belonging to various types $[CuCl_2]^-$; $[CuCl_3]^{2-}$ and $[CuCl_4]^{3-}$ are roughly in the ratio 10:5:1. In fact complexes such as $(NH_4)_4CuCl_2$ and potassium dichlorocuprate (I), $K\ CuCl_2$, have been prepared. Similarly, sodium dichlorocuprite and potassium trichlorocuprite have also been prepared. The step-wise formation of chlorocomplexes in KCl solution with increasing CuCl/KCl ratio may be represented as[19]

$$CuCl + 2Cl^- \rightleftharpoons [CuCl_3]^{2-} \quad K = 1.45\times10^{-6} \text{ at } 25^\circ C$$

$$CuCl + Cl^- \rightleftharpoons [CuCl_2]^{2-} \quad K = 11.4\times10^{-6} \text{ at } 25^\circ C$$

$$CuCl + [CuCl_2]^- \rightleftharpoons [CuCl_3]^{2-}$$

In these copper has a filled $3d^{10}$ shell. The most common co-ordination number adopted by copper (I) is four, the metal atom being tetrahedrally surrounded by the four ligands. Coordination number of two and three are also known, but are less common[20,21]. Many of the compounds having a composition L CuX, where L = ligand and X = halogens might be expected to

contain two co-ordination number. Indeed, X-ray studies show them to be tetrameric[22], having tetrahedral cluster of copper atoms. Non-linear trimers of CuCl with two co-ordination number occur in the gas phase. These are only few compounds of copper with co-ordination number four.

In a few compounds, stoichiometry or X-ray diffraction studies suggest that cuprous copper may adopt a co-ordination number of five. Ethylammonium dichlorocuprate (I) when treated with ethylamine forms complexes having the composition $C_2H_5NH_3CuCl_2.nC_2H_5NH_2$, n = 1,2 or 3. It is suggested that $C_2H_5NH_3CuCl_2.3C_2H_5NH_2$ may contain five co-ordinate copper in a complex anion[23]. However, the majority of cuprous compounds adopt tetrahedral co-ordination both in discrete ions or molecules, and in polymeric structures found in the crystalline state.

Corresponding and similarly behaving complex bromo-cuprate ion is formed. The di-iodo cuprate (I) ion is also known, but is considerably less stable than the corresponding chloro and bromo complexes. $[CuBr_2]^-$; $[CuBr_3]^{2-}$ and $[CuBr_4]^{3-}$ complexes of copper (I) are known as also that of $[CuI_2]^-$; $[CuI_3]^{2-}$ and $[CuI_4]^{3-}$. Several copper (I) halide-ammonia complexes have been prepared by the reaction of Cu-X with NH_3. Copper (I) bromide in different proportions of CuBr to NH_3 forms from $CuBr.NH_3$ to $CuBr.3NH_3$. Similarly

with CuI forms different ammine complexes of which $[Cu(NH_3)_3I]$ is typical. However, all such univalent dihalocuprate (I) and divalent trichlorocuprate (I) ion are stable only in sufficiently high concentration of chloride ions. The first X-ray structural determination of $[CuCl_2]^-$ complex has been reported by Caughman and Taylor[24]. He synthesized the complex $[E\text{-}\overset{+}{\underset{H}{N}}\text{-}P\text{-}O]CuCl_2^-$ from the reaction of CuCl and hydrochloride of 2-(diphenylphosphino)ethyl-dimethylammine (E-PN), for the structural studies. In contrast, the compound $Cu(NH_3)_4[CuI_2]$ contains a distorted tetrahedral arrangement of iodine atoms about the copper (I) atom[25].

K. Monkemeyer obtained[26] a series of mixed crystals between copper (I) bromide and copper (I) iodide, between cuprous chloride and cuprous bromide, and cuprous chloride and cuprous iodide. Batronov and coworkers[27] oxidised cuprous chloride with bromine and iodine to obtain CuClBr and CuClI. X-ray examination of these products showed that they were merely mixtures of copper dihalides but no information on the chemical properties of the compounds is available.

Recently, halocomplexes of copper (I) such as $[Cu_2I_6]^{4-}$; $[Cu_2Br_5]^{3-}$ and $[Cu_2Br_6]^{4-}$ have been reported by Ahrland and Tegesson[28]. The complex fluorides A_3MF_6, where A is alkali metal of copper is reported as pale green cubic crystal of K_3CuF_6[29].

All the mercuric halides, except HgF_2 and HgI_2, have orthorhombic structures. HgF_2 has cubic crystal lattice, while HgI_2 is tetrahedral (fig. 1).

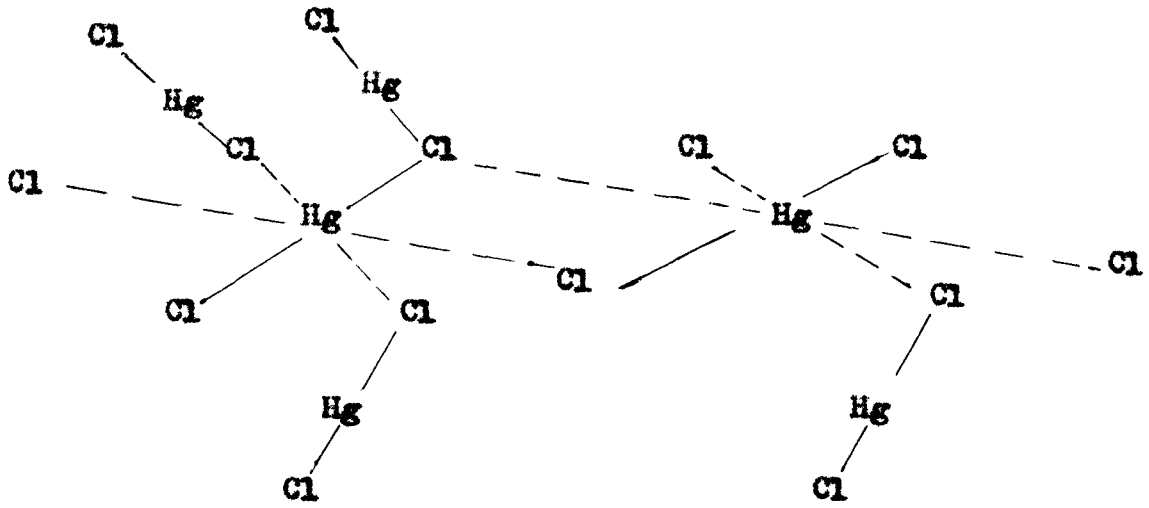

(a)

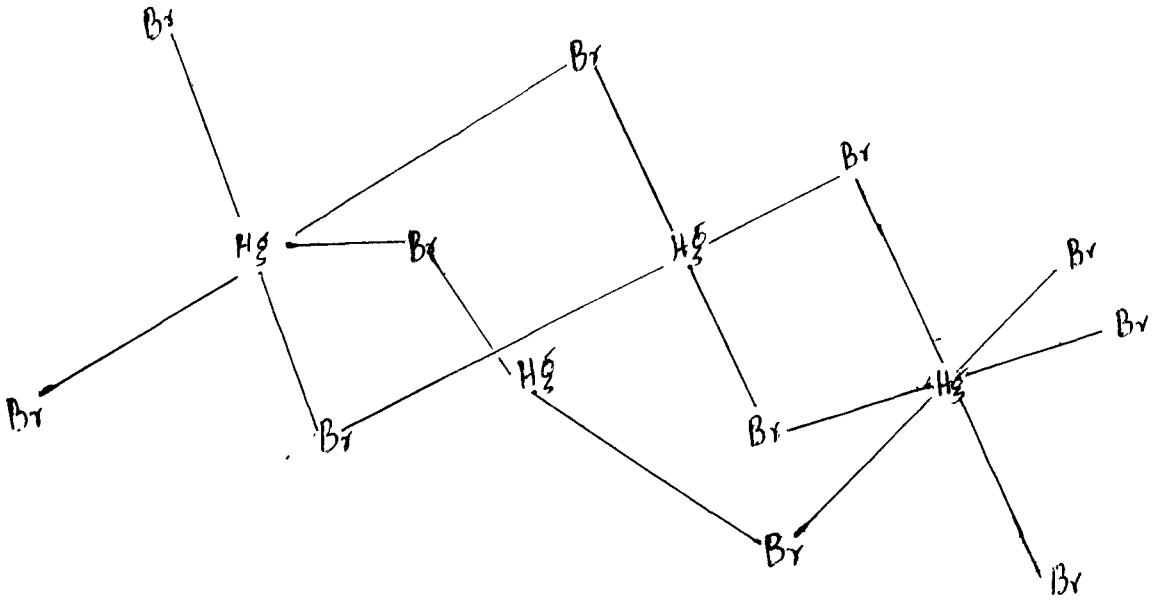

(b)

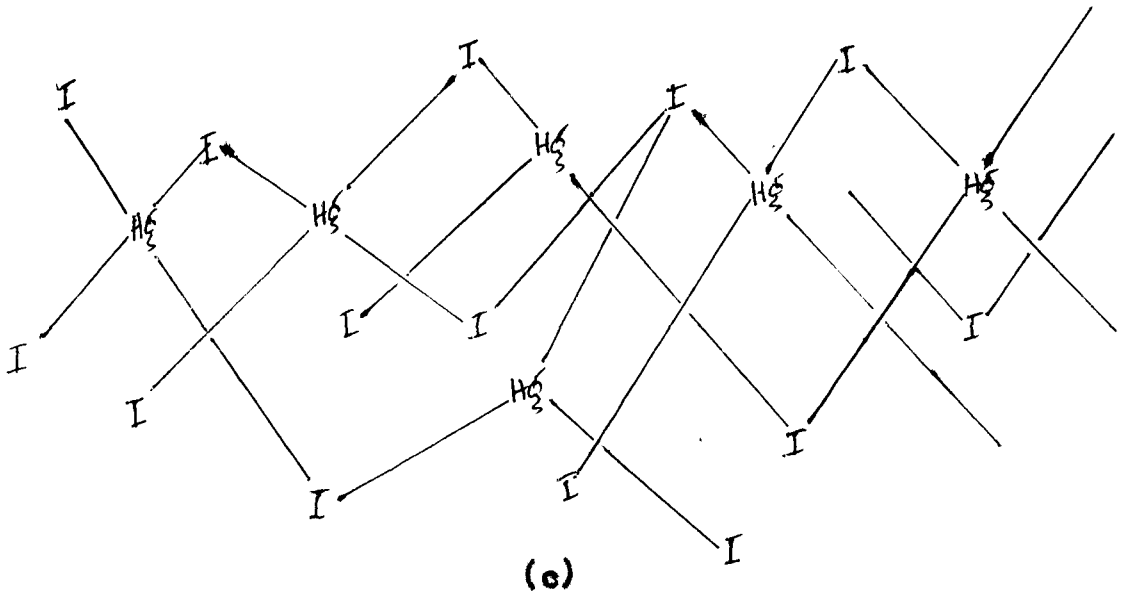

Fig.1. The environment of mercury in the crystal structure of $HgCl_2$(a), $HgBr_2$(b) and HgI_2(c)

The crystal structures of the mercuric halides are example of a morphotropic transition dependent upon the electronegativity of the halogen (4.0, 3.0, 2.8, and 2.5 for F, Cl, Br and I respectively). While mercury has distorted octahedral stereochemistry in the chloride, the structure is essentially molecular[30-32], having discrete linear Cl-Hg-Cl molecules. These are arranged in sheets stacked one above another along the C-axis[21] (Fig. 1a).

Mercuric bromide has a related structure of $HgCl_2$ in which linear Br-Hg-Br units may be distinguished. These are arranged in a deformed brucite structure[33,34], with six Hg-Br distance being less than R(Hg) - R(Br). Instead of being

regularly octahedrally co-ordinated, the mercury atoms have two close and two distorted version of the mixed hexagonal cubic close packing arrangement (Fig. 1b).

There are at least three forms of crystalline mercuric iodide, that stable at room temperature, the red α-form has an infinite layer structure in which iodine atoms are in distorted cubic close packing and mercury atoms occupy one fourth of the tetrahedral holes[35,36]. Above 129°C, the yellow β-form is the stable form with a structure like that of $HgBr_2$. Recent work[37] has confirmed the existence of another orange form, which has almost similar structure as that of α-form HgI_2.

HgF_2 has an ionic structure with each mercury atom having eight nearest neighbour fluorides. In the vapour phase, mercuric halides, but for HgF_2 consist of linear molecules. Bond lengths in the vapour phase as obtained by electron-diffraction have been given in Table II.

TABLE - II

Hg-X bond length in A^0 in the vapour phase

Hg - Cl	Mercuric chloride	2.20[38]; 2.34[39]; 2.27[40]
Hg - Br	Mercuric bromide	2.40[38]; 2.44[39]
Hg - I	Mercuric iodide	2.55[38]; 2.60[39]

Some of the physical properties of mercuric halides are tabulated in Table III.

TABLE - III

Physical properties of mercuric halides

Properties	HgF_2	$HgCl_2$	$HgBr_2$	HgI_2
ΔH_{vap} (KCal/mole)	22.0	14.08	14.15	14.14
ΔS_{vap} ($Cal.deg^{-1} mole^{-1}$)	-	24.4	23.8	22.7
Transition temperature (^oC)	-	-	-	129°
ΔH_f^o (KCal/mole)	-101.0	- 55.0	-40.5	-25.2
ΔG_f^o (KCal/mole)	-89.43	- 43.99	-36.37	-24.43
Solubility (g/100g water)	-	6.6 at 20°C	0.62 at 25°C	6×10^{-3} at 25°C
Resistance ohm cm x 10^{-3})	-	1.22 at 294°	6.9 at 243°	0.12 at 260°
Colour	White	White	White	White
Molecular structure	-	linear	linear	linear
Crystal	Cubic, CaF_2 structure[2]	Orthorhombic molecular	Ortho-rhombic molecular	(i) Red, Tetragonal layer (ii) Yellow, Orthorhombic like $HgBr_2$ (iii) Orange
d (Hg-X) A^o	2.46	2.23, 2.27	2.48	(i) 2.78 (ii) 2.62 3.51

The coordination of metal in molecules, complex ions and crystal structures depend upon the electronegativity of the ligands. Normally the atoms surrounding the metal at a distance of less than the sum of the Vander Waals radii are considered to belong to the metal coordination sphere.

In free molecules or complex ions characteristic coordination number of two, three and four for covalent bonding and eight for ionic bonding are known. Although Garlin et al.[41] claim to have prepared complex of mercury but this structure for a mercury compound has not been backed by complete structure determinations. A series of halomercury arsenites have been reported by Puff et al.[42]. Masalov[43] has proposed a general formula for the calculation of thermodynamic properties of complexes of mercury (II). Heat of formation of mixed halide complexes and complex ions are listed in Table IV.

The mercuric halides but for HgF_2 are not dissociated in aqueous media. In excess of alkali halides stable species HgX_3^- and HgX_4^{2-} are formed. The sparingly soluble HgI_2 is also soluble in excess of mercuric salts. Raman spectroscopic studies[44] have shown that the species present are as $[HgCl]^+$, $[HgBr]^+$ and $[HgI]^+$; and also in the case of iodide as $[Hg - I - Hg]^{3+}$.

Several investigation of mercury (II) halides complexes in aqueous solution, applying different methods have been

reported in the literature[45,46]. E.m.f. measurements on dilute solutions have shown that HgX^+, HgX_3^- and HgX_4^{2-} complexes are formed. Van Eck[47] showed that HgX_4^{2-} are probably tetrahedron but highly distorted with Hg-I= 2.80A° in HgX_4^{2-}.

Spectroscopic studies show that the complex ion HgX_4^{2-} in solution is a regular tetrahedron[48,49], X-ray scattering data have shown that HgI_3^- is approximately a pyramidal and HgI_4^{2-}, tetrahedral[50]. For concentrated mercury (II) chloride solution containing a large ratio of chloride ion, the data are consistent with a dominant $HgCl_4^{2-}$ complex with Hg-Cl=2.47A°[51] Linhart[52], by measuring the distribution of $HgCl_2$ between water and benzene phase showed that the species Hg_2Cl_4; $Hg_2Cl_5^-$ and $Hg_2Cl_6^{2-}$ are formed.

Table - IV

A. Heat of formation of complex ions of mercury(II) at 25°C in Kcal/mole.

	ΔH_f^o		ΔH_f^o
$[HgCl_2Br]^-$	83.0	$[HgCl_2I_2]^{2-}$	92.8
$[HgClBr_2]^-$	75.6	$[HgI_3Cl]^{2-}$	76.0
$[HgCl_3Br]^{2-}$	122.2	$[HgI_3Br]^{2-}$	66.0
$[HgCl_3I]^{2-}$	111.6	$[HgCl_2BrI]^{2-}$	103.6
$[HgBr_3I]^{2-}$	87.4	$[HgBr_2ClI]^{2-}$	95.5
$[HgClBr_3]^{2-}$	106.2	$[HgI_2ClBr]^{2-}$	84.8
$[HgCl_2Br_2]^{2-}$	114.3		

B. Heat of formation of mixed halide complexes of potassium and mercury at 25°C in Kcal/mole.

	ΔH_f^o		ΔH_f^o
$K[HgCl_2Br]$	151.1	$K_2[HgBr_3I]$	217.8
$K[HgCl_2I]$	142.0	$K_2[HgI_3Cl]$	205.8
$K[HgBr_2Cl]$	142.5	$K_2[HgI_3Br]$	196.6
$K[HgBr_2I]$	124.6	$K_2[HgCl_2Br_2]$	247.0
$K[HgI_2Cl]$	124.1	$K_2[HgCl_2I_2]$	225.8
$K[HgI_2Br]$	115.5	$K_2[HgBr_2I_2]$	207.5
$K[HgClBrI]$	133.3	$K_2[HgCl_2BrI]$	236.4
$K_2[HgCl_3Br]$	256.2	$K_2[HgBr_2ClI]$	227.1
$K_2[HgCl_3I]$	245.6	$K_2[HgI_2ClBr]$	216.4
$K_2[HgBr_3Cl]$	237.8		

No structural determination have, however, been carried out on mercury (II) complexes of fluorine although pyridinium complex (pyH^+), HgF_4^{2-} have been prepared[53]. All mercury (II) chloro-complexes of known structure contain more or less distorted $HgCl_6$; these may be linked into chains or layers by sharing of edges or corners as shown in figures (a) and (b).

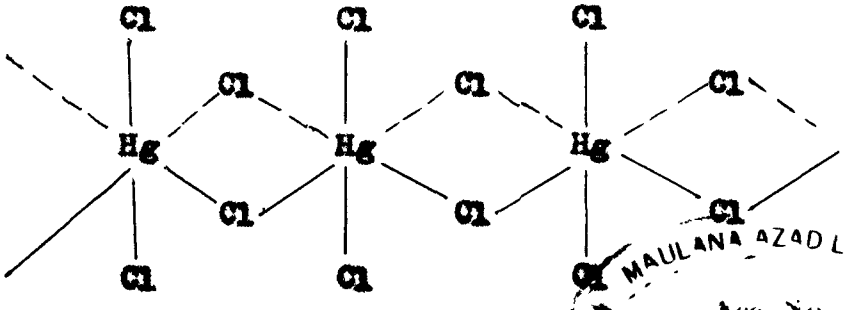

(Fig. a)

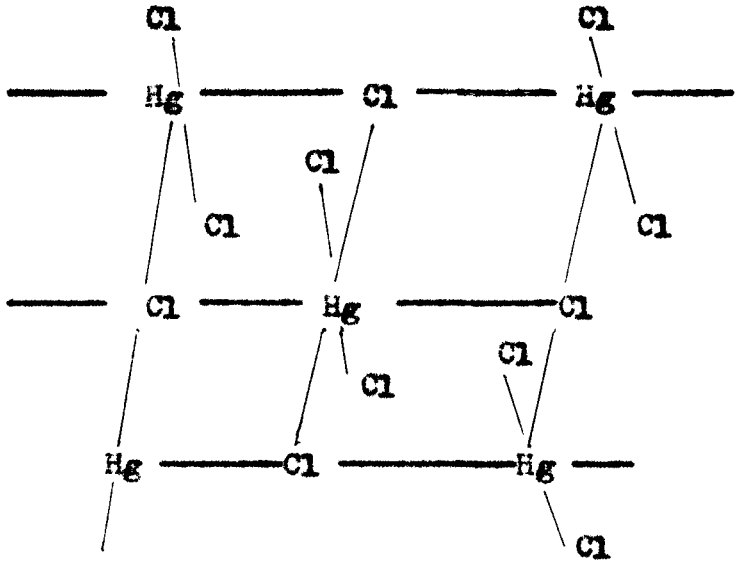

(Fig. b)

The only structure with discrete $HgCl_4^{2-}$ groups appear to be a derivative of the alkaloid peroline of composition $C_{27}H_{17}N_2O_3$. 0.5 $HgCl_4.H_2O$[54]. Recently, two new complexes and their structures have been worked out by Beg et al.[55]

Bromocomplexes are not well documented apart from a rather dubious assignment of the provksite structure to $C_8H_8Br_3$. The only known structure is that of NMe_4HgBr_3, which consists of NMe_4^+ and pyramidal $HgBr_3^-$ ions loosely linked into chains[56]. Mercury thus has a distorted four coordination.

In iodocomplexes, the large iodine atoms seems to form only three and four coordinate complex with mercury (II). The sulphonium compounds $(Me_3S)^+ HgI_3^-$ and $(Me_3S)_2HgI_4$ are apparently ionic, as formulated[57]. Both CuI and AgI form remarkable complexes with Hg(II) iodide, which exist in high and low

temperature form (α & β). The crystal structure of the yellow, tetragonal Ag_2HgI_4 has cube close packed iodine atoms, with some of the tetrahedral holes filled by Ag^+ and Hg^{2+} atoms in a regular manner. Its red modification has cube structure of zincblende[58]. The isomorphous Cu_2HgI_4 shows analogous thermochromic properties.

Redistribution reaction between individual mercury (II) halides have been carried out by Marcus and Elizer[59] and they found the result in the affirmative. However, the first evidence for the existence of mixed halide of mercury (II) were obtained by Raman Spectra in MeOH[60-63] and in molten state by Zangen[64]. In gaseous state the discrete absorption band spectra have been obtained by Muller[64a]. In solid state, several mixed halides of mercury have been reported by Rastogi and coworkers[66,67]. Formation of HgClI in various conditions and that of HgBrI was also reported much earlier[68-73]. Physical properties of mixed halides of mercury have been studied by various authors. For example, Maltsev et al.[74] have studied the force constant in the binding by I.R. spectral observations. The bond-bond interaction in mixed halides have been studied by Duchesne and Brunella[75]. Recently, Rastogi et al.[76] have reviewed the various aspects of mixed halides in detail.

The formation of Cu_2HgI_2 from HgI_2 and CuI in solid state is well known[77]. It is expected that HgI_2 vapourises to react with CuI to give Cu_2HgI_4 via counter diffusion of Cu^+ and Hg^{2+} through Cu_2HgI_4. However, no work is reported to have been done to investigate the reaction of copper(I) halides and mercuric halide in solid state. The lack of this information and the possibility of getting new mixed halides and different modes of solid solutions, has tempted to carry out the reactions of copper(I) halides with Mercury(II) halides in solid state.

Studies on the kinetics and mechanisms of the reaction between mercuric bromoiodide and copper(I) iodide mercuric bromide and copper(I) iodide, mercuric chloride and cuprous iodide, and mercuric chloride and cuprous bromide in solid state were carried out by X-ray, chemical analysis, thermal and electrical conductivity measurements. Rate measurements were carried out in the manner as described elsewhere[65]. The solid solutions formed during the reaction were not studied quantitatively, but there evidences have been ascertained by measuring the deviation in the d-values from the d-values of the standard X-ray diffraction patterns.

REFERENCES

1. Ahrland, S., Chatt. J. and Davies, N.R.: Quart. Rev. 12, 265 (1958).

2. Bodlaender, G. and Storabeck, O.: Z. anorg. Chem. 31, 1; 458 (1902).

3. Ryss, I.M.: Zhur. Fiz. Khim. 29, 936 (1955).

4. Wartenberg, H. Von: Z. anorg. allgem. Chem. 241, 381 (1939).

5. Billy, C. and Haender, H.M.: J. Am. Chem. Soc. 79,1049 (1957).

6. Wyckoff, R.W.G. and Ponsjak, E.: J. Am. Chem. Soc. 44, 30 (1922).

7. Schubert, K.: Z. Naturforsch, 59, 345 (1950).

8. Biltz, H. and Meyer, V.: Z. Physik Chem. 4, 267 (1889).

9. Terrien, J.: Ann. Phys. [XI], 9, 447 (1938).

10. Brewer, L. and Lofgren, N.L.: J. Am. Chem. Soc. 72, 3038 (1950).

11. Wong, C.H. and Schomaker, V.: J. Phys. Chem. 72, 358 (1957).

12. Sidgwick, N.V.: The Chemical Elements and Their Properties (Oxford University Press), 1950.

13. Shelton, R.A.J.: Trans. Farad Soc. 57, 2113 (1961).

14. Smithells, C.J. (editor): Metals Reference Book. 3rd edition (Butterworth, London), 1962.

15. Farha, F. and Iwamoto, R.T.: Inorg. Chem. 4, 844 (1965).

16. Kubota, M. and Johnston, D.L.: J. Inorg. Nucl. Chem. 29, 719 (1967).

17. Peters, D.G. and Caldwell, R.L.: Inorg. Chem. 6, 1478 (1967).

18. Remy, H. and Laves, G.: Ber. 66, 571 (1933).

19. Chaltykrav, O.A.: Zhur. Obschei Khim. 18, 1626 (1948).

20. Block, B.P.: in Inorganic Polymers, editors: Stone, F.G.A. and Graham, W.Z.G. (Academic Press, New York), Chap. 8(1962).

21. Wells, A.F.: Structural Inorganic Chemistry, 3rd edition, (Oxford Univ. Press), 1962.

22. Wilkins, R.G. and Berkin, A.R.: J. Chem. Soc. 127,154 (1950).

23. Clifton, J.R. and Yoke, J.T.: Inorg. Chem. 6, 1258 (1967).

24. Caughman, E.D. and Taylor, R.C.: Inorg. Nucl. Chem. Letter. 6, 623 (1970).

25. Baglio, J.A. et al.: J. Inorg. Nucl. Chem. 32, 795 (1970).

26. Monkemyer, K.: Neues. Jahrb. Min. B.B. 22, 42 (1906).

27. Batsonov, S.S. et al.: Dokl. Akad. Nank. SSSR, 181, 599(1968).

28. Ahrland, S. and Tagesson, B.: Acta Chem. Scand. A31, 615 (1977).

29. Klemn, W. and Huss, E.: Z. anorg. Chem. 258, 221 (1949).

30. Braekken and Harang: Z. Krist. 68, 123 (1928).

31. Braekken and Scholten: Ibid. 89, 448 (1934).

32. Gradenic: Archiv. Kem. 22, 14 (1950).

33. Verweel and Bijvoet: Z. Krist. 77, 122 (1931).

34. Braekken, H.: Z. Krist. 81, 152 (1932).

35. Havighurst: Americ. J. Sci. 10, 556 (1925).

36. Bijvoet, et al.: Proc. K. ned. Akad. Westenschap. 29, 529 (1926).

37. Jeffery, G.A. and Vlasse, M.: Inorg. Chem. 6, 396 (1967).

38. Braune and Knocke: Z. Physik. Chem. B25, 165 (1933).

39. Gregg et al.: Trans. Farad. Soc. 33, 852 (1937).

40. Maxwell and Mosley: Phys. Rev. 57, 21 (1940).

41. Garlin et al.: Inorg. Chem. 1, 182 (1962).

42. Puff, H. et al.: Naturwissenschaften, 52, 494 (1965).

43. Maslov, P.G.: I.V.U.Z. Khim i Khim. Tekhnol. 2, 335 (1959).

44. Clark, J.H.R. and Woodward, L.A.: Trans. Farad. Soc. 61, 207 (1965).

45. Deacon, G.B.: Rev. Pure appl. Chem. 13, 189 (1963).

46. Sillen, L.G. and Martell, A.E.: Stability constants Specl. Publ. No.17 (1964) and Suppl. No.1, Specl. Publ. No.25, The Chemical Society (London) (1971).

47. Van Panthaleon Van Eck et al. Recl. Trav. Chim. Pays. Bas. 75, 802 (1956).

48. Hooper, M.A. and James, D.W.: Aust. J. Chem. 24, 1345 (1971).

49. Macklin, J.W. and Plane, R.A.: Inorg. Chem. 9, 821 (1970).

50. Gaizer, F. and Johansson, G.: Acta Chem. Scand. 22, 3013(1968).

51. Sandstran, M.: Acta Chem. Scand. A31, 141 (1977).

52. Linhart, G.A.: J. Am. Chem. Soc. 38, 272 (1916).

53. Dotzer, R. et al.: Z. anorg. und. allgem. Chem. 308,79 (1961).

54. Jeffreys, J.A.D. et al.: Proc. Chem. Soc. (1963), pp. 171.

55. Beg, M.A. and Ansari, S.M.: J. Solid State Chem. 20, 1 (1978).

56. White, J.G.: Acta Cryst. 16, 397 (1963).

57. Penn, R.H.: Acta. Cryst. 20, 20; 24 (1966).

58. Ketelaar: Z. Krist. 80, 190 (1934); (A)87, 435 (1934).

59. Marcus, Y. and Eliezer, I.: J. Phy. Chem. 66, 1661 (1962).

60. Clark, J.H.R. and Solomons, C.: J. Chem. Phys. 48, 528 (1968).

61. Francois, F.: Compt. rend. 207, 425 (1938).

62. Delwaille, M.L. and Francois, F.: Bull. Soc. Chim. 7, 359 (1940).

63. Delwanlle, M.L.: Spectrochim. Acta, Suppl. 565 (1957).

64. Zangen, M.: J. Inorg. Nucl. Chem. 31, 867 (1969).

64a. Muller, P.: Helv. Phys. Acta. 15, 233 (1942).

65. Rastogi, R.P. and Lubey, B.L.: J. Am. Chem. Soc. 89, 200 (1967).

66. Rastogi, R.P. et al.: J. Inorg. Nucl. Chem. 37, 1167 (1975).

67. Boullay, P.F.G.: Ann. Chim. Phys. 29, 201 (1882).

68. Kohler, H.: Ber. 12, 608, 1188 (1879).

69. deLuca, S.: Ann. Chim. Phys. 43, 271 (1885).

70. Reinders, W.: Z. Phys. Chem. 32, 503 (1900).

71. Luczizky, W.C.: Z. Krist. 46, 297 (1909).

72. Van Nest, J.S.: Z. Krist. 47, 263 (1910).

73. Oppenheim, A.: Ber. 2, 571 (1869).

74. Maltsev, A.A. et al.: Phys. Sci. 231, 157 (1971).

75. Duchesne, J. and Brunelle, L.: J. Chem. Phys. 19,1191 (1951).

76. Rastogi, R.P. et al.: J. Sci. Indust. Res. 37, 622 (1978).

77. Pinnock, A.T.: J. Soc. Chem. Ind. 38, 78 (1919).

C H A P T E R - III

PREPARATION OF MATERIALS

COPPER (I) HALIDES

Since cuprous halides are sensitive to light, fresh cuprous iodide, cuprous bromide and cuprous chloride were prepared before the start of each set of experiments.

Preparation of Copper (I) iodide

Copper (I) iodide was prepared following the methods of Berthemot[1] and Guichard[2].

Two moles of KI (BDH, Analar Grade) in 150 ml double distilled water and one mole of cupric sulphate (BDH, Analar Grade) in three litres double distilled water were mixed, and the mixture boiled to remove the excess iodine. The resulting white CuI crystals were washed and purified with double distilled water and alcohol respectively, and then kept for few days in a thermostat maintained at 80-100°C to get rid of any moisture present. X-ray diffraction studies showed it to be single phase CuI, and its d values and the related intensities matched well to that of γ-CuI[3]. To avoid the exposure by light, CuI was kept in a dark bottle.

Preparation of Copper (I) bromide

Cuprous bromide was prepared following the method of Lean and Whatmough[4]. About 20 gms of cupric sulphate and 8 gms. of sodium bromide (both BDH, Analar Grade) were dissolved in 300 ml double distilled water. Sulphur dioxide, prepared by the standard laboratory method, was passed through this solution. Small white shining crystals of cuprous bromide separated out. This was filtered out, and the filtrate was boiled to remove the excess sulphur dioxide, which again produced crystals of CuBr. The crystals were washed out immediately with sulphurous acid, and spread on porous tiles. This was dried over potassium hydroxide in vaccum and dark. X-ray diffraction pattern showed it to be single phase CuBr, and its d values and intensities correspond well to that of γ-CuBr[5].

Preparation of Copper (I) chloride

Cuprous chloride was prepared by the method as recommended by Wöhler[6] and Rosenfeld[7]. 20 gms of Cupric sulphate and 4.25 gms of sodium chloride (both BDH, Analar Grade) in 300 ml double distilled water were taken. The mixture was saturated with SO_2 gas when crystals of CuCl slowly separated out. The crystals were washed immediately and in dark by sulphurous acid, and then with glacial acetic acid. The crystals were put in

between porous tiles and dried in vaccum and dark. X-ray diffraction pattern showed it to be single phase CuCl, and its d values and intensities conform well to that of CuCl[8].

Preparation of Cuprous Iodo Mercurate, Cu_2HgI_4

Cu_2HgI_4 is known to be formed[9] in solid state by the interaction of CuI and HgI_2. However, this method is not followed in its preparation, but this was done by simultaneous precipitation from solution containing stoichiometric amounts of reactants. This method yielded more satisfactory results than solid state reaction. Aqueous solutions containing mixtures of cupric nitrate (BDH, Analar Grade) with total metal concentration about 0.4M was added to boiling solution of approximately 0.1M K_2HgI_4 which was earlier prepared by mixing stoichiometric solution of mercuric nitrate and potassium iodide, and further adding sufficient potassium iodide to remove the iodine formed[10], and to decrease the loss of material remaining in solutions. If this was not done, results were found to be poor, the product consisting largely of cuprous iodide rather than Cu_2HgI_4.

Cu_2HgI_4 obtained as dark red mass was filtered and washed with potassium iodide solution and double distilled water, dried thereby over porous plate in a thermostat at about 100°C. Cu_2HgI_4 exists in two forms, the low temperature

β-Cu_2HgI_4 which is stable below 69°C, and the high temperature α-Cu_2HgI_4 which is stable above 69°C[11].

X-ray diffraction studies showed it to be low temperature single phase β-Cu_2HgI_4. The calculated d values resemble that of ASTM powder diffraction file[12] but the intensities do not correspond exactly. The d values and corresponding intensities are given in Table I.

TABLE - I

X-ray Diffraction of β-Cu_2HgI_4, taken by 'Norelco, (Philips-1010) Diffractometer using $CuK\alpha$ radiation and Ni-filter.

d, in A°	I/Io	d in A°	I/Io
5.43	23	1.84	58
3.52	100	1.67	12
3.43	22	1.55	35
3.03	15	1.52	42
2.71	8	1.47	41
2.68	28	1.39	45
2.27	30	1.38	8
2.14	85(100)	1.32	22
2.01	25	1.24	40

MERCURY (II) HALIDES

Preparation of mercuric bromoiodide

HgBrI was prepared by Oppenhein's method[13]. Equimolar mixture of $HgBr_2$ and HgI_2 (both a. Merck) in acetone were taken, and mixed. Yellow shining crystals separate out after standing for sometime. These were filtered off and washed with double distilled water. The X-ray analysis showed it to be single phase HgBrI.

HgBrI was also prepared by equimolar mixing of $HgBr_2$ and HgI_2 in solid state[14] at elevated temperature, about 100°C. After keeping this mixture for more than five days, yellow shining crystals appeared. X-ray analysis showed it to be single phase HgBrI. The patterns in either cases were almost the same. However, the d values and intensities are different from the one reported by Rastogi, et al.[14]

TABLE - II

X-ray diffraction pattern for HgBrI using CuKα radiation recorded on 'Norelco, diffractometer (Philips - 1010) and using Ni-filter.

d in A°	I/Io	d in A°	I/Io
6.51	100	2.19	16
3.88	9	2.09	14
3.71	69	2.06	8
3.36	50	1.99	12
2.90	35	1.90	8
2.75	30	1.77	14
2.40	14	1.64	10
2.33	18	1.50	10

$HgBr_2$ and HgI_2 (E. Merck) and $HgCl_2$ were used without further purification. The purity was checked by X-ray. The X-ray data were same as reported[15,16] for $HgCl_2$ and HgI_2. The data has, however, been found different from that published recently for $HgBr_2$[17]. The observed d values and corresponding intensities are reported in Table III.

TABLE - III

X-ray diffraction pattern for $HgBr_2$ using CuK_α radiation with Ni-Filter. 32 Kv at 12 mA. $\lambda = 1.5405 A^\circ$

d in A°	I/Io	d in A°	I/Io
6.18	100	2.08	25
3.81	9	2.07	69
3.64	58	2.03	13
3.25	43	2.00	20
2.98	11	1.93	19
2.80	45	1.82	21
2.62	33	1.81	8
2.41	11	1.76	12
2.31	29	1.70	9
2.29	14	1.68	11
2.16	19	1.66	5
		1.58	43
		1.55	33
		1.51	11

REFERENCES

1. Berthemot, J.B.: Jour. Pharm. 14, 614 (1830).
2. Guichard, M.: Compt. rend. 144, 1430 (1907).
3. ASTM, Powder Diffraction File, No.6-0246.
4. Lean, B. and Whatmough, W.H.: J. Chem. Soc., 73, 148 (1898).
5. ASTM, Powder Diffraction File, No. 6-0292.
6. Wöhler, F.: Liepzigs Ann. 130, 373 (1864).
7. Rosenfeld, M.: Gazz. Chim. Ital. 12, 954 (1879).
8. ASTM, Powder Diffraction File, No.6-0344.
9. Pinnock, A.T.: J. Soc. Chem. Ind. 38, 78 (1919).
10. Meyer, M.: J. Chem. Educ. 20, 145 (1943).
11. Ketelaar, J.: Z. Krist. 87, 440 (1934).
12. ASTM, Powder Diffraction File, No.18-0450.
13. Oppenheim, A.: Ber. 2, 571 (1869).
14. Rastogi, R.P. and Dubey, B.L.: J. Inorg. Nucl. Chem. 31, 1530 (1969).
15. ASTM, Powder Diffraction File, No.4-0335.
16. ASTM, Powder Diffraction File, No.4-0456.
17. ASTM, Powder Diffraction File, No.24-0753.

C H A P T E R - IV

REACTION OF CuI - HgBrI

EXPERIMENTAL

Cuprous iodide and mercuricbromoiodide give scarlet product immediately after they are mixed which turns to dark brown colour when heated above 70°C.

Kinetic Measurements

CuI and HgBrI were powdered in a agate mortar and sieved to 300 mesh. The kinetics of the reaction in the solid state were studied by placing HgBrI powder over CuI powder in a vertical pyrex glass tube of 0.5 cm internal bore. An approximately 10 cm long tube of uniform diameter was chosen for this purpose. One end of the tube was sealed and a weighed amount of CuI was introduced into the tube through the open end, and pressed gently by placing a 20 cm long glass rod of 0.5 cm external diameter. A weighed amount of HgBrI on a tissue paper and the tube containing CuI were placed in an incubator maintained at the desired temperature. After about half an hour, HgBrI was placed over CuI layer in the tube. To press the HgBrI, the same glass rod was used, and after gently pressing HgBrI, it was removed immediately. The whole criterion was done in the incubator controlled at $\pm$ 0.5°C. Since there is every possibility that change of

pressure will affect the reaction kinetics, mainly due to its action on elementary processes such as sintering, recrystallisation and diffusion etc, the same amounts of the reactants were always used. The progress of the reaction was followed by measuring the total thickness of the product layer formed at the interface by travelling microscope having a caliberated scale in its eyepiece. Each experiment was run in triplicate and the average of different set is reported (Table I) here.

Soonafter the placement of the HgBrI powder over the CuI in the reaction tube, a brown red boundary formed at the interface and this grew with time on CuI side. After sometimes, a gap developed between the HgBrI and the brown colour product, while another layer of light or pale yellow colour product also appeared. On cooling to room temperature the dark brown product turned to scarlet colour. Cu_2HgI_4 is dark brown above 70°C and scarlet below this temperature[1]. The kinetics were studied at different temperatures in a similar way. Later, when the reactants were placed in a tube with some gap, the product layers were similar as when they were in contact. This implied that HgBrI reacts with CuI via vapour phase.

TABLE - I

Dependence of Parameters of equation $X_1^n = Kt$ on temperature for CuI-HgBrI reaction

Temperature (°C ± 0.5)	K(cm./hr)	n
64	1.064×10^{-6}	2.67
75	2.559×10^{-6}	2.40
87	7.079×10^{-6}	2.50
95	14.96×10^{-6}	2.50
104	39.81×10^{-6}	2.60
116	64.46×10^{-6}	2.44

Analysis of the product layer

A reaction tube having the scarlet product and yellow layer was broken carefully and the layers were separated. The amounts thus obtained were dissolved in concentrated nitric acid separately. In the yellow product layer, Cu^+ and Br^- ions were confirmed by the spot tests[2]. X-ray diffraction pattern was identical with that of γ-CuBr.

The spot tests for the scarlet product layer showed the presence of Cu^+, Hg^{2+} and I^-. X-ray diffraction pattern showed it to be single phase β-Cu_2HgI_4.

X-ray studies

The reactants CuI and HgBrI (both about 300 mesh size) were mixed thoroughly in an agate mortar in different molar ratios. One part of each mixture was heated in an air oven thermostat at 120 ± 0.5°C and one part was maintained at room temperature (30°C). Both were analysed by Norelco Geiger Counter X-ray Diffractometer (PW 1010 Philips) by CuKα radiation applying 32 KV at 12 mA current with a Ni-filter.

The compounds present were identified by calculating the d values and the corresponding intensities of the lines and comparing them with the standard values of the expected compounds. The compounds obtained in different mixtures are given in Table II.

TABLE - II

Compounds present in different molar ratio mixtures of CuI and HgBrI

Mixture	Molar Ratio of CuI:HgBrI	Compounds identified at room temperatures(30°C) after about 1 hr.	Compounds identified at 120°C after 60 hrs.
I	4:1	CuI, Cu_2HgI_4, CuBr and HgI_2	CuI, Cu_2HgI_4 and CuBr
II	3:1	Cu_2HgI_4, CuBr and HgI_2	Cu_2HgI_4, CuBr
III	1:2	Cu_2HgI_4, CuBr, HgBrI and HgI_2	Cu_2HgI_4, CuBr and HgBrI

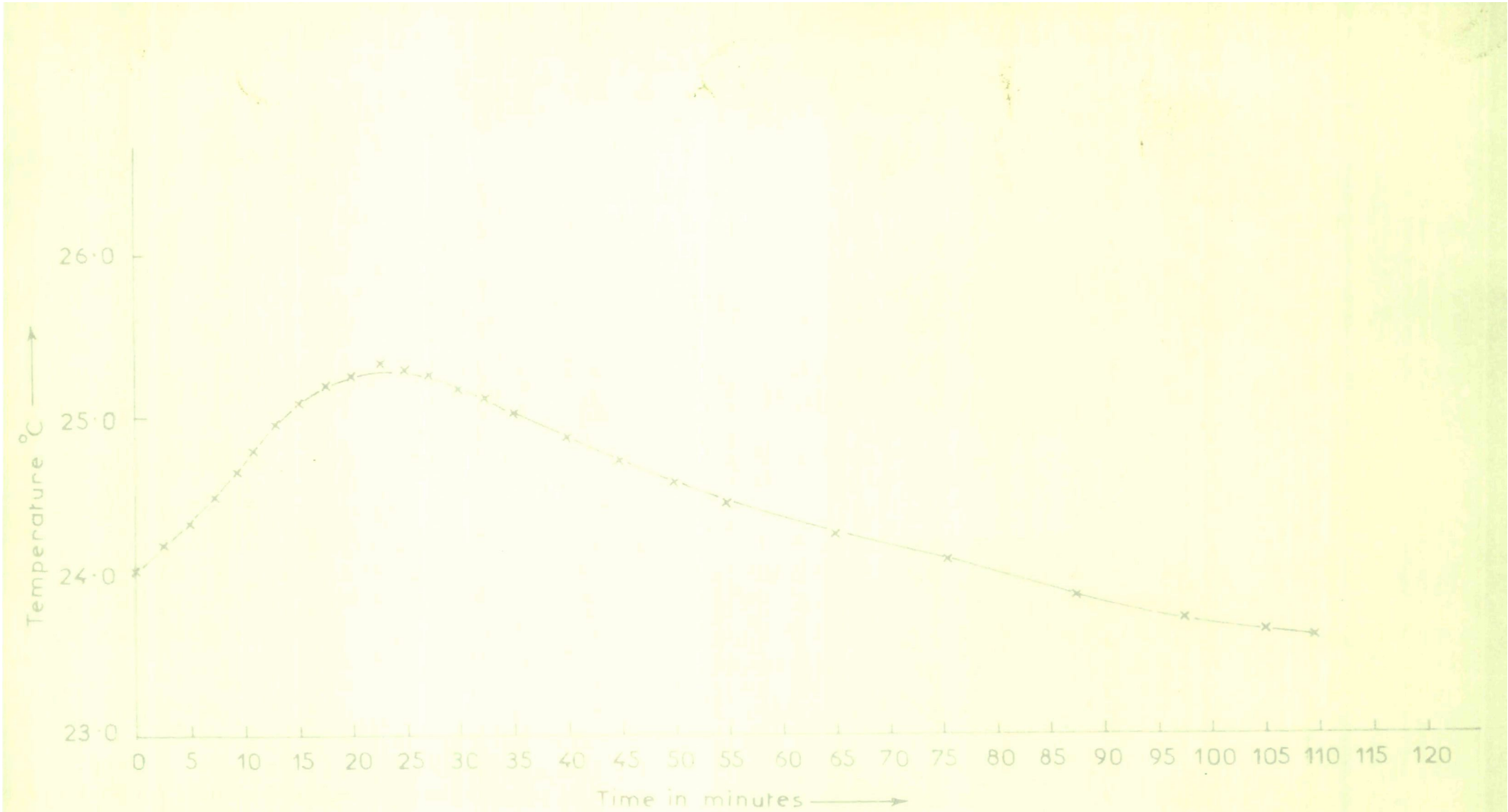

FIG. 1a TEMPERATURE RISE AS A FUNCTION OF TIME FOR THE REACTION CuI – HgBrI IN A MOLAR RATIO 3:1

Thermal studies

Amounts of CuI and HgBrI in molar ratio 3:1 were weighed separately on tissue papers. Reactants mixture in molar ratio 3:1 were poured into the Dewar flask calorimeter and mixed thoroughly. The rise in temperature was noted against time. Similar experiments were repeated with other molar ratio mixtures. The results are shown in the figure (Ia,1).

Conductivity Measurements

CuI and HgBrI in molar ratio 3:1 were thoroughly mixed with each other, and immediately poured into a die and pressed into a pellet. This pellet was then fixed between platinum electrodes, and the change in conductance against time was noted at room temperature by current I.C. Bridge, applying 0.2V at frequency 5×10^3 Hz. Similar experiments were carried out with 2:1 and 1:1 molar mixture. The results are depicted in the figure (Ib,1).

Dispersion

The X-ray diffraction measurements (Table II) revealed that CuI and HgBrI react in the 3:1 molar ratio in the solid state.

$$3\ CuI + HgBrI \longrightarrow CuBr + Cu_2HgI_4 \qquad (1)$$

It was noticed that when the reactants were mixed at room temperature, a scarlet product was formed which later became faint in colour. The appearance of the light yellow colour is probably due to the formation of pale yellow CuBr. The X-ray pattern of the reactants maintained at room temperature showed the presence of HgI_2, which means that HgI_2 is formed as soon as the reactants were mixed. The presence of HgI_2 in the mixture at room temperature could not be conceived by simple visual observation, because Cu_2HgI_4 at room temperature is also reddish in colour. This HgI_2 immediately reacted with CuI to give the addition product, Cu_2HgI_4[3]. The reaction sequence may be written as:

$$HgBrI + CuI \longrightarrow HgI_2 + CuBr \qquad (Ia)$$

$$HgI_2 + 2CuI \longrightarrow Cu_2HgI_4 \qquad (Ib)$$

$$HgBrI + 3CuI \longrightarrow CuBr + Cu_2HgI_4$$

Thermal and conductance measurements (figure Ia & Ib) show only one peak and therefore no evidence for a two step reaction is obtained. This is understandable because step (Ib) is much faster than step (Ia). Step (Ia) will be slow because the ionic radii of Cu^+ and Hg^{2+} are very close to each other. Step (Ib) is known to be very fast[3] even at room temperature and below room temperature too. This is why no indication is obtained for step (Ia) during the thermal and conductance measurements. X-ray measurements for 3:1 ratio at 120°C is given in Table III.

TABLE - III

X-ray measurements for the reaction mixture 3CuI + HgBrI

d in A°	I/Io	d in A°	I/Io
5.40+	21	1.81	-
3.49+	100	1.73*	35
3.41+	20	1.55+	30
3.33*	100		
3.00+	10	1.50+	30
2.64+	20	1.39+	40
2.24+	25	1.31+*	15
2.14+	68	1.23+	40
2.03*	56	-	-
2.00+	25	-	-
1.83+	56	-	-

\+ lines of β-Cu_2HgI_4
* lines of γ-CuBr.

The X-ray analysis of 4:1 molar mixture of CuI and HgBrI showed that at room temperature, HgI_2, Cu_2HgI_4, CuI, and CuBr, were formed whereas at higher temperature, Cu_2HgI_4 and CuBr were the products. In both cases, excess CuI is left unreacted. The reaction sequence is similar to that in 3:1 molar mixture.

$$4CuI + HgBrI \longrightarrow 3CuI + HgI_2 + CuBr \qquad \text{slow}$$

$$\underline{HgI_2 + 2CuI \longrightarrow Cu_2HgI_4} \qquad \text{fast}$$

$$HgBrI + 4CuI \longrightarrow Cu_2HgI_4 + CuBr + CuI$$

The thermal and conductance measurements, however, gave only one infliction in the curve, which has been explained a little earlier. The X-ray diffraction pattern of this mixture is shown in Table IV.

TABLE - IV

X-ray diffraction pattern for the molar ratio 4CuI + HgBrI

d in A^0	I/Io	d in A^0	I/Io
5.38x	20	1.98x	25
3.49+x	100	1.82+	35
3.42x	16	1.80*x	35
3.36*	100	1.55x	30
3.00x	10	1.52x	30
2.98x	10	1.51+	6
2.65x	20	1.39x	40
2.25	25	1.37x	15
2.14+x	56	1.27x	15
2.10x	65	1.23x	50
2.05*	59	-	-

x lines for Cu_2HgI_4[4]
+ lines for γ-CuI[6]
* lines for γ-CuBr[5].

The X-ray diffraction analysis of a 1:2 molar mixture of CuI and HgBrI maintained at room temperature showed the presence of Cu_2HgI_4, HgI_2, CuBr and HgBrI while at 120°C,

Cu_2HgI_4, CuBr and excess of HgBrI were present. The overall reactions may be as the following:

$$3CuI + 6HgBrI \longrightarrow HgI_2 + CuBr + 2CuI + 5HgBrI$$
$$2CuI + HgI_2 \longrightarrow Cu_2HgI_4$$
$$3CuI + 6HgBrI \longrightarrow Cu_2HgI_4 + CuBr + 5HgBrI$$

The steps involved here seem to be the same as those in 3:1 molar mixture except that the excess of HgBrI is left unreacted. The X-ray diffraction pattern are shown in Table V.

TABLE - V

X-ray measurements for the reaction CuI + 2HgBrI reaction

d in A^0	I/Io	d in A^0	I/Io
6.55x	100	2.50+	8
5.38+	20	2.37x	15
3.95x	8	2.22x	15
3.78x	65	2.13+	68
3.48+	100	2.03	56
3.40+x	55	1.97x	10
3.30	100	1.80x	10
2.94x	30	1.73	35
2.84	2	1.51+x	8
2.71+	10	1.40+	60
2.63+	25		

+ lines for β-Cu_2HgI_4 [4] Unmarked lines are for γ-CuBr [5]
x lines for HgBrI [7]

Miscibility of reactant and product phases

During the X-ray analysis of products obtained in different molar mixtures of reactants (Table II) it was observed that the d values of Cu_2HgI_4 has decreased in all the molar ratios, while those of CuBr and HgBrI have increased. Wherever CuI was present in excess, it was miscible with CuBr to some extent. This is understood by the fact that both CuI and CuBr have cubic structure, which will facilitate the miscibility. Both CuBr and HgBrI are soluble very slightly in Cu_2HgI_4, but Cu_2HgI_4 is soluble in CuBr and HgBrI. Miscibility of Cu_2HgI_4 and HgBrI was checked by mixing them in 2:1 molar ratio and keeping it at 120°C for more than three days. Although, the colour of the mixture was altogether different from that of the original one, but the X-ray analysis showed that no new product was obtained. However, the d values of HgBrI were significantly increased while that of Cu_2HgI_4 were diminished to about the same extent.

Mechanism of Lateral diffusion

During the lateral experiments it was observed that immediately after mixing HgBrI with CuI, a red boundary formed at the interface, which grew on the CuI side with time. Soon it separated into brown and white pale layers. A gap developed between HgBrI and product layers at the same time. In another

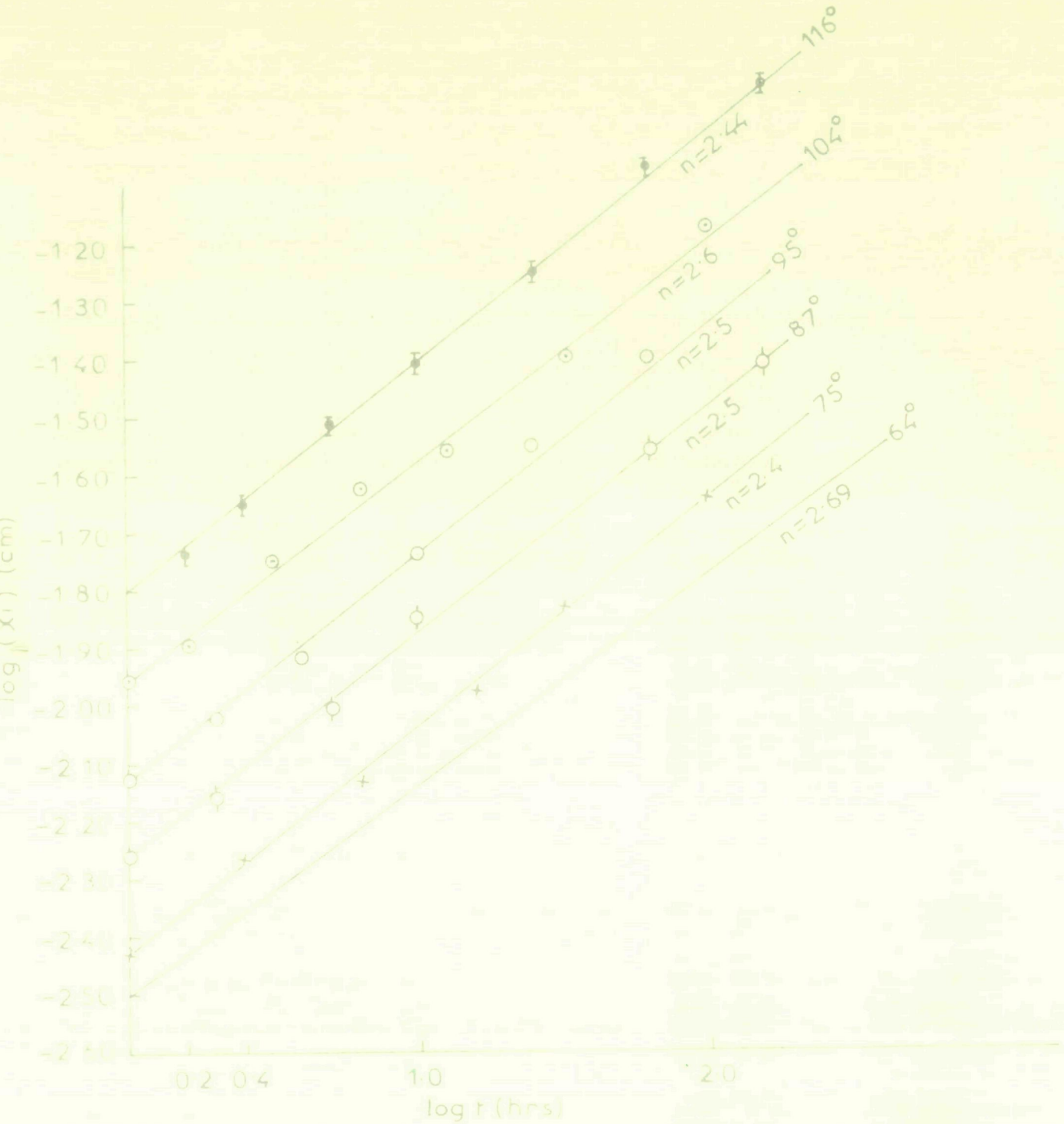

FIG. 3. KINETIC DATA FOR LATERAL DIFFUSION AND THE TEST OF EQUATION $x^n = Kt$ FOR THE REACTION BETWEEN CuI AND HgBrI

experiment with an air gap between HgBrI and CuI, it was observed that similar layers were formed which clearly demonstrate that HgBrI reacts via gaseous phase. At the reaction zone, HgBrI vapour surrounds each CuI grain and reacts through counter diffusion of Cu^{+} and Hg^{2+} with the simultaneous separation of CuBr and Cu_2HgI_4.

Reaction at the interface, where HgBrI vapours are in contact with CuI, are represented as

$$HgBrI + 2Cu^{+} \longrightarrow CuBr + CuI + Hg^{2+} \qquad (2a)$$

Reaction at the interface, where CuI grains are in contact with Hg^{2+} ions beyond CuBr layer, are represented as

$$\frac{4CuI + Hg^{2+} \longrightarrow Cu_2HgI_4 + 2Cu^{+}}{HgBrI + 3CuI \longrightarrow Cu_2HgI_4 + CuBr} \qquad (2b)$$

The CuI formed in reaction (2a) is immediately consumed. As the reaction proceeds, the rate of reaction decreases with time. In other words, with the increase in the thickness of the product layers, the rate decreases. The initial increase in the thickness is due to the fact that the chemical reaction is much faster than the diffusion process. The increase in thickness results in decrease of the diffusion in the reactions, and hence reaction rate falls gradually.

FIG. 4 DEPENDENCE OF K ON TEMPERATURE FOR THE REACTION BETWEEN HgBrI AND CuI

For lateral diffusion, the kinetic data fit best (fig. 1c) in the equation

$$x_i^n = Kt$$

Where x_i is the total thickness of the product at time t and K and n are constant. K is related to the diffusion co-efficient and follows the Arrehenius equation (fig. 4). The activation energy, measured from log K vs. $\frac{1}{T}$ plot, is 21.07 Kcal/mole.

REFERENCES

1. Fiegel, F. and Anger, V.: Spots Tests in Inorganic Analysis (Elsevier Publishing Company) 1972, pp. 203, 145 and 147 respectively.

2. Ibid. pp. 307 and 309; 203 and 249 respectively.

3. Wagner, C.: B34, 317 (1936).
Pinnock, A.T.: J. Soc. Chem. Ind. 38, 78 (1919).

4. X-ray Diffraction Data pp. 89 Chapter III.

5. ASTM X-ray Diffraction Data File No. 6-0292.

6. ASTM X-ray Diffraction Data File No. 6-0246.

7. X-ray Diffraction Data File (In press). Cf. pp 88 Chapter III.

C H A P T E R - V

REACTION OF CuI - $HgBr_2$

Cuprous iodide and mercuric bromide give scarlet colour product immediately after they are mixed, which becomes dark brown coloured when put above 70°C.

Rate Measurements

The kinetics of the reaction were studied by placing mercuric bromide over cuprous iodide (both about 300 mesh size) in a vertical pyrex glass tube as described in the preceding chapter.

As soon as $HgBr_2$ powder was placed over cuprous iodide in the tube, a scarlet colour boundary appeared at the interface which grew with time on the cuprous iodide side. After sometime, a pale yellow product started to develope between $HgBr_2$ and the scarlet product, and a gap developed between $HgBr_2$ and the light yellow product. On cooling, the dark brown product turned to scarlet below 70°C (Cu_2HgI_4 is scarlet below 70°C and dark brown above this temperature). The brown and light yellow layers grew simultaneously. The rate of the reaction was followed by measuring the total thickness of the brown and light layers. The rate constants for different sets are tabulated in Table I.

TABLE - I

Dependence of parameters of equation $x_1^n = Kt$ on temperature for CuI-$HgBr_2$ reaction

Temperature °C	K (cm/hr)	n
98	7.58×10^{-6}	2.0
110	2.18×10^{-5}	1.99
124	6.60×10^{-5}	1.90
131	8.31×10^{-5}	1.91
142	9.33×10^{-5}	2.01
155	10.50×10^{-5}	1.99

Analysis of the product layers

A reaction tube having thick distinct scarlet and light yellow product layers was broken carefully, and the layers were separated. Each layer was analysed for Cu^+, Hg^{2+} and I^- and Cu^+, Br^- ions respectively by spot tests[1] after dissolving them in concentrated nitric acid separately. X-ray diffraction pattern showed light yellow layer to be single phase γ-CuBr; and scarlet layer to be single phase β-Cu_2HgI_4. The results of chemical analyses agreed with this finding.

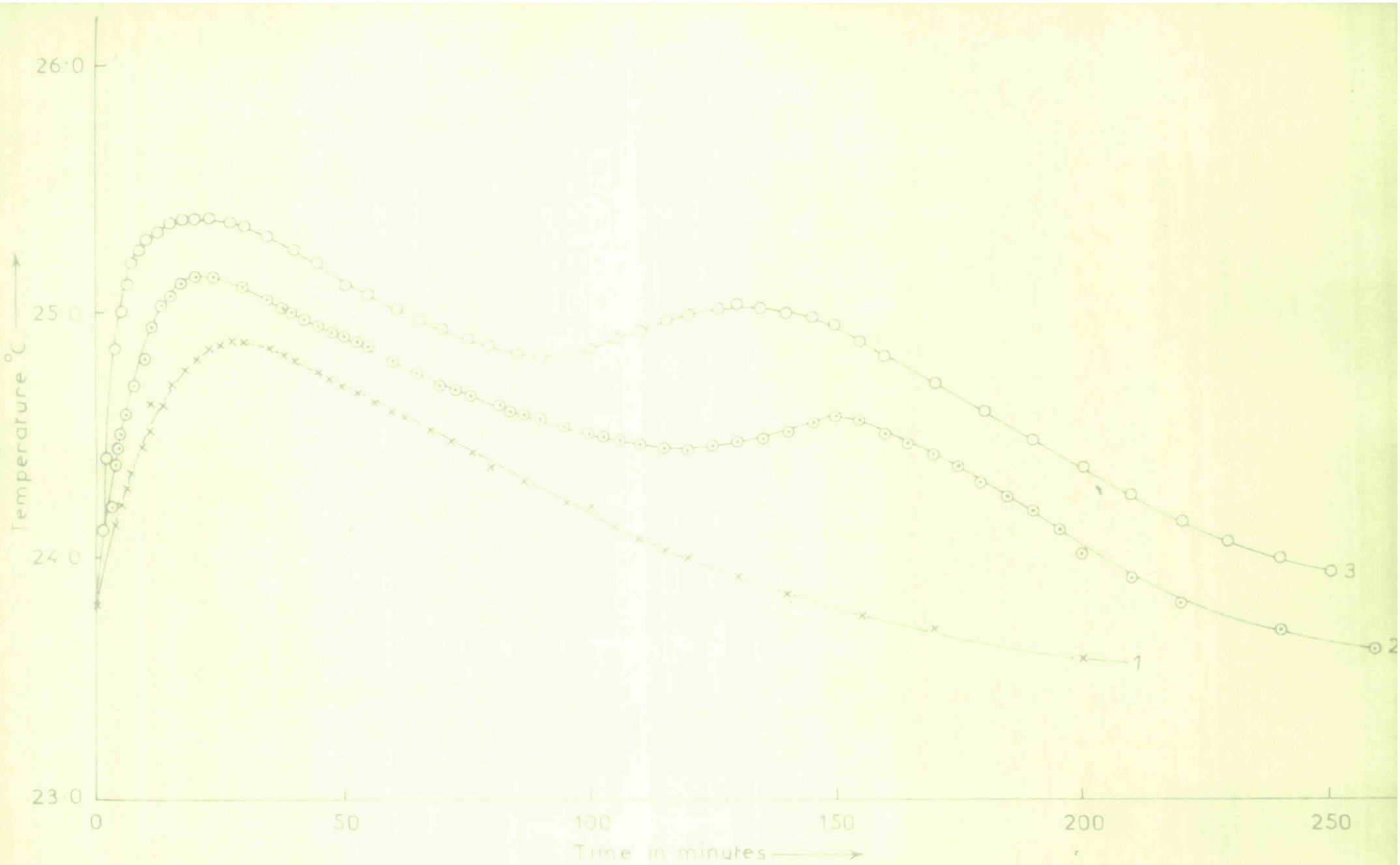

FIG. 2a TEMPERATURE RISE AS A FUNCTION OF TIME FOR THE REACTION BETWEEN CuI AND $HgBr_2$ AT MOLAR RATIOS OF (1) 4:1 (2) 2:1 & (3) 1:2.

X-ray Studies

The reactants cuprous iodide and mercuric bromide in different molar ratios were mixed thoroughly in a mortar. One part of the mixtures were kept at about 120°C in an air thermostat for three days. X-ray diffraction patterns of all reaction mixtures were taken at the room temperature by a Norelco Geiger Counter X-ray Diffractometer by CuK_{α} radiation with a Ni-filter, applying 32KV at 12 mA current. The compounds were identified by calculating the d values of the lines and corresponding intensities of the lines and comparing them with the standard values of the expected compounds. The compounds obtained in different mixtures at room temperature and at 120°C are given in Table II. The X-ray diffraction patterns at room temperatures were taken after half an hour by mixing cuprous iodide and mercuric bromide in the similar molar mixture ratios.

Thermal and conductance measurements

Thermal studies, with amounts of CuI and $HgBr_2$ in molar ratios of 4:1, 2:1 and 1:1 weighed separately, were carried out in the similar fashion as described earlier, and the results are shown in figure (2a).

Conductivity measurements for the molar mixture 4:1, 3:1, 2:1, 1:1 and 1:2 of cuprous iodide and mercuric bromide were done as described earlier, and the results are depicted in figure (2b).

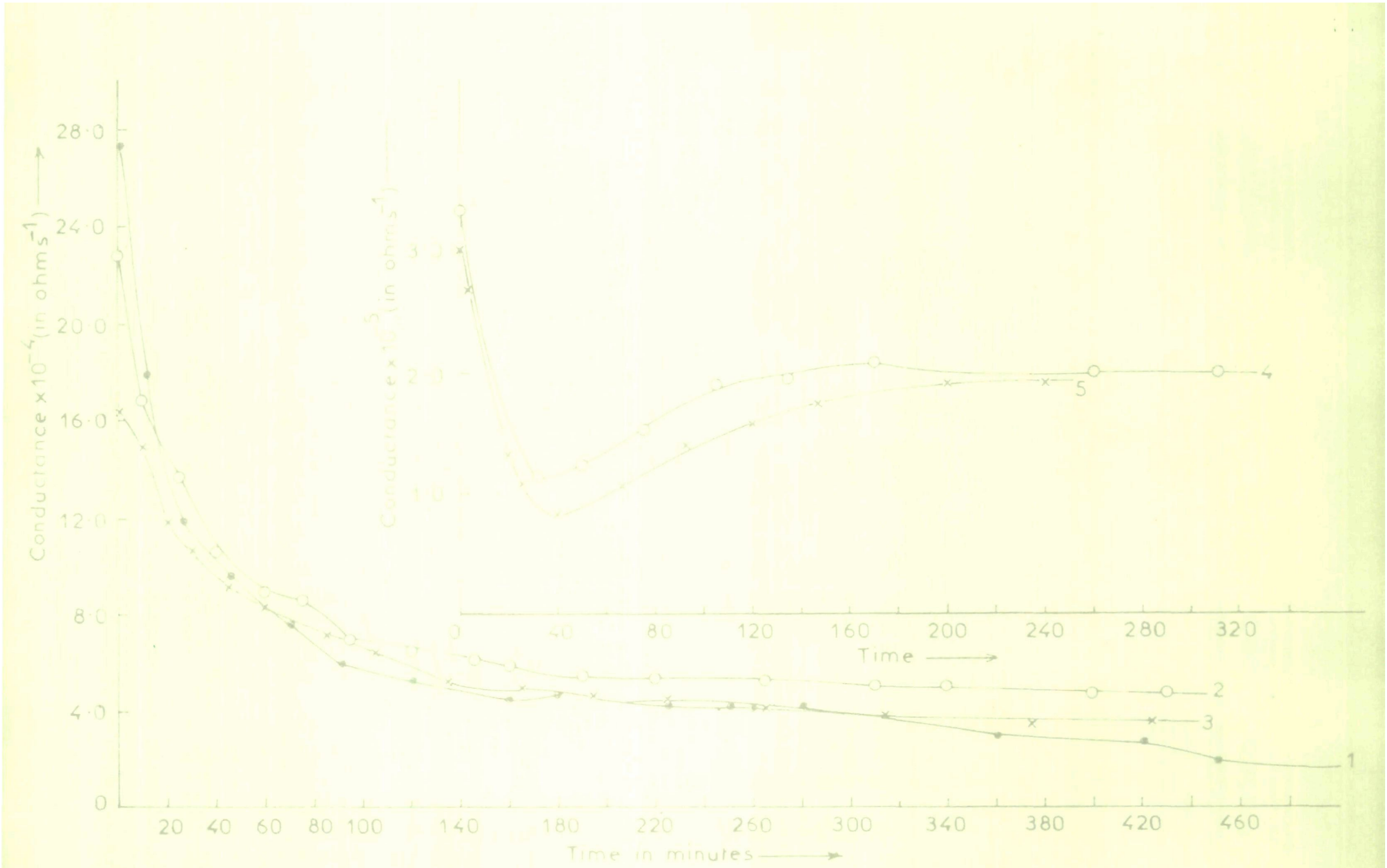

FIG.2b CONDUCTIVITY CHANGE AS A FUNCTION OF TIME FOR THE REACTION BETWEEN CuI & $HgBr_2$ AT 30 °C. MOLAR RATIOS OF CuI: $HgBr_2$ ARE (1) 4:1, (2) 3:1, (3) 2:1, (4) 1:1, (5) 1:2.

TABLE - II

Compounds present in different molar ratio mixtures of CuI and $HgBr_2$

Mixture	Molar Ratio of CuI:$HgBr_2$	Compounds identified at room temperature	Compounds identified at 120°C
a	4:1	Cu_2HgI_4, CuBr, HgI_2	Cu_2HgI_4, CuBr
b	3:1	Cu_2HgI_4, CuBr, HgBrI, HgI_2	Cu_2HgI_4, CuBr and HgBrI
c	2:1	Cu_2HgI_4, CuBr, HgBrI and HgI_2	Cu_2HgI_4, CuBr, Cu_2HgI_4
d	1:1	CuBr, HgBrI, Cu_2HgI_4	CuBr, HgBrI
e	1:2	$HgBr_2$, HgBrI, Cu_2HgI_4, CuBr	$HgBr_2$, HgBrI and $CuHgBr_3$

Results and Discussion

Table II clearly indicates that $HgBr_2$ and cuprous iodide react differently in different molar mixtures.

A 4:1 molar mixture of cuprous iodide and $HgBr_2$ maintained at 120° for about three days after mixing them together gave the evidence of only Cu_2HgI_4 and CuBr as the end products.

$$HgBr_2 + 4\ CuI \longrightarrow Cu_2HgI_4 + 2CuBr \qquad (1)$$

Thermal measurements (fig. 2a,1) made with a 4:1 molar mixture of CuI and $HgBr_2$ at room temperature gave no indication of any sub-step involved in reaction described by (1). Conductance measurements also leads to the same conclusion, because there is only one inflection in the curve (fig. 2b,1). The decrease in the curve is due to the fact that the conductivity of cuprous iodide is higher than that of the resulting product Cu_2HgI_4. In fact, it is almost a conductor[2]. Nevertheless, X-ray pattern of molar mixture 4:1, kept at room temperature for about 24 hours after mixing showed the presence of HgI_2 lines, besides Cu_2HgI_4 and CuBr. This is indeed a clear indication that HgI_2 is also formed during the reaction, which is being consumed immediately after by CuI in the mixture to form Cu_2HgI_4; and ultimately disappears at higher temperatures. Therefore, the reaction is proceeding via the formation of HgI_2. Hence, at room temperature,

$$4CuI + HgBr_2 \longrightarrow 2CuBr_2 + HgI_2 + 2CuI \qquad (2a)$$

The formation of HgI_2 raises two questions:
Firstly, soon after the formation, HgI_2 may react with $HgBr_2$ to give HgBrI by the following reaction:

$$HgI_2 + HgBr_2 \longrightarrow 2HgBrI \qquad (2b)$$

which is known to be formed in solid state at high temperatures more easily[3].

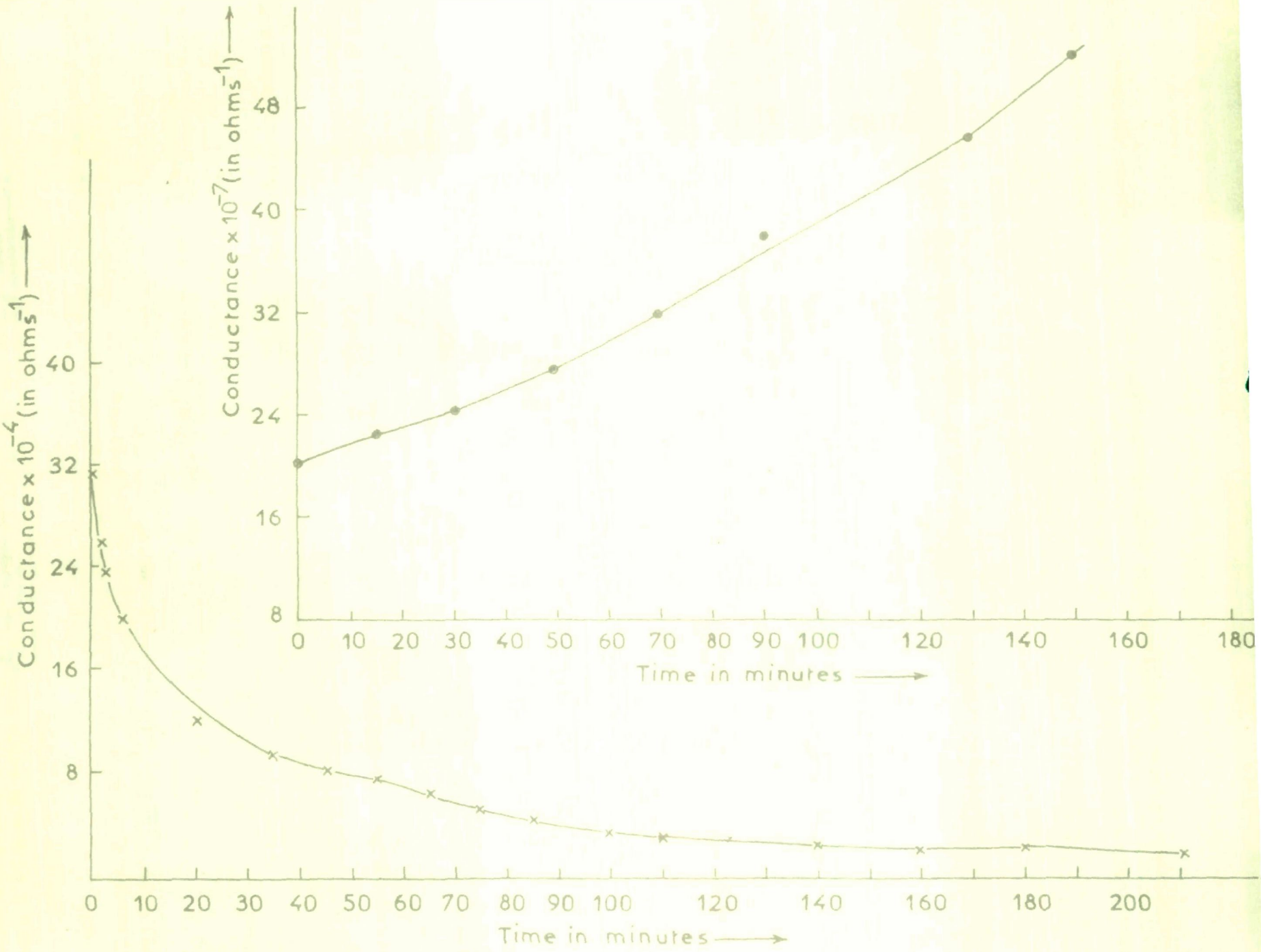

FIG. CHANGE IN CONDUCTANCE AS A FUNCTION OF TIME FOR (i) $2CuI + HgI_2$ & (ii) $HgI_2 + HgBr_2$ REACTION.

Secondly, HgI_2 may react with the excess of CuI in the reaction mixture to give Cu_2HgI_4:

$$2CuI + HgI_2 \longrightarrow Cu_2HgI_4 \qquad (2c)$$

To check these two alternatives, conductance measurements had been carried out for the individual reaction of (2b) and (2c). The results for (2b) reaction showed that conductance increase constantly, while for the reaction given by (2c), it decreases with time. Also, the former reaction was very very slow, almost not occurring at room temperature, while the latter seems to be comparatively much faster, and which is known to be occurring very fast[4]. Therefore, it appears that consumption of HgI_2 formed in the initial stage, by $HgBr_2$ to give HgBrI is not as probable as the one which leads to the formation of Cu_2HgI_4 according to equation (2c); because in the conductivity measurement studies for 4:1 molar mixture of CuI and $HgBr_2$ (fig. 2b,1), there is a gradual decrease in the conductivity.

The overall reaction may be written as:

$$2CuI + HgBr_2 \longrightarrow HgI_2 + 2CuBr \qquad (1a)$$

$$2CuI + HgI_2 \longrightarrow Cu_2HgI_4 \qquad (1b)$$

$$4\ CuI + HgBr_2 \longrightarrow Cu_2HgI_4 + 2\ CuBr$$

The d values and the intensities of the lines of the X-ray pattern of 4:1 molar mixture of CuI and $HgBr_2$ at 120°C are given in Table III.

TABLE - III

X-ray measurements for the reaction mixture 4 CuI + $HgBr_2$

d in A^0	I/Io	d in A^0	I/Io
5.39x	20	1.81x	58
3.45x	100	1.80x	8
3.34+	100	1.74+	30
2.98x	8	1.49x	30
2.11x	65	1.48x	30
2.04+	56	1.37x	12

+ lines correspond to $CuBr$[4]
x lines correspond to Cu_2HgI_4[5]

The X-ray patterns for molar mixture 3:1 of CuI and $HgBr_2$ (Table II) showed that the compounds identified in the mixture maintained at 120°C for three days and cooled to room temperature are Cu_2HgI_4, HgBrI and CuBr:

$$9\ CuI + 3\ HgBr_2 \longrightarrow 2\ Cu_2HgI_4 + HgBrI + 5\ CuBr \qquad (3)$$

The thermal and conductance measurements showed only one clear inflection. There was, however, a slight second inflection in the thermal measurement after about an hour, which was not observed in the conductivity measurements (fig. 2a,2 & 2b,2). The presence of HgI_2 in the mixture maintained at room temperature shows that this reaction of 3:1 molar ratio also

goes via HgI_2 formation; which resulted in the formation of Cu_2HgI_4 (Step 2a). HgBrI formation is explained by the fact that HgI_2 formed in the initial step may combine with $HgBr_2$ in equimolar ratio to give HgBrI, but as described in the case of the 4:1 molar mixture reaction, this is not likely to occur as compared to the formation of Cu_2HgI_4 in the presence of CuI in the reaction mixture. Hence, it is more likely that excess $HgBr_2$ reacts with Cu_2HgI_4 formed in the reaction to produce HgBrI and CuBr. HgBrI formed in this way, may combine with the remaining CuI in the mixture to form Cu_2HgI_4 and CuBr. The overall reaction may therefore, be written as:

$$6\ CuI + 3\ HgBr_2 \longrightarrow 6\ CuBr + 3\ HgI_2 \qquad (3a)$$

$$6\ CuI + 3\ HgI_2 \longrightarrow 3\ Cu_2HgI_4 \qquad (3b)$$

$$Cu_2HgI_4 + 3\ HgBr_2 \longrightarrow 2\ CuBr + 4\ HgBrI \qquad (3c)$$

$$6\ CuI + 2\ HgBrI \longrightarrow 2\ Cu_2HgI_4 + 2\ CuBr \qquad (3d)$$

$$18\ CuI + 6\ HgBr_2 \longrightarrow 4\ Cu_2HgI_4 + 2\ HgBrI + 10\ CuBr$$

The step (3c) was confirmed by mixing Cu_2HgI_4 and $HgBr_2$ in the molar ratio 1:3 and heated for two days and the products were analysed by X-ray diffraction (Table IV); which showed that only CuBr and HgBrI were present in the product. The step (3c) has been already discussed in the preceding chapter. Nevertheless, in the reaction mixture 3:1 CuI and $HgBr_2$, the steps (3c) and (3d) are supposed to take place simultaneously

which is perhaps the reason that when conductance measurements studies were carried out, there was no evidence for these steps (fig. 2b,2).

TABLE - IV

X-ray pattern for the reaction Cu_2HgI_4 + 3 $HgBr_2$

d in A°	I/Io	d in A°	I/Io
6.50x	100	2.76x	28
3.91x	8	2.69	
3.69x	61	2.07x	7
3.37x	48	2.02+	56
3.32+	100	1.77+	34
2.89x	30	1.49x	7

x lines for $HgBrI$[6]
+ lines for $CuBr$[4]

The d values and I/Io of 3:1 molar mixture of CuI and $HgBr_2$ measured from the X-ray diffraction patterns are tabulated in Table V.

TABLE - V

X-ray diffraction pattern for the reaction 3 CuI + $HgBr_2$

d in A°	I/Io	d in A°	I/Io
6.56+	100	2.37+	10
5.39x	21	2.15x	68
3.76+	62	2.05x*	55
3.49x	100	1.98+	10
3.39x	30	1.82x	52
3.36+	45	1.81x	15
3.29*	100	1.75*	30
2.98+		1.59x	20
2.62x	25	1.23x	20

+ lines for $HgBrI$[6] * lines for $CuBr$[4]
x lines for Cu_2HgI_4[3]

The X-ray diffraction pattern taken with 2:1 molar mixture of CuI and $HgBr_2$ showed that Cu_2HgI_4, CuBr and HgBrI were the end product at the temperature 120°C (Table II). At room temperature, however, HgI_2 was also present in addition to all other products present at high temperature.

Thermal and conductance measurements studies at room temperature showed (fig. 2a, 3 and fig. 2b,3) that the reaction might be occurring in a way similar to that in 3:1 molar mixture of CuI and $HgBr_2$. The mechanism may, therefore, be written as:

$$6\ CuI + 3\ HgBr_2 \longrightarrow 6\ CuBr + 3\ HgI_2$$

$$6\ CuI + 3\ HgI_2 \longrightarrow Cu_2HgI_4$$

$$Cu_2HgI_4 + 3\ HgBr_2 \longrightarrow 2\ CuBr + 4\ HgBrI$$

$$12\ CuI + 6\ HgBr_2 \longrightarrow 8\ CuBr + 4\ HgBrI$$

The identification of products in 1:1 molar mixture and 1:2 molar mixture of CuI and $HgBr_2$ revealed that CuBr and HgBrI; and HgBrI and $CuHgBr_3$ were present respectively at the temperature 120°C (Table II):

$$CuI + HgBr_2 \longrightarrow CuBr + HgBrI \qquad (4)$$

and $$CuI + 2\ HgBr_2 \longrightarrow HgBrI + CuHgBr_3 \qquad (5)$$

Looking at the reaction, it seems as if simple exchange reaction is taking place. But this is not indeed the case. When the two reactants in the former case were mixed at room temperature, they formed a scarlet product which gradually turned to

yellow. This is an ample proof that an intermediate of scarlet colour is formed, and the reaction is not a mere exchange reaction. The thermal and conductance measurements also showed that this reaction is a multi-step reaction (fig. 2a,4 and fig. 2b,4). X-ray diffraction pattern taken after about 6 hour indicated the presence of Cu_2HgI_4. However, X-ray studies of the same molar mixture kept at room temperature taken just after half an hour showed the presence of HgI_2. HgI_2 immediately react with CuI to give Cu_2HgI_4[7]. X-ray diffraction studies after 5 days showed only the presence of HgBrI and CuBr, as the same in the reaction mixture at 120°C. In the light of all these facts, the reaction sequence in 1:1 molar mixture of CuI and $HgBr_2$ may be described as:

$$2\ CuI + HgBr_2 \longrightarrow 2\ CuBr + HgI_2 \qquad (4a)$$

$$2\ CuI + HgI_2 \longrightarrow Cu_2HgI_4 \qquad (4b)$$

$$Cu_2HgI_4 + 3\ HgBr_2 \longrightarrow 4\ HgBrI + 2\ CuBr \qquad (4c)$$

Predominant

$$4\ CuI + 4\ HgBr_2 \longrightarrow 4\ HgBrI + 4\ CuBr$$

The fall in conductance (fig. 2b,4) is the indication that Cu_2HgI_4 is formed, and the rise in conductance shows the formation of HgBrI.

The X-ray diffraction pattern for equimolar mixture of CuI and $HgBr_2$ are shown in Table VI.

TABLE - VI

X-ray measurements for the reaction CuI + $HgBr_2$

d in A°	I/Io	d in A°	I/Io
6.58x	100	2.32x	15
3.89x	8	2.30x	15
3.76x	63	2.20x	11
3.35x	50	2.01+	55
3.29+	100	1.92x	10
		1.78x	10
2.93x	25	1.72+	30
2.77x	25	1.66x	8

+ lines correspond to CuBr[4]
x lines correspond to HgBrI[6]

The X-ray analysis showed that CuI and $HgBr_2$ in the molar ratio 1:2 react in a way similar to the 1:1 molar mixture of CuI and $HgBr_2$. Unlike in 1:1 molar mixture, CuBr was not found in the ultimate analysis of X-ray diffraction pattern. This is because CuBr formed during the reaction combined with the excess of $HgBr_2$ to give $CuHgBr_3$; which was earlier prepared by mixing equimolar ratio of CuBr and $HgBr_2$, which produced a yellow product. $[HgBr_3]^-$ ion is known and its salts are also prepared in non-aqueous media[7] with potassium. However, the

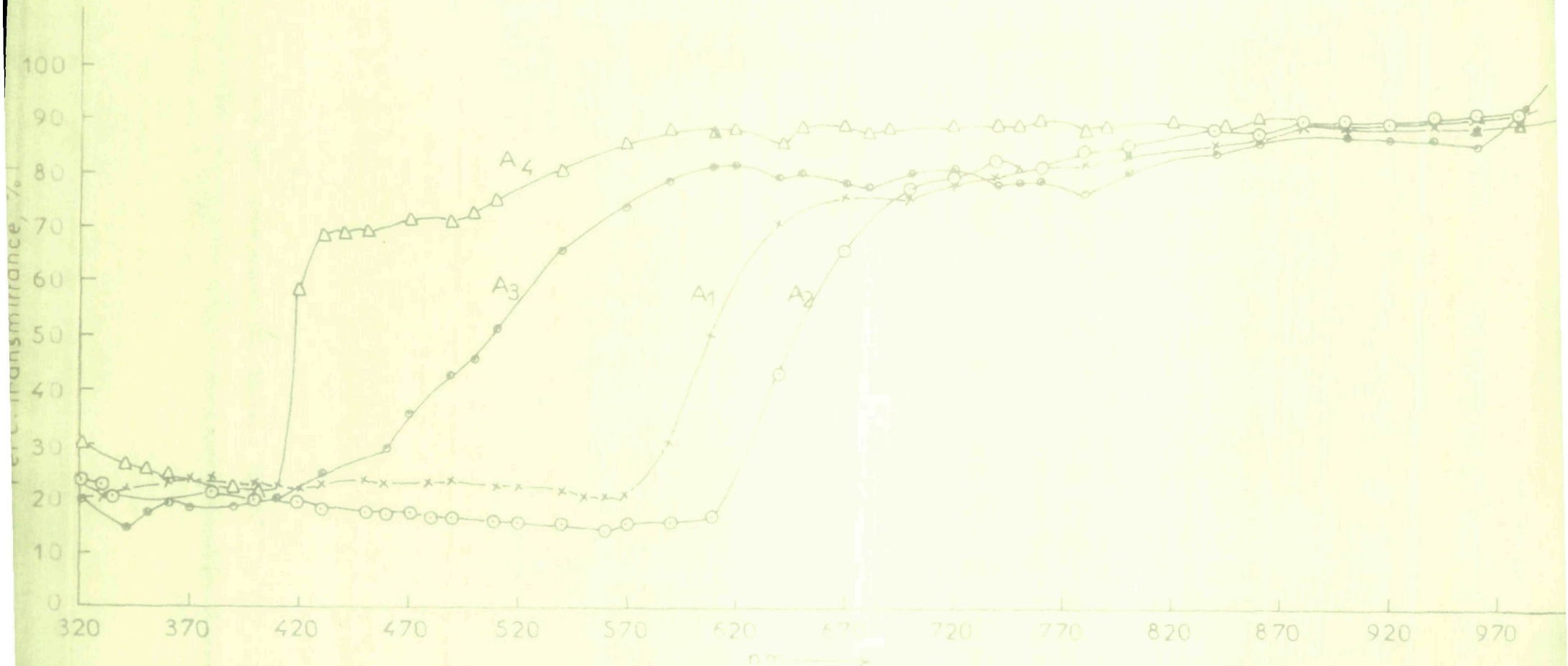

FIG. 3 REFLECTANCE SPECTRA FOR THE REACTION BETWEEN CuI + $HgBr_2$

(i) A_2, 4:1 (ii) A_1, 3:1 (iii) A_3, 2:1 (iv) A_4, 1:1

complex ion is not seemed to be reported in solid state. The compound $CuHgBr_3$ was prepared by mixing cuprous bromide and $HgBr_2$ in a molar ratio 1:1, and heating at 70°C for about five days. The reflectance studies (fig. 3) for 1:2 molar mixture showed that the product formed is different from the one obtained in 1:1 molar mixture reaction. The product is yellow. The X-ray data for this compound is given in Table VII.

TABLE - VII

X-ray measurements for the reaction product of CuBr + $HgBr_2$

d in A°	I/Io	d in A°	I/Io
5.99	42	2.15	56
4.92	25	2.13	70
3.86	42	2.07	50
3.74	71		
3.10	46	2.03	28
2.75	64		
2.59	12	1.92	20
2.49	35	1.87	15
2.28	100	1.72	14
2.19	15	1.64	8
2.17	48	1.54	28
		1.37	25
		1.24	18

The reaction sequence of 1:2 molar ratio of CuI and $HgBr_2$ may be written as:

$$4\ CuI + 8\ HgBr_2 \longrightarrow 7\ HgBr_2 + 2\ CuI + HgI_2 + 2\ CuBr$$

$$2\ CuI + HgI_2 \longrightarrow Cu_2HgI_4$$

$$3\ HgBr_2 + Cu_2HgI_4 \longrightarrow 4\ HgBrI + 2\ CuBr$$

$$4\ CuBr + 4\ HgBr_2 \longrightarrow 4\ Cu\ HgBr_3$$

$$4\ CuI + 8\ HgBr_2 \longrightarrow 4\ HgBrI + 4\ Cu\ HgBr_3$$

The X-ray studies for this molar mixture is given in table VIII.

TABLE - VIII

X-ray measurements for the reaction between CuI and $HgBr_2$ in the molar ratio 1:2

d in A^o	I/Io	d in A^o	I/Io
6.55x	100	2.35x	15
5.99+	40	2.28+	100
3.85+	25	2.13+	62
3.71x	65	2.04+	25
3.36x	45	1.98+	
3.10+	45	1.76+x	14
2.92x	35	1.69+	7
2.75x	28	1.61+	5
2.49+	25	1.54+	25

x lines correspond to $HgBrI$[6]

+ lines correspond to $CuHgBr_3$[7]

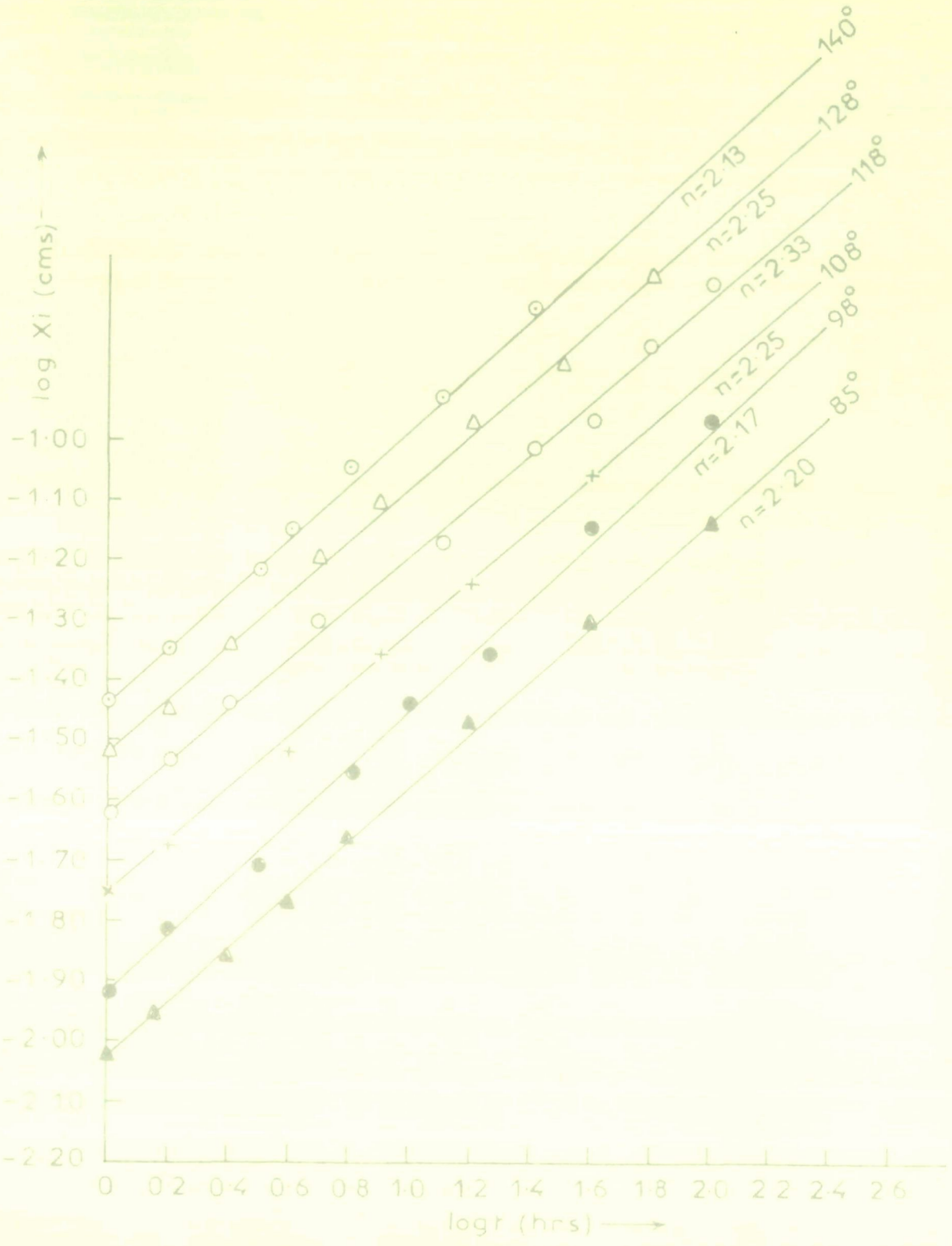

FIG 3 KINETIC DATA FOR LATERAL DIFFUSION AND TEST FOR EQUATION $X_i^n = Kt$ FOR CuI AND $HgBr_2$ REACTION.

FIG 4 DEPENDENCE OF K ON TEMPERATURE FOR THE REACTION BETWEEN CuI & $HgBr_2$.

Mechanism of lateral diffusion

In lateral diffusion experiments, it was observed that a dark red chocklate colour formed at the interface immediately after placing $HgBr_2$ over CuI, which grew with time on CuI side and soon separated into pale yellow and chocklate colour layers. A gap developed between $HgBr_2$ and the product layers. This implies that $HgBr_2$ reacts with CuI via gaseous state. $HgBr_2$ like HgBrI react with the CuI grain at the interface via counterdiffusion of Cu^+ and Hg^{2+} through product layers. Growth of the thickness of the product layers follows the Jander's equation $X_1^n = Kt$ (fig. 4), where X_1 is the total thickness of the product layers at time t and n and K are constants. The values for n and k at various temperature are given in Table I. The values of n are almost constant, and varies within 2.13 to 2.33, which may be taken almost equal to 2. The activation energy was calculated by plotting lok K Vs 1/T (fig. 5), which came out to be 22.91 Kcal/mole. The activation energy clearly suggest that this is a diffusion controlled reaction, in other words, diffusion is slower than the chemical reaction between $HgBr_2$ and CuI.

The formation of solid solutions between the systems CuBr - CuI; Cu_2HgI_4 - CuBr, and HgBrI - Cu_2HgI_4 which was noted during the study of HgBrI-CuI reaction was also observed during X-ray analysis of the product in this system. However, no attempt have been made to study it systematically.

REFERENCES

1. Fiegel, F. and Anger, V.: Spots Tests in Inorganic Analysis (Elsevier Publishing Company, Amsterdam), 1972, pp. 203; 145; 307, 309 and 249.

2. Badeker, K.: Ann. Physik (4), 22, 749 (1907); Phys. Zeit. 9, 437 (1908); Trumpler, G: Zeit. Phys. Chem. 99, 9 (1921).

3. Pinnock, A.T.: J. Soc. Chem. Ind. 38, 78 (1919).

4. ASTM Diffraction Data File No. 6-0292.

5. X-ray Diffraction data, pp.88 Chapter III.

6. X-ray Diffraction data (In press), Cf. pp.89 Chapter III.

7. Wagner, C.: B34, 317 (1936).

8. Yankov, P. and Krasnousova, I.G.: Zh. Neorg. Khim. 16(2), 557 (1971).

9. X-ray Diffraction data, pp.117, Chapter III.

C H A P T E R - VI

REACTION OF CuI - $HgCl_2$

Experimental

The mixing of powdered cuprous iodide and mercuric chloride produced scarlet colour product immediately; the colour of this product gradually fainted with time. At temperature above 70°C, the colour of the product changed to dark brown, which was restored again to its original colour below 70°C.

Kinetic Measurements

The kinetic measurements of CuI and $HgCl_2$ (both about 300 mesh size) were carried out as in the case of CuI and HgBrI or CuI-$HgBr_2$ reaction, described in the preceeding chapters.

As soon as $HgCl_2$ powder was placed over CuI layer in the tube, a dark brown layer appeared immediately at the interface which grew on CuI side. After sometime, there appeared another layer of white colour, and at the same time a gap developed between the white layer and $HgCl_2$ interface. The kinetics were followed by measuring the total thickness of the product layers. The rates were measured at different temperatures. At each temperature, three sets under as an identical condition as possible were run and the averages of the respective values of the three different sets are reported in Table 1.

Analysis of the product layers

A reaction tube having two distinct layers of the product was broken carefully and the two layers were collected separately. The chemical analyses by Spot Tests[1] of the white layer showed it to be CuCl and the scarlet layer β-Cu_2HgI_4. The X-ray analysis showed it to be single phase CuCl[2] and βCu_2HgI_4[3].

X-ray studies

Powdered cuprous iodide and mercuric chloride (about 300 mesh size) in different molar ratios were thoroughly mixed in an agate mortar. One part of it was heated in an air oven maintained at 120 $\pm$ 0.5°C for about two days. The other parts were allowed to stand at room temperature for about an hour. The X-ray patterns of either samples were recorded at room temperature. In both cases CuK_α radiation with a Ni-filter was always utilized. The compounds present in the various molar mixtures as identified on the basis of X-ray diffraction are given in Table II.

TABLE - I

Dependence of parameters of equation $x^2 = Kt$ on temperature for CuI-$HgCl_2$ reaction.

Temperature °C	K (cm/hr)	n
80	4.01×10^{-9}	
95	11.11×10^{-9}	2
110	23.33×10^{-9}	
115	43.25×10^{-9}	
121	80.00×10^{-9}	

TABLE - II

Mixture	Molar ratio of CuI $HgCl_2$	Compounds identified in mixtures	
		at room temperature (30°C)(kept for about one hr)	at 120°C (kept for about two days)
a	4:1	CuCl, Cu_2HgI_4, HgI_2	CuCl, Cu_2HgI_4
b	3:1	CuCl, Cu_2HgI_4, HgI_2	CuCl, Cu_2HgI_4, HgI_2
c	2:1	CuCl, Cu_2HgI_4, HgI_2	CuCl, HgI_2
d	1:1	CuCl, Cu_2HgI_4, HgI_2 and $HgCl_2$	CuCl, HgI_2, $HgCl_2$
e	1:2	CuCl, HgI_2 and $HgCl_2$	CuCl, HgI_2, $HgCl_2$

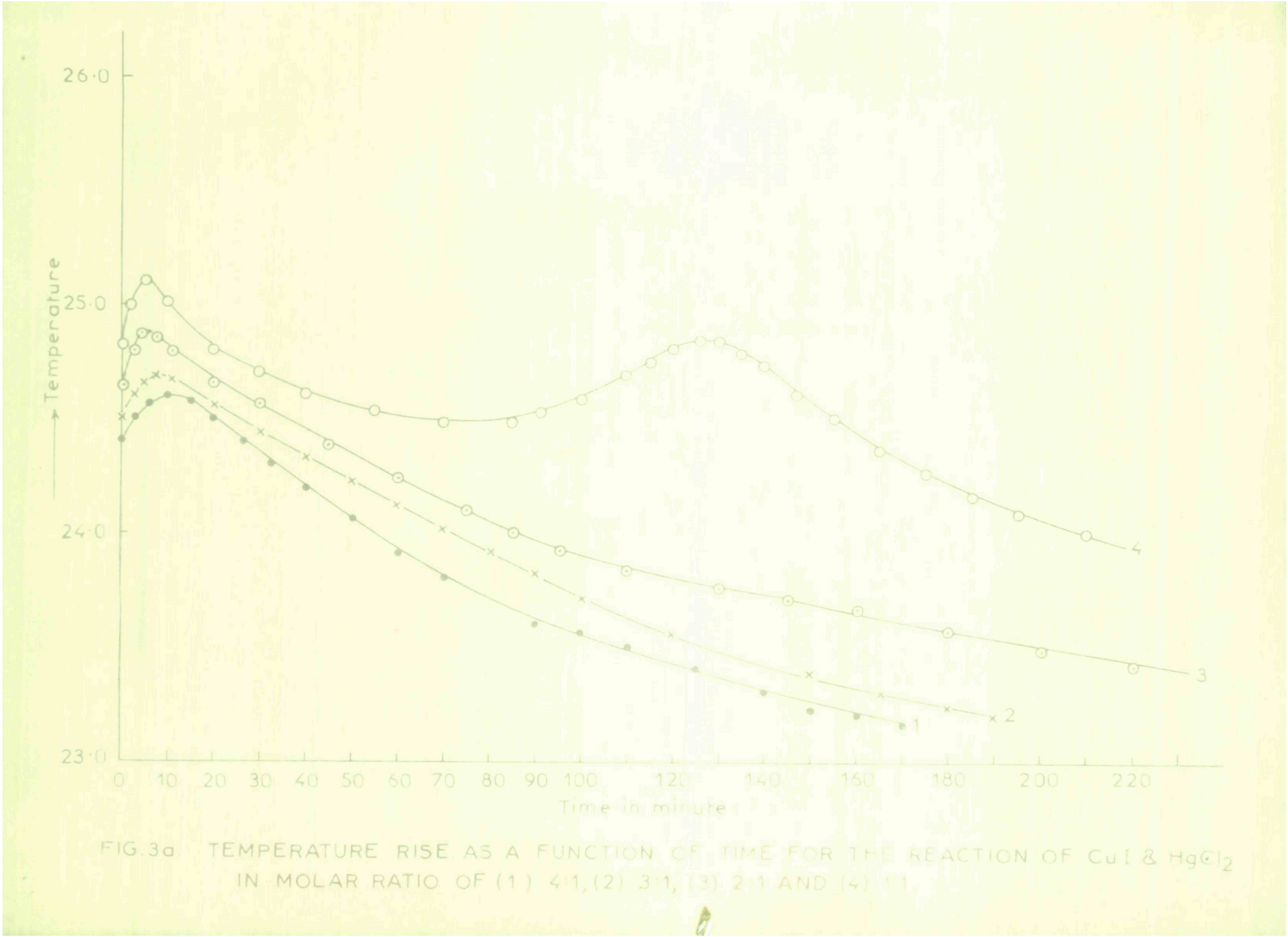

FIG. 3a TEMPERATURE RISE AS A FUNCTION OF TIME FOR THE REACTION OF CuI & $HgCl_2$ IN MOLAR RATIO OF (1) 4:1, (2) 3:1, (3) 2:1 AND (4) 1:1

Thermal analysis and conductance measurements

Thermal studies with amounts of CuI and $HgCl_2$ in molar ratios 4:1, 3:1, 2:1 and 1:1 weighed seperately, were carried out as described earlier for the reaction of CuI-HgBrI and CuI-$HgBr_2$. The results are presented as plot of rise in temperature versus time in figure 3a.

Same proportions of CuI and $HgBr_2$ as weighed for thermal studies, were weighed seperately, mixed thoroughly and pressed into tablets. Conductance of each tablet was measured as described in earlier reactions. The results are shown in figure 3b.

Discussion

It is evident from Table II that CuI reacts with $HgCl_2$ differently in different molar ratios.

In 4:1 molar mixture of cuprous iodide and mercuric chloride heated at 120°C for about two days showed that Cu_2HgI_4 and CuCl were the end product.

$$4\ CuI + HgCl_2 \longrightarrow Cu_2HgI_4 + 2\ CuCl \qquad (1)$$

Thermal as well as conductance measurements (fig. 3a,1 and fig. 3b,1) carried out at room temperature showed no evidence for any sub-steps involved in the 4:1 molar ratio.

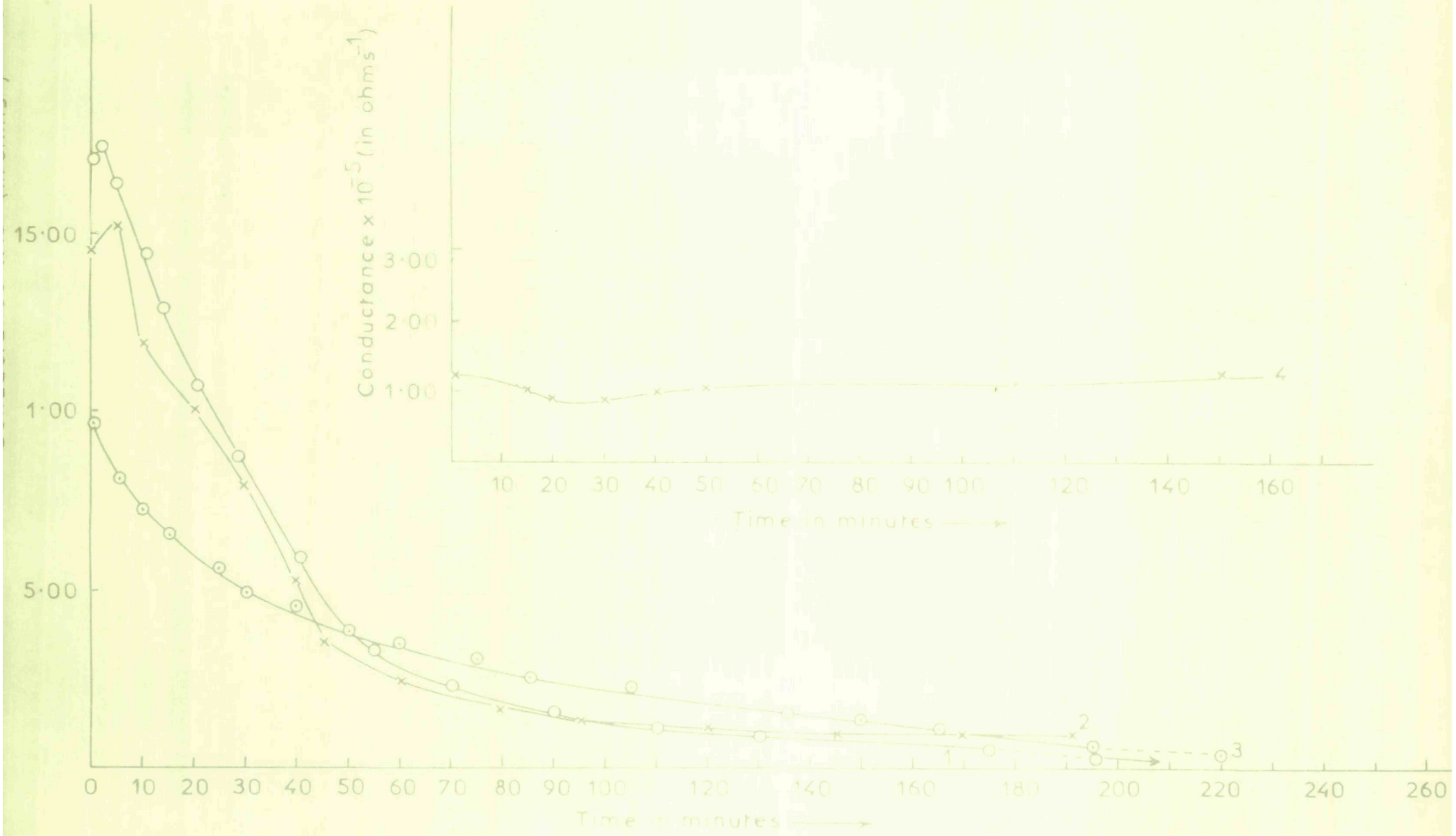

FIG. 3b CHANGE IN CONDUCTANCE AS FUNCTION OF TIME FOR CuI & $HgCl_2$ REACTION.
MOLAR RATIOS (i) 4:1, (ii) 3:1, (iii) 2:1, (iv) 1:1

However, X-ray pattern for 4:1 molar mixture maintained at room temperature gave no evidence for the presence of reactants in the reaction mixture and had lines for CuCl, Cu_2HgI_4 and HgI_2. This suggests that HgI_2 was formed in the initial stage which was immediately taken up either by excess of CuI or $HgCl_2$.

$$2\ CuI + HgCl_2 \longrightarrow 2\ CuCl + HgI_2 \qquad (1a)$$

HgI_2 this formed initially apparently competes to react with CuI and $HgCl_2$ present in the reaction mixture. In other words, the following two reactions are possible

$$2\ CuI + HgI_2 \longrightarrow Cu_2HgI_4 \qquad (1b)$$

$$HgCl_2 + HgI_2 \longrightarrow 2\ HgClI \qquad (1c)$$

The reaction described by (1b) has been established to be very fast[4]; while HgClI is unstable at room temperature, reverting back to its component molecules[5,6]. The X-ray pattern for 4:1 molar mixture heated at 120°C was taken at room temperature, which means that had HgClI formed, there would have been HgI_2 in the final analysis, but the lines for HgI_2 were not to be found. Only Cu_2HgI_4 and CuCl are confirmed. Moreover, equimolar mixture of $HgCl_2$ and HgI_2 at room temperature did not give any evidence for the formation of HgClI at room temperature even after about six days. Hence the possibility that HgI_2 reacts with $HgCl_2$ to form HgClI by step (ii) is a distant

possibility. Furthermore, this is a much slower reaction[5] as compared to the formation[4] of Cu_2HgI_4 and from CuI and HgI_2. Hence the step (i) may be the predominant in comparison to the step (iii). Hence the overall reaction may be written as far a 4:1 molar mixture of CuI and $HgCl_2$:

$$2\ CuI + HgCl_2 \longrightarrow 2\ CuCl + HgI_2 \qquad (i)$$

$$2\ CuI + HgI_2 \longrightarrow Cu_2HgI_4 \qquad (ii)$$

$$4\ CuI + HgCl_2 \longrightarrow Cu_2HgI_4 + 2\ CuCl$$

The X-ray analysis for the 4:1 molar mixture are given in Table III.

TABLE - III

X-ray measurements for 4:1 molar mixture of CuI and $HgCl_2$ heated at 120°C.

d in A°	I/Io	d in A°	I/Io
5.37+	20	1.91x	53
3.49+	100	1.83+	68
3.36+	30	1.63x	28
3.13x	100	1.61+	10
3.02+	12	1.52+	40
2.71x+	8	1.40+	58
2.63+	25	1.27+	15
2.25+	30	1.24+	41
1.99+	30		

x lines correspond to CuCl[2]

+ lines correspond to Cu_2HgI_4[3]

The X-ray analysis for 3:1 molar mixture of cuprous iodide and mercuric chloride, heated at 120°C for about two days, showed the presence of Cu_2HgI_4, CuCl and HgI_2 (Table II). The mixture maintained at room temperature also indicated the same end product (Table II):

$$6\ CuI + 2\ HgCl_2 \longrightarrow Cu_2HgI_4 + 4\ CuCl + HgI_2 \qquad (2)$$

The thermal and conductance measurements did not give evidence for any sub-steps (fig. 3a,? and fig. 3b,2). Nevertheless, the colour changes in the mixture and presence of HgI_2 in the product suggest that mechanism is similar to that of the 4:1 molar ratio of CuI and $HgCl_2$. The presence of HgI_2 lines in the final product is probably due to the fact that CuI and $HgCl_2$ react stoichiometrically in 4:1 molar ratio; whereas, in 3:1 molar mixture, the quantity of CuI is not enough to consume all HgI_2 produced in the initial stage. Therefore, some HgI_2 which is being removed through (2b) will remain unreacted in the mixture. Further, it may be clarified that the presence of HgI_2 in the reaction product can not be due to the formation of HgClI it being unstable, and its subsequent decomposition into $HgCl_2$ and HgI_2. Had it been so, there would have been lines for $HgCl_2$ also. Hence, it can be safely concluded that the lines for HgI_2 in the product is due to the formation of HgI_2 in the initial step:

$$4\ CuI + HgCl_2 \longrightarrow 2\ HgI_2 + 4\ CuCl \qquad (2a)$$
$$2\ CuI + HgI_2 \longrightarrow Cu_2HgI_4 \qquad (2b)$$

$$6\ CuI + HgCl_2 \longrightarrow Cu_2HgI_4 + HgI_2 + 4\ CuCl$$

The d values and the intensity of lines in the 3:1 molar mixture of CuI and $HgCl_2$ are given in Table IV.

TABLE - IV

X-ray measurements for CuI and $HgCl_2$ reaction in 3:1 molar ratio

d in A°	I/Io	d in A°	I/Io
6.20x	25	2.16x	70
5.37+	22	2.13+	68
4.10x	80	1.97+	25
3.56x	100	1.89x*	40
3.49+	100	1.81+	55
3.36+	23	1.74+	8
3.10*	100	1.61*	30
3.00+	10	1.54+	35
2.71+	8	1.39+	40
2.66+	25	1.24+	40
2.23+	30		

x lines for HgI_2 [7]
+ lines for Cu_2HgI_4 [3]
* lines for CuCl [2]

The X-ray analysis of the product of 2:1 molar mixture of CuI and $HgCl_2$ maintained at 120° indicated the presence of only CuCl and HgI_2 (Table II).

$$2\ CuI + HgCl_2 \longrightarrow 2\ CuCl + HgI_2 \qquad (3)$$

Thermal and conductance measurements showed only one clear inflection in the curve (fig. 3a,3 and 3b,3). From equation (3), it appears as if simply exchange reaction is occurring. But, the X-ray analysis of mixture maintained at room temperature showed the presence of Cu_2HgI_4, in addition to CuCl and HgI_2. As Cu_2HgI_4 was not detected in the mixture heated at high temperature (Table II), it is presumed that Cu_2HgI_4 is totally consumed in this condition. The thermal studies (fig. 3a,3) though did not show the second inflection, there was some rise in temperature after about two hours. In other words, the curve does not exactly conform to that of either 4:1 or 3:1 molar mixture of CuI and $HgCl_2$ reaction (fig. 3a,1 or 3a,2). Therefore it may be inferred that some other reaction may be occurring. Since $HgCl_2$ is in excess according to the stoichiometry of the reaction, it may be assumed that this excess amount of $HgCl_2$ reacts with Cu_2HgI_4 to produce HgI_2 and CuCl.

$$Cu_2HgI_4 + HgCl_2 \longrightarrow 2\ HgI_2 + 2\ CuCl \qquad (3e)$$

This step was separately confirmed by heating equimolar mixture of Cu_2HgI_4 and $HgCl_2$ at 120°C. The X-ray pattern of its product showed only the presence of HgI_2 and CuCl. Hence, the overall reaction sequence of the CuI and $HgCl_2$ reaction in 2:1 molar ratio may be described as:

$$2\ CuI + HgCl_2 \longrightarrow HgI_2 + 2\ CuCl \qquad (3a)$$

$$2\ CuI + HgI_2 \longrightarrow Cu_2HgI_4 \qquad (3b)$$

$$Cu_2HgI_4 + HgCl_2 \longrightarrow 2\ HgI_2 + 2\ CuCl \qquad (3c)$$

$$4\ CuI + 2\ HgCl_2 \longrightarrow 2\ HgI_2 + 4\ CuCl$$

The d values and intensities for the expected compounds in 2:1 molar ratio of CuI and $HgCl_2$ are given in Table V.

TABLE - V

X-ray measurements for CuI and $HgCl_2$ reaction in 2:1 molar ratio heated at 120°C

d in A°	I/Io	d in A°	I/Io
6.21x	25	1.90+	50
4.08x	75	1.87x	8
3.56x	100	1.77x	8
3.10+	100	1.65+	31
2.98x	24	1.55+	5
2.75x	35	1.51+	3
2.17x	55	1.43+	2
2.15x	5	1.35x	5
2.07x	3	1.32+	3
1.92x	9	1.24x	8

x lines correspond to HgI_2 [7]
+ lines correspond to CuCl [2]

The identification of products in 1:1 molar mixture of CuI and $HgCl_2$ heated at 120°C for about two days, showed that CuCl, HgI_2 and $HgCl_2$ are the end products (Table II).

$$2\ CuI + 2\ HgCl_2 \longrightarrow 2\ CuCl + HgI_2 + HgCl_2 \qquad (4)$$

The X-ray pattern of the mixture kept at room temperature however, showed the presence of Cu_2HgI_4, in addition to CuCl, HgI_2 and $HgCl_2$.

The detection of Cu_2HgI_4 at room temperature shows that this is, however, not a simple exchange reaction as suggested by equation (4). For, at room temperature, thermal and conductance measurements clearly show that the reaction is a multi-step reaction (fig. 3a,4 and fig. 3b,4). The first inflection in the curve may be due to the formation of HgI_2 in the initial stage by the reaction of CuI and $HgCl_2$. HgI_2 thus formed immediately reacted with CuI to give Cu_2HgI_4. The fall in conductance confirms this step, because Cu_2HgI_4 has much lower conductance value than that of CuI, which is almost a conductor . These may be described as:

$$2\ CuI + HgCl_2 \longrightarrow HgI_2 + 2\ CuCl \qquad (4a)$$

$$2\ CuI + HgI_2 \longrightarrow Cu_2HgI_4 \qquad (4b)$$

The second inflection in the thermal or conductance curve may be due to the slight formation of HgClI by the reaction of Cu_2HgI_4 and excess $HgCl_2$ in the reaction system; which is perhaps the cause of the increase in the conductance. It is interesting to note that in 2:1 molar mixture of CuI and $HgCl_2$, Cu_2HgI_4 reacted with $HgCl_2$ in equimolar ratio to produce HgI_2 and

CuCl (cf. equation 3e). In this case, we have assumed that HgClI is formed by the reaction of Cu_2HgI_4 and $HgCl_2$ as:

$$Cu_2HgI_4 + 3\ HgCl_2 \longrightarrow 4\ HgClI + 2\ CuCl \qquad (4e)$$

This assumption has got some understandable reasoning. When this reaction mixture was heated, the colour of the product mass was yellow. *HgClI is yellow in colour in its stable form* that is at elevated room temperature. When the reaction product was brought to room temperature, the colour becomes red. HgClI is not stable at room temperature, and decomposes into its component HgI_2 and $HgCl_2$ molecules[5,6] as described by the reaction;

$$2\ HgClI \longrightarrow HgI_2 + HgCl_2$$

The colour of HgI_2 which is red gives the product a total red look. The formation of HgClI at room temperature is therefore, difficult, but not an impossible one, hence the second inflection in the thermal and conductance curves may not be ruled out. It may be recalled that in 2:1 molar mixture, there was also some distinction in the latter part of the curve in comparison to 4:1 or 3:1 molar mixture curves (fig. 3a, 3). In 1:1 molar mixture, this distinction has to be more evident, which is the result of the second inflection.

Now, the formation of HgClI from Cu_2HgI_4 and $HgCl_2$ may be explained in two ways:

Firstly, Cu_2HgI_4 may stoichiometrically combine with three molecules of $HgCl_2$ (cf. equation 4c)

$$Cu_2HgI_4 + 3\ HgCl_2 \longrightarrow 2\ CuCl + 4\ HgClI \qquad (4c)$$

Mercury chloro iodide decomposes into HgI_2 and $HgCl_2$ at lower temperature:

$$2\ HgClI \longrightarrow HgI_2 + HgCl_2 \qquad (4d)$$

Formation of HgClI by equation (4c) would lead to the following overall mechanism:

$$2\ CuI + HgCl_2 \longrightarrow HgI_2 + 2\ CuCl \qquad (4a)$$

$$2\ CuI + HgI_2 \longrightarrow Cu_2HgI_4 \qquad (4b)$$

$$Cu_2HgI_4 + 3\ HgCl_2 \longrightarrow 4\ HgClI + 2\ CuCl \qquad (4c)$$

$$2\ HgClI \longrightarrow HgI_2 + HgCl_2 \qquad (4d)$$

$$4\ CuI + 4\ HgCl_2 \longrightarrow 2HgI_2 + 2\ HgCl_2 + 4\ CuCl$$

Secondly, Cu_2HgI_4 formed in step (4b) may combine in equimolar ratio with $HgCl_2$ to form HgI_2 and CuCl as in the case of 2:1 molar ratio reaction

$$Cu_2HgI_4 + HgCl_2 \longrightarrow 2\ HgI_2 + 2\ CuCl \qquad (4e)$$

This HgI_2 reacts with $HgCl_2$ molecules present in excess in the system at elevated temperatures to give HgClI, which decomposes into its component molecules when cooled

$$2\ HgCl_2 + HgI_2 \underset{-\Delta}{\overset{+\Delta}{\rightleftharpoons}} 2\ HgClI \qquad (4f)$$

This assumption would lead to the following reaction sequence.

$$2\ CuI + HgCl_2 \longrightarrow HgI_2 + 2\ CuCl \qquad (4a)$$

$$2\ CuI + HgI_2 \longrightarrow Cu_2HgI_4 \qquad (4b)$$

$$Cu_2HgI_4 + HgCl_2 \longrightarrow 2\ HgI_2 + 2\ CuCl \qquad (4c)$$

$$2\ HgI_2 + 2\ HgCl_2 \longrightarrow 4\ HgClI\ (hot) \qquad (4d')$$

$$2 \times 2\ HgClI \longrightarrow HgI_2 + HgCl_2\ (cool) \qquad (4e')$$

$$4\ CuI + 4\ HgCl_2 \longrightarrow 2\ HgI_2 + 2\ HgCl_2 + 4\ CuCl$$

The step (4c) could not be confirmed because HgClI is unstable at room temperature and the X-ray measurements are made at a different laboratory. The step (4c') was, however, confirmed in the study of 2:1 molar mixture of this system. Considering the 2:1 molar mixture reaction, the later mechanism appears to be more reasonable. The X-ray diffraction pattern of this molar mixture is described in Table VI.

The X-ray analysis of 1:2 molar mixture of CuI and $HgCl_2$ at 120°C showed the presence of CuCl, HgI_2 and $HgCl_2$ (Table II).

$$2\ CuI + 4\ HgCl_2 \longrightarrow 2\ CuCl + HgI_2 + 3\ HgCl_2 \qquad (5)$$

By all account, the reaction sequence occurring in this mixture is the same as that in 1:1 molar mixture.

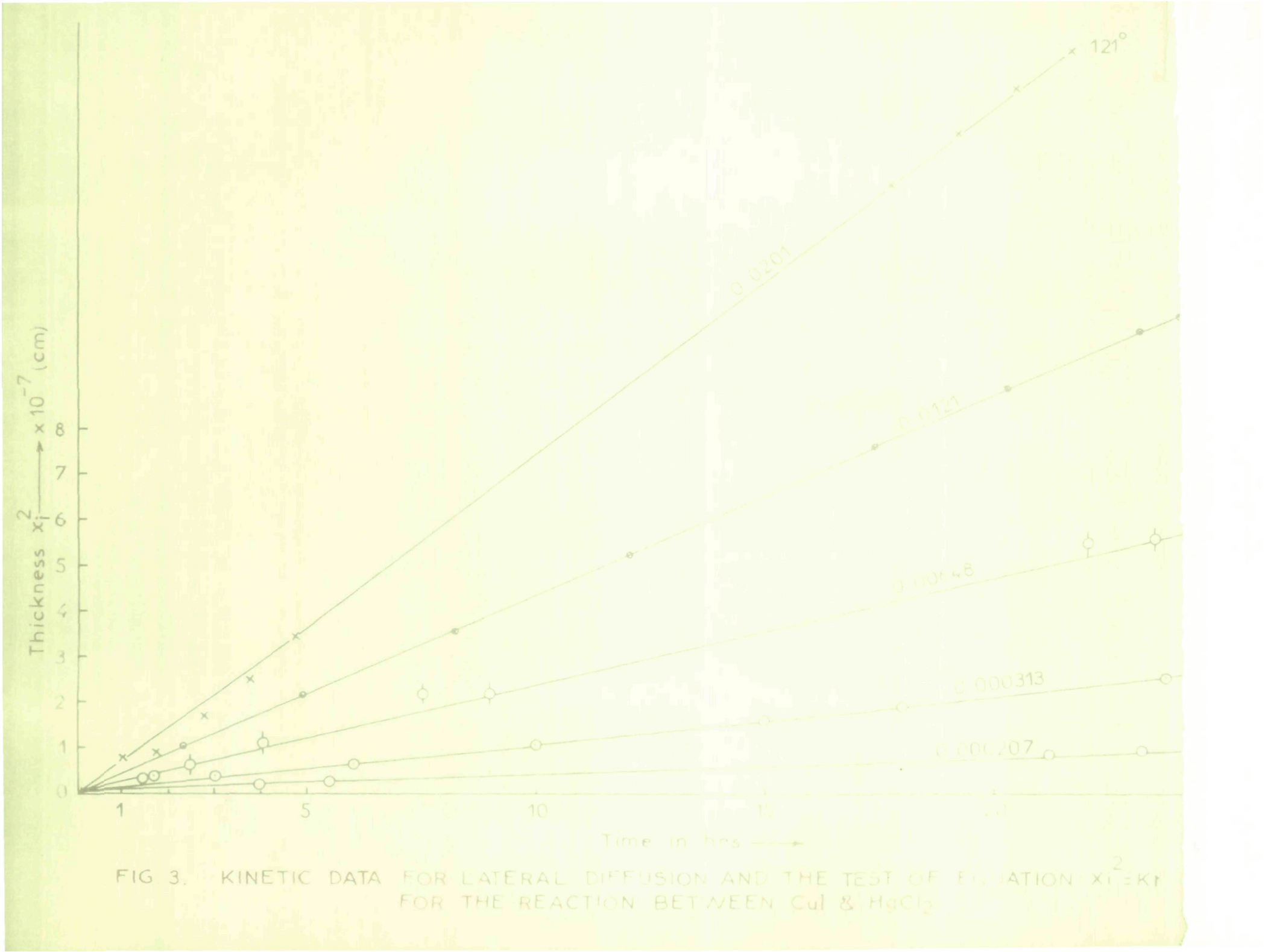

FIG 3. KINETIC DATA FOR LATERAL DIFFUSION AND THE TEST OF EQUATION $x_i^2 = Kt$ FOR THE REACTION BETWEEN CuI & $HgCl_2$

TABLE - VI

X-ray measurements for 1:1 molar mixture of CuI and $HgCl_2$ at 120°C

d in A°	I/Io	d in A°	I/Io
6.20x	24	2.43*	15
4.38*	100	2.34*	5
4.08x*	70	2.17x	5
3.60x	100	2.13*	5
3.13+	100	2.07x	5
3.02*	10	2.01*	15
3.00x	25	1.91+	50
2.75x	5	1.81*	v. low
2.71+*	15	1.67*	v. low
2.		1.63+	30

* lines correspond to $HgCl_2$ [8]
x lines correspond to HgI_2 [7]
+ lines correspond to CuCl [2]

Mechanism of lateral diffusion

The dark brown colour product layer that appears at the interface between CuI and $HgCl_2$ grows on the CuI side in the tube. This implies that it is only $HgCl_2$, that moves towards the CuI side. Soon after the dark brown colour layer appeared, another white layer was also seen between $HgCl_2$ and dark brown layer followed by an air gap between white layer and $HgCl_2$.

FIG. 4 DEPENDENCE OF K ON TEMPERATURE FOR THE REACTION BETWEEN $HgCl_2$ AND CuI

$HgCl_2$ reacts via gaseous phase. Gaseous $HgCl_2$ reacts with CuI like HgBrI and $HgBr_2$ with CuI grains via counter-diffusion of Cu^+ and Hg^{2+} through product layers. Growth of the thickness in CuI side of the product layers follows the equation $x^2 = Kt$, where x is the total thickness of the product layers at a time t. K is a constant. The plot of x^2 versus t are given in fig. 3, and the values of K at various temperatures are given in Table - I. The plot of log K inverse temperature (fig. 4) gave the activation energy 18.77 Kcal/mole. The magnitude of activities energy suggests that the reaction is diffusion controlled.

The formation of solid solution between CuI-CuCl, CuCl-Cu_2HgI_4 were also noticed during the X-ray analysis of the reaction mixtures. No attempts have, however, been made to study the extent of dissolution.

REFERENCES

1. Feigel, F. and Anger, V.: Spot Tests in Inorganic Chemistry 6th rev. edition, Elsevier, Amsterdam (1972), pp. 179, 203, 307 and 249.

2. ASTM Powder Diffraction File No. 6-0344.

3. ASTM Powder Diffraction File No. 18-0450, Cf. Chapter III Table I.

4. Pinnock, A.T.: J. Soc. Chem. Ind. 38, 78 (1919).

5. Rastogi, R.P. et al.: J. Inorg. Nucl. Chem. 37, 1167 (1975).

6. ASTM Powder Diffraction File No. 4-0456.

7. ASTM Powder Diffraction File No. 4-0335.

C H A P T E R - VII

REACTION OF CuBr - $HgCl_2$

Reaction between CuBr and $HgCl_2$

At room temperature, when CuBr and $HgCl_2$ were mixed, the resulting pale white colour product appeared after sometime. The colour of the product did not change on temperature increase.

Rate Measurements

$HgCl_2$ (below 300 mesh size) powder compact was placed over CuBr (also below 300 mesh size) powder compact in the reaction tube, and the progress of the reaction was noted by measuring the thickness of the product layer as described earlier. Rate constants at different temperatures are reported in Table I.

TABLE - I

Dependence of parameters of equation $x_1^n = Kt$ on temperature for CuBr-$HgCl_2$ reaction.

Temperature ($^oC \pm 0.5$)	K (cm/hr)	n
75	0.4×10^{-7}	
85	0.72×10^{-7}	2
96	1.11×10^{-7}	
101	1.50×10^{-7}	
107	1.75×10^{-7}	

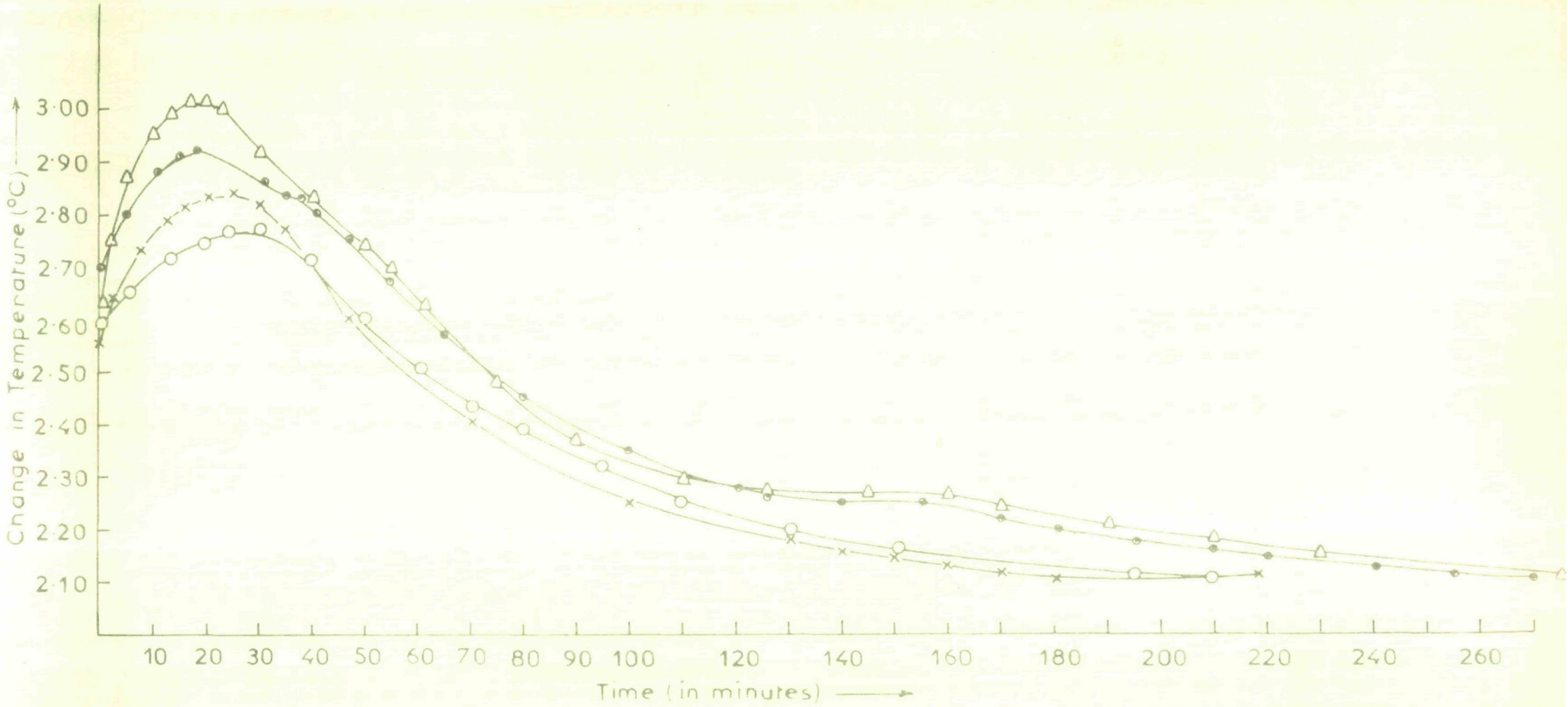

FIG.4a TEMPERATURE RISE AS A FUNCTION OF TIME FOR THE REACTION BETWEEN CuBr AND $HgCl_2$ MOLAR RATIOS (i) 4:1, (ii) 3:1, (iii) 2:1 & (iv) 1:1.

X-ray Studies

Different molar mixtures of powdered (below 300 mesh size) $HgCl_2$ and CuBr were mixed thoroughly in an agate mortar. One part of each mixture was allowed to stand at room temperature, and the other was heated for about 80 hours in an air oven maintained at $100^{\circ}C \pm 0.5^{\circ}C$. The mixtures at room temperature and $100^{\circ}C$ were analysed by Norelco Geiger counter X-ray diffractometer by CuK_{α} radiation applying 32 Kv at 12 mA with Ni-filter. The compounds identified in the different reaction mixtures are given in Table II.

Thermal Studies

A weighed amount of CuBr was taken in a Dewar flask. Thereafter, its half molar equivalent of $HgCl_2$ was weighed on a tissue paper and poured into the flask. The mixture was first stirred thoroughly and then allowed to stand undisturbed. The rise in temperature was noted with time (fig. 4a).

Conductivity measurement

Powdered $HgCl_2$ and CuBr in 1:2 molar ratio were thoroughly mixed, and the mass was immediately poured into a die and pressed into a disc. The disc was fixed between two platinum electrodes (applied voltage 0.2V and frequency 5×10^3 Hz). The change in conductance with time at room temperature was recorded with current ratio L-C Bridge.

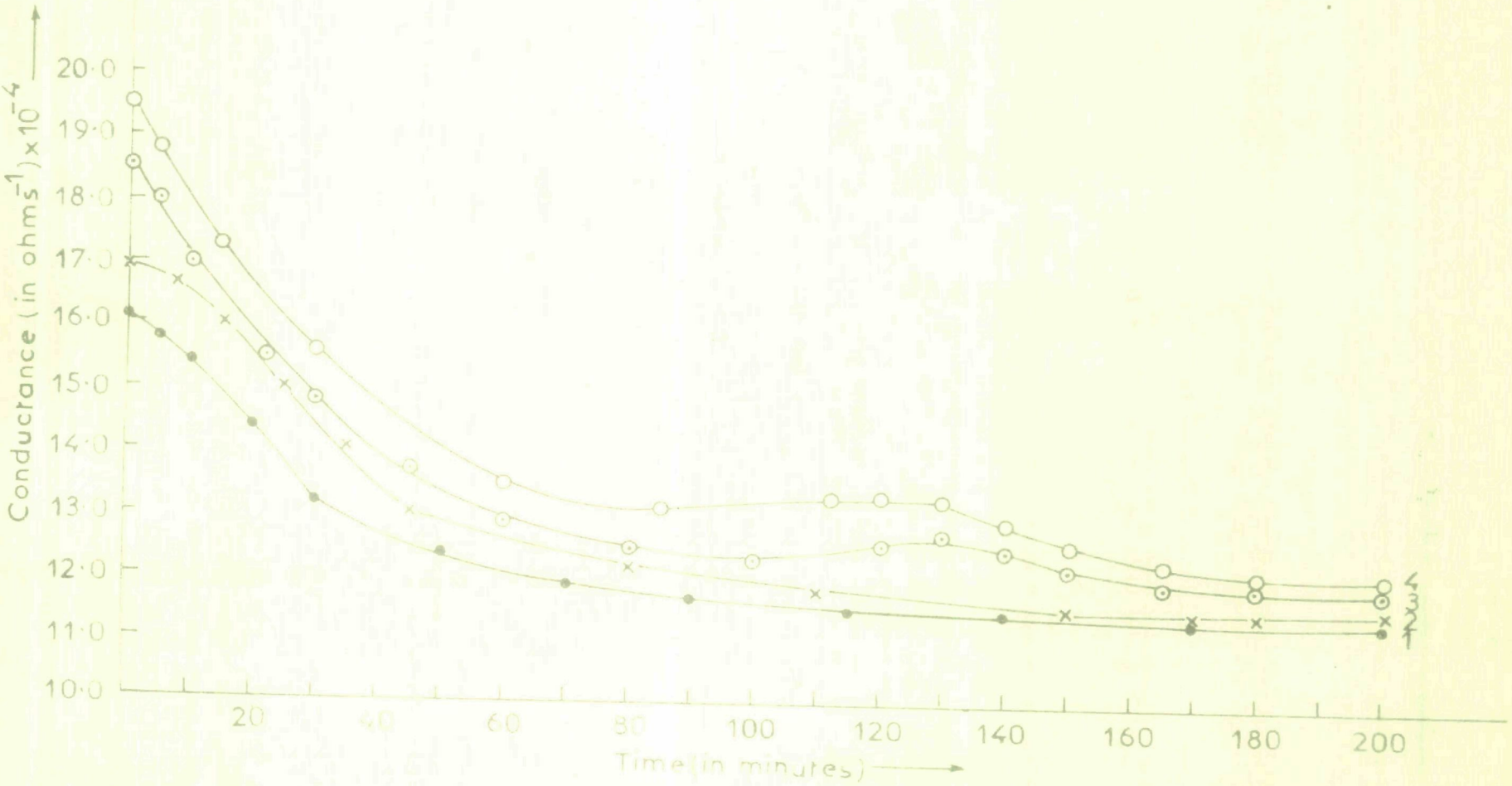

FIG. 4b CHANGE IN CONDUCTANCE AS FUNCTION OF TIME FOR CuBr AND $HgCl_2$ REACTION MOLAR RATIOS (i) 4:1, (ii) 3:1, (iii) 2:1, (iv) 1:1.

Analysis of product layers

A reaction tube having the yellow and white layers of the product was broken and the two layers collected separately with great care.

White layer was analysed for Cu^{+1} and Cl^{-2} by Spot Tests. X-ray analysis show it to be single phase CuCl. Similarly pale white layer was analysed for Hg^{2+}[3], Cl^{-2} and Br^{-}[4].

Discussion

The X-ray diffraction analysis showed that CuBr and $HgCl_2$ react in 2:1 molar ratio in the solid state; giving CuCl and $HgBr_2$ as the final product.

$$2\ CuBr + HgCl_2 \longrightarrow 2\ CuCl + HgBr_2 \qquad (1)$$

At the first sight, it seems that the reaction is a simple exchange reaction. The thermal and conductivity measurements (fig. 4a-3) and (fig. 4b-3) also suggest that the reaction is a single step reaction, because there is no second inflection observable in the plot of temperature rise with time in the case of thermal analysis or in the plot of conductance increase with time in the case of conductivity measurements. It may be assumed that as soon as $HgBr_2$ are formed, it may combine with $HgCl_2$ to form HgClBr at high temperature[5]

(HgClBr is formed by reaction of $HgCl_2$ and $HgBr_2$ when mixed in equimolar ratio in solid state at high temperature). But, this possibility is ruled out by the fact that exchange reaction are very fast.[6] Furthermore, the formation of HgClBr by the reaction

$$HgCl_2 + HgBr_2 \longrightarrow 2\ HgClBr \qquad (2)$$

is comparatively very slow (which was checked earlier by the thermal analysis. Since no lines for HgClBr were obtained, it is concluded that the formation of HgClBr was not probable. It might be forming but the amount may be so little as to be practically negligible. The X-ray pattern of 2:1 molar ratio of the mixture is dipicted in Table III.

TABLE - II

X-ray diffraction analysis for CuBr + $HgCl_2$ reaction

Mix. No.	Molar ratio of CuBr and $HgCl_2$	Reaction product at 100°C
0	4:1	CuCl, $HgBr_2$, CuBr
1	3:1	CuCl, $HgBr_2$, CuBr
2	2:1	CuCl, $HgBr_2$
3	1:1	CuCl, HgClBr

TABLE - III

X-ray data for the product of the reaction 2:1 molar ratio of CuBr and $HgCl_2$ at 60°C

d in A°	I/Io	d in A°	I/Io
6.21+	100	2.24+	10
3.82+	6	2.17+	10
3.66+	50	2.07+	55
3.26+	35	2.02+	10
3.24		1.99+	8
3.13x	100	1.92x	50
3.10+	10	1.73+	8
2.82+	40	1.64x+	30
2.74x	8	1.54+	5
2.62+	30	1.45+	8
2.43+	8	1.44+	5
2.29+	10		

+ lines belong to $HgBr_2$ [7]
x lines belong to CuCl [8]

The examination of Table II shows that the reaction product for 4:1 and 3:1 molar ratios of CuBr and $HgCl_2$ are CuCl, $HgBr_2$ and CuBr. The X-ray analysis clearly shows that the reaction is taking place exactly in the similar manner as that of the reaction for the 2:1 molar mixture. The excess amount of CuBr present in the reaction mixtures remains unreacted. The thermal and conductivity measurements supports the conclusion (fig. 4a-1,2) and (fig. 4b-1,2).

The X-ray data for the product of reaction CuBr and $HgCl_2$ in the molar ratio of 3:1 and 4:1 are given in Tables IV and V.

X-ray analysis for the reaction mixture of CuBr and $HgCl_2$ in molar ratio 1:1 showed that (Table II), CuCl and HgClBr were the final product.

$$CuBr + HgCl_2 \longrightarrow CuCl + HgClBr \qquad (3)$$

Thermal and conductivity measurement did show (fig. 4a,4) and (fig.4b,4) the second inflection after about the same time. This means that the reaction proceeds via two steps. The first step is the formation of $HgBr_2$ and CuCl as in the other molar ratios

$$2\ CuBr + 2\ HgCl_2 \longrightarrow 2\ CuCl + HgBr_2 + HgCl_2 \qquad (3a)$$

The excess amount of $HgCl_2$ in the reaction mixture, which were left unreacted, then combined with $HgBr_2$ to form HgClBr.

$$HgCl_2 + HgBr_2 \longrightarrow 2\ HgClBr \qquad (3b)$$

Earlier, the formation of HgClBr was not observed, because the amount of $HgCl_2$ was always stoichiometrically balanced. Hence, the overall reaction may be written as

$$2\ CuBr + 2\ HgCl_2 \longrightarrow 2\ CuCl + 2\ HgClBr$$

The X-ray data for the product of reaction CuBr and $HgCl_2$ in the molar ratio of 3:1 and 4:1 are given in Table IV and V.

TABLE - IV

X-ray analysis for the reaction 4:1 molar ratio CuBr and $HgCl_2$

d in A^o	I/Io	d in A^o	I/Io
6.21	100	2.17	12
3.83	5	2.08	30
3.66	50	2.03	5
3.32x	100	2.01x	56
3.21	35	1.96	15
3.10+	100	1.93+	50
2.96	10	1.82	15
2.82	35	1.74x	35
2.62	30	1.68+	25
2.32	20	1.54	20
		1.52	10

x lines of CuBr[9]
+ lines of CuCl[8]
Remaining lines are of $HgBr_2$[7]

TABLE - V

X-ray analysis for the reaction 3 CuBr + $HgCl_2$

d in A^0	I/Io	d in A^0	I/Io
6.21*	100	2.03+	50
3.80*	5	2.00*	10
3.63*	50	1.95x	50
3.24+	100	1.93*	15
3.15x	100	1.83*	12
2.92+	8	1.81*	5
2.79+	5	1.73*	8
2.71x	7	1.69+	30
2.62*	25	1.65x*	30
2.41*	8	1.64*	3
2.30*	20	1.55*	15
2.16*	12	1.51*	8
2.08*	15	1.50*	8
2.07*	40	1.46+*	5
		1.37x	5

x lines for CuCl[8]
+ lines for CuBr[9]
Remaining are for $HgBr_2$[7]

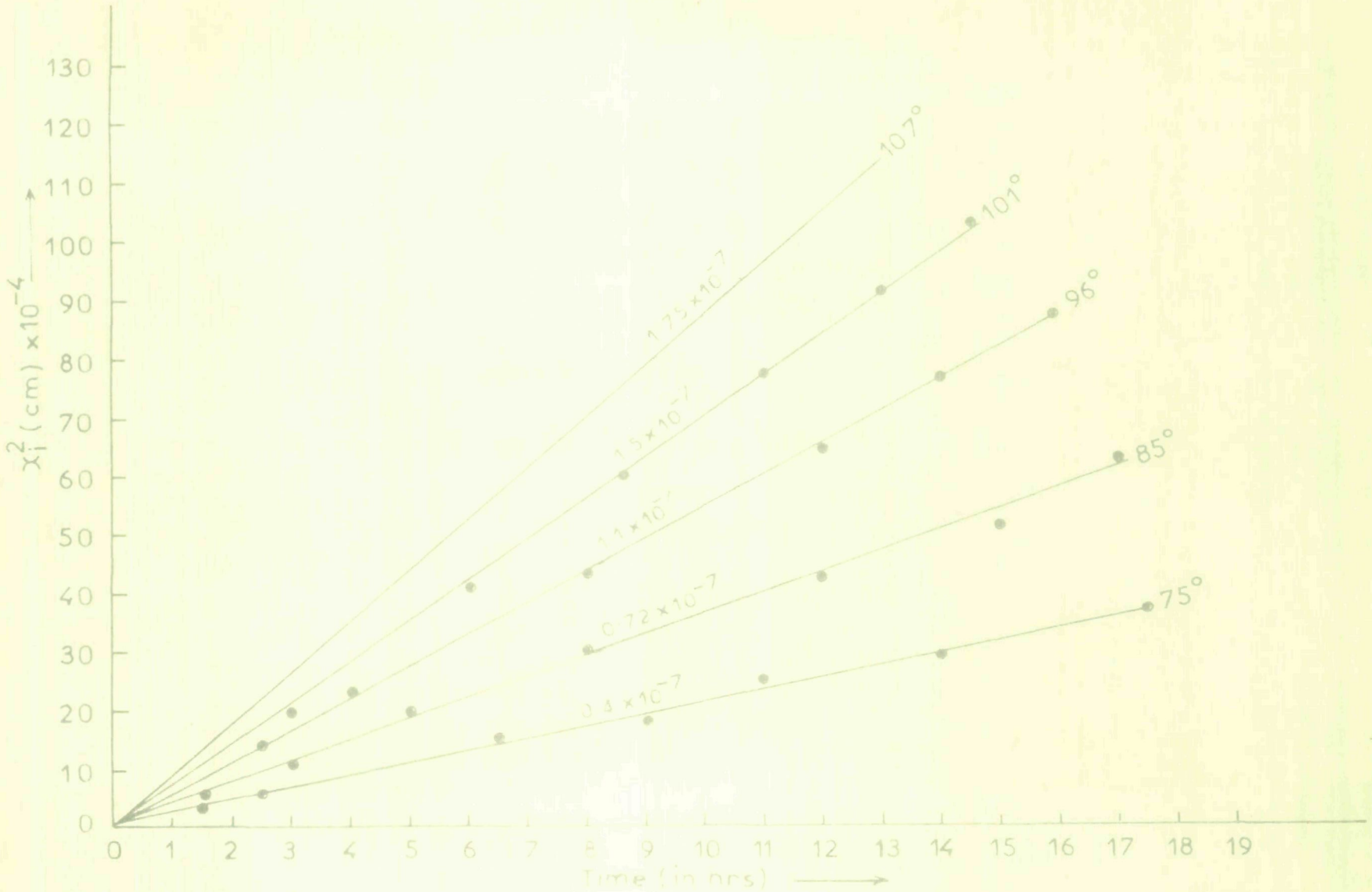

FIG. 4 KINETIC DATA FOR LATERAL DIFFUSION AND TES FOR EQUATION $x_i^2 = Kt$ FOR THE REACTION BETWEEN CuBr & $HgCl_2$.

The d values and the corresponding intensities of the identified compounds in 1:1 molar mixture are given in Table VI.

TABLE - VI

X-ray data for the reaction CuBr + $HgCl_2$

d in A^o	I/Io	d in A^o	I/Io
5.92x	20	2.75+	7
5.06x		2.73x	21
4.62x	20	2.49x	20
4.30x	15	2.30x	30
4.17x	20	2.11x	35
3.63x	15	2.05x	15
3.46x	15	1.94+	50
3.13+	100	1.88x, 1.86+	8
3.10x			
3.02x	100	1.67x	25
2.81x	35	1.63+	30

x lines belong to $HgClBr$ [5]

+ lines belong to $CuCl$ [8]

FIG 4d DEPENDENCE OF K ON TEMPERATURE FOR REACTION BETWEEN CuBr AND $HgCl_2$

Mechanism of lateral diffusion

In lateral diffusion experiments, it was observed that after placing powdered $HgCl_2$ over CuBr, a whitish yellow boundary appeared at the interface after sometimes, which grew in CuBr side. Soon it separated into white and yellow layers. $HgCl_2$ is highly vapourising material, hence $HgCl_2$ vapour surrounds the CuBr grain at the reaction zone to form $HgBr_2$ and CuCl by exchange reaction. But since $HgCl_2$ molecules are in excess and in the immediate vicinity of the formed $HgBr_2$, therefore, it combine with $HgBr_2$ to produce yellow colour HgClBr which is an addition product. The appearance of whitish yellow colour after sometimes is perhaps due to this fact.

Growth of the product layers satisfies the equation $x^2 = Kt$ (fig. 4), where x is the total thickness of the product layers in time t and n and K are constants. The value of n in equation is 2 at all temperatures. The activation energy measured from log K Vs 1/T plot, comes out to be 14.41 Kcal/mole.

The deviation of d values in the X-ray patterns suggest that formation of solid solution between CuBr and CuCl which are cubic, is taking place.

REFERENCES

1. Fiegel, F. and Anger, V.: Spots Tests in Inorganic Analysis (Elsevier Publishing Company, Amsterdam), pp 179.
2. Ibid, pp. 203.
3. Ibid. pp. 307, 309.
4. Ibid. pp. 145, 147.
5. Rastogi, R.P. et al.: J. Inorg. Nucl. Chem. 37, 1167-72(1975).
6. Link, H.L. and Wood, L.J.: J. Am. Chem. Soc. 62, 766 (1940).
7. ASTM X-ray Diffraction File No. (In Press) Cf. pp 90, Chapter III.
8. ASTM X-ray Diffraction File No.6-0344.
9. ASTM X-ray Diffraction File No.6-0292.